POLITECNICO
MILANO 1863

Politecnico di Milano
Department of Electronics, Information, and Bioengineering
Doctoral Program In Information Technology

OPTIMAL DESIGN OF OFF-GRID WATER-ENERGY SYSTEMS IN SMALL MEDITERRANEAN ISLANDS

Doctoral Dissertation of:
Federico Giudici

Advisor:
Prof. Andrea Castelletti

Co-Advisor:
Elisabetta Garofalo

Tutor:
Prof. Luigi Piroddi

The Chair of the Doctoral Program:
Prof. Barbara Pernici

2019 – XXXII Cycle

If we knew what it was we were doing,
it would not be called research, would it?
— Albert Einstein

Abstract

Small Mediterranean islands represent a paradigmatic example of remote, off-grid systems facing a large number of sustainability issues, mainly due to their distance from the mainland, the lack of accessible water sources, and the high seasonal variability of both water and electricity demand. Energy security is generally reliant on carbon intensive diesel generators, which are usually oversized to meet peak summer electricity demand driven by high touristic fluxes. Potable water is often produced by energy intensive desalination technologies, which strongly impact on the electricity system, increasing air pollution and greenhouse gas emissions. In order to improve the economic and environmental sustainability of small islands, the design of hybrid energy systems, combining traditional power generation with renewable energy sources and storage technologies, represents a viable and promising solution. However, traditional methods for designing such systems usually neglect important aspects and challenges. Major challenges include (i) the optimal control of the electricity system as well as its interconnection with other energy vectors (e.g., gas, heat) and domains (e.g., water system) for fully exploiting renewable power, (ii) the interdependency between system planning and its operation, (iii) the presence of multiple, potentially conflicting, objectives reflecting economic, environmental and other sustainability aspects, (iv) deep uncertainty in climate, technological and socio-economic conditions that may affect the system performance over a medium-to-long term horizon.

Driven by these challenges, this thesis contributes novel methodologies for supporting energy systems transition towards decarbonization, helping decision makers to identify viable solutions at different temporal scales in light of plausible future conditions that might unfold. In particular, we develop a set of modelling and optimization tools for optimizing both the design and the operations of off-grid water-energy systems, also considering the uncertainty related to future changes in the main external drivers. The proposed methodologies allow us to (i) investigate the benefits of explicitly considering the interdependency between system design and operation with respect to multiple economical, environmental and efficiency objectives, (ii) assess the vulnerability of hybrid en-

ergy systems to the future uncertainty in the main external drivers, and (iii) design solutions that are robust with respect to this uncertainty.
The first deliverable of this research is a novel multi-objective, dynamic approach for conjunctively optimizing design and operation of water-energy systems by focusing on the interconnection between electricity generation and water supply through the optimal control of desalination plant. Secondly, we propose a methodological framework to assess the vulnerability of hybrid energy systems with respect to changes in the main climate drivers (i.e., solar radiation, wind speed, temperature). More precisely, we evaluate how historical variability and future uncertainty in these climate variables affect the performance of highly renewable hybrid energy systems, designed under average historical conditions, in terms of different sustainability indicators. Finally, we focus on the challenge of directly including deep uncertainty in future climate drivers within the system design phase. Since the performance of hybrid energy systems in small Mediterranean islands strictly depends on multiple, deeply uncertain covarying drivers, a very large number of future scenarios should be considered and, consequently, included within the optimization process for generating robust solutions, leading to very high, or even intractable, computational time for solving the problem. To address this issue, we develop ROSS (Robust Optimal Scenario Selection), a novel algorithm that uses active learning for adaptively selecting the smallest scenario subset to be included into a robust optimization process.
We test our novel approaches on the real case study of the Italian Ustica island, which represents a paradigmatic example of off-grid Mediterranean island.
Main thesis outcomes show that considering the interdependency between system design and operation by dynamically modelling the nexus between water production and electricity generation allows to significantly improve system performance by reducing the structural interventions, the investment costs and the environmental impacts. In addition, results suggest that wind speed represents the climate variable that mainly influences the performance of hybrid energy systems, which will likely degrade on a medium-to-long term horizon. Finally, our novel ROSS algorithm allows to obtain robust hybrid energy system designs reducing computational requirements between 23% and 84% compared with traditional robust optimization methods, depending on the complexity of the robustness metrics considered. Moreover, it is able to identify very small regions of the scenario space containing the most informative scenarios highlighting the main system vulnerabilities.
Part of this research has appeared (or has to appear) in the following journal publications:

- Giudici, F., Castelletti, A., Garofalo, E., Giuliani, M., Maier, H. R., 2019a. Dynamic, multi-objective optimal design and operation of water-energy

systems for small, off-grid islands. Applied Energy 250, 605–616;

- Giudici, F., Castelletti, A., Giuliani, M., Maier, H. R., 2019c. An active learning approach for identifying the smallest subset of informative scenarios for robust planning under deep uncertainty. Environmental Modelling & Software (Under Review);
- Giudici, F., Castelletti, A., Garofalo, E., Maier, H. R., 2019b. Exploring the effects of climate change and technological innovation on the robust design of off-grid hybrid energy systems. Nature Energy (in preparation).

Sommario

Le piccole isole del Mediterraneo rappresentano un esempio paradigmatico di sistemi remoti fuori rete che affrontano un gran numero di problemi di sostenibilità, principalmente a causa della loro distanza dalla terraferma, della mancanza di sorgenti d'acqua accessibili e dell'elevata variabilità stagionale della domanda di acqua ed elettricità. La sicurezza energetica dipende generalmente da generatori diesel, che di solito sono sovradimensionati per soddisfare il picco della domanda di elettricità estiva dovuta agli elevati flussi turistici. L'acqua potabile è spesso prodotta da tecnologie di dissalazione altamente energivore, che incidono fortemente sul sistema elettrico, aumentando l'inquinamento atmosferico e le emissioni di gas serra. Al fine di migliorare la sostenibilità economica e ambientale delle piccole isole, la progettazione di sistemi energetici ibridi, che combinano generazione elettrica da fonti tradizionali con fonti di energia rinnovabili e tecnologie di stoccaggio, rappresenta una soluzione praticabile e promettente. Tuttavia, i metodi tradizionali per la progettazione di tali sistemi di solito trascurano aspetti importanti. I principali aspetti includono (i) il controllo ottimale del sistema elettrico e la sua interconnessione con altri vettori energetici (ad es. gas, calore) e sistemi (ad es. sistema idrico) per sfruttare pienamente la risorsa rinnovabile, (ii) l'interdipendenza tra la pianificazione del sistema e la sua gestione, (iii) la presenza di molteplici obiettivi, potenzialmente conflittuali, che riflettono aspetti economici, ambientali e di sostenibilità, (iv) la profonda incertezza in condizioni climatiche, tecnologiche e socio-economiche che possono influire sulle prestazioni del sistema in un orizzonte di medio-lungo termine.

Spinto da queste sfide, questa tesi propone nuove metodologie per supportare la transizione dei sistemi energetici verso la decarbonizzazione, aiutando i decisori a identificare soluzioni praticabili su diverse scale temporali, alla luce di possibili condizioni future che potrebbero verificarsi. In particolare, sviluppiamo una serie di strumenti di modellizzazione e ottimizzazione per ottimizzare sia la progettazione che le operazioni dei sistemi acqua-energia fuori rete, anche considerando l'incertezza relativa ai futuri cambiamenti nelle principali forzanti esterne. Le metodologie proposte ci consentono di (i) studiare i vantaggi di

considerare esplicitamente l'interdipendenza tra la progettazione del sistema e il suo funzionamento rispetto a molteplici obiettivi economici, ambientali e di efficienza, (ii) valutare la vulnerabilità dei sistemi energetici ibridi rispetto all'incertezza futura nelle principali forzanti esterne, e (iii) identificare soluzioni che siano robuste rispetto a questa incertezza.
Il primo risultato di questa ricerca è un nuovo approccio dinamico, multi-obiettivo per ottimizzare congiuntamente la progettazione e il funzionamento dei sistemi energetici ibridi, concentrandosi sull'interconnessione tra produzione di elettricità e fornitura di acqua attraverso il controllo ottimale dell'impianto di dissalazione. In secondo luogo, proponiamo un quadro metodologico per valutare la vulnerabilità dei sistemi energetici ibridi rispetto ai cambiamenti nei principali fattori climatici (ovvero radiazione solare, velocità del vento, temperatura). Più precisamente, valutiamo in che modo la variabilità storica e l'incertezza futura nelle variabili climatiche influenzano le prestazioni dei sistemi energetici ibridi progettati in condizioni storiche medie, in termini di diversi indicatori di sostenibilità. Infine, ci concentriamo sull'inclusione della profonda incertezza nelle forzanti climatiche nella fase di pianificazione del sistema. Siccome le prestazioni dei sistemi energetici ibridi nelle piccole isole del Mediterraneo dipendono fortemente da molteplici forzanti incerte e co-varianti, un numero molto alto di scenari dovrebbe essere considerato e, di conseguenza, incluso nel processo di ottimizzazione per generare soluzioni robuste, portando a tempi computazionali molto alti o addirittura intrattabili. Per affrontare questo problema, sviluppiamo ROSS (Robust Optimal Scenario Selection), un nuovo algoritmo che utilizza l'apprendimento attivo per selezionare in modo adattivo il sottoinsieme di scenari più piccolo da includere in un processo di ottimizzazione robusta.
Testiamo i nostri nuovi approcci sul caso di studio reale dell'isola italiana di Ustica, che rappresenta un esempio paradigmatico di isola del Mediterraneo fuori rete.
I principali risultati della tesi mostrano che considerare l'interdipendenza tra la progettazione e il funzionamento del sistema modellando dinamicamente il nesso tra produzione di acqua e generazione di elettricità consente di migliorare significativamente le prestazioni del sistema, riducendo gli interventi strutturali, i costi di investimento e gli impatti ambientali. Inoltre, i risultati suggeriscono che la velocità del vento rappresenta la variabile climatica che influenza maggiormente le prestazioni dei sistemi energetici ibridi, le quali molto probabilmente degraderanno in un orizzonte a medio-lungo termine. Infine, il nostro nuovo algoritmo ROSS consente di ottenere soluzioni di pianificazione robuste riducendo i requisiti computazionali tra il 23% e l'84% rispetto ai metodi tradizionali, a seconda della complessità delle metriche di robustezza considerate. Inoltre, ROSS è in grado di identificare regioni molto piccole dello spazio degli

scenari contenenti gli scenari che evidenziano le principali vulnerabilità del sistema.
Parte della ricerca presentata in questa tesi appare (o apparirà prossimamente) nelle seguenti pubblicazioni scientifiche:

- Giudici, F., Castelletti, A., Garofalo, E., Giuliani, M., Maier, H. R., 2019a. Dynamic, multi-objective optimal design and operation of water-energy systems for small, off-grid islands. Applied Energy 250, 605–616;
- Giudici, F., Castelletti, A., Giuliani, M., Maier, H. R., 2019c. An active learning approach for identifying the smallest subset of informative scenarios for robust planning under deep uncertainty. Environmental Modelling & Software (Under Review);
- Giudici, F., Castelletti, A., Garofalo, E., Maier, H. R., 2019b. Exploring the effects of climate change and technological innovation on the robust design of off-grid hybrid energy systems. Nature Energy (in preparation).

Contents

1 Introduction

1.1 The water and energy nexus

Tackling climate change by mitigating its impacts on nature, society and national economies is one of the major challenges of this century. The scientific community widely recognises that climate is changing due to a significant increase in greenhouse gas emissions resulting from human activities. In particular, the energy sector accounts for about 72% of global manmade emissions (WRI, 2017), of which 82% is carbon dioxide (EPA, 2017) mainly produced by fossil fuel combustion for electricity generation. In recent years, several decarbonization policies have been thus implemented to improve the sustainability and the efficiency of the energy systems both globally and locally.
At the global scale, the United Nations recognise within the 17 Sustainability Development Goals for shaping a more sustainable future the need to ensure access to affordable, reliable and clean energy by defining specific targets to be reached by 2030. These prescribe to substantially increase the renewable energy share in the global energy mix, double the global rate of improvement in energy efficiency, and ensure clean energy in developing countries by enhancing international cooperation and expanding infrastructures (UN, 2019).
At the European scale, the "2020 Climate and Energy Package" established in 2009 by the European Union (EU) identifies three key targets to be reached by 2020, namely 20% of greenhouse gas emissions reduction with respect to 1990 levels, 20% of EU energy production from renewables and 20% of improvement in energy efficiency (EC, 2009). The "Roadmap to 2050" of the European Commission provides instead a practical guide to achieve a low carbon economy, in line with the sustainability goals of the EU, aiming at reducing between 80% and

90% the greenhouse gas emissions by 2050 (EC, 2011).

As highlighted, the energy sector will have a central role for succeeding in development and sustainability goals, and thus tackling and mitigating climate change (EC, 2016). In particular, electricity generation represents a key aspect of climate change mitigation policies, as the transition from fossil fuel to renewable energy sources (RES) is crucial to reduce manmade greenhouse gas emissions, air pollution, and global warming (Lechón et al., 2018).
However, future changes in the electricity generation mix could have significantly impacts on other important resources, such as water. Water and energy systems are in fact intrinsically coupled (Olsson, 2015) as large amounts of electricity is needed for extraction, treatment, conveyance, and distribution of water and wastewater (Pate et al., 2007), and significant volumes of water are withdrawn and consumed for electricity generation processes such as fuel production, thermoelectric cooling, and hydropower generation (Macknick et al., 2012). This nexus between water and energy (Lubega and Farid, 2014) implies that decisions made in one domain might affect positively or negatively the other, and vice-versa, over different spatio-temporal scales (Scott et al., 2011) and multiple dimensions (e.g., environmental, economic, technological, social) (Hamiche et al., 2016). These implications become amplified when global trends, such as growth in total and per capita demand of both water and energy, climate change, and the increasing pressure of droughts, strengthen the interactions between water and energy systems, negatively impacting their reliability and sustainability (Scott et al., 2015). In this context, considering the energy system along with its interconnection with other domains (e.g., water, land) becomes essential to foster more effective policies and strategies that lead to a more sustainable future.

1.2 Remote, off-grid energy systems

When dealing with energy security issues and electricity system decarbonization, off-grid renewable power systems play a crucial role in both developing and developed countries (IRENA, 2015). With more than one billion people living without electricity connection, local power systems constitute a reliable solution to provide sustainable electricity access to about 17% of the world's population living in developing countries (Sovacool, 2012). Conversely, renewable off-grid energy systems in developed countries are a promising alternative to replace carbon intensive diesel generators for producing clean energy at lower costs and, at the same time, improving power quality and reliability, avoiding power blackouts due to extreme events.

In this developed context, remote communities in rural areas or small islands rely on fossil fuels for producing electricity and face specific challenges typical of closed and disconnected systems (Beal et al., 2016) such as geographic isolation, high cost for electricity supply due to the transport of fuel, and highly variable electricity demand that causes difficulties in balancing electricity supply and demand (Kaygusuz, 2011; Mohtar and Lawford, 2016). However, recent decreasing costs of photovoltaic (PV), wind turbines and storage technologies as well as their increasing efficiency are making renewable systems particularly competitive and attractive for these communities (IRENA, 2013), which are starting their energy transition towards more sustainable power systems.
In this thesis, we focus on small Mediterranean islands as a paradigmatic example of remote, off-grid communities, where the above mentioned issues are further intensified by a strict interconnection between electricity generation and water supply. In particular, we concentrate on the Italian Ustica island, for which we provide a detailed description in Chapter 2.

1.3 Small Mediterranean islands

Small Mediterranean islands represent a paradigmatic example of remote off-grid systems facing a large number of sustainability issues, mainly due to their distance from the mainland, the lack of accessible water sources, and the high seasonal variability of both water and electricity demand.
Energy security is generally reliant on carbon intensive diesel generators (Duić and Da Graça Carvalho, 2004; Patlitzianas et al., 2007), which are usually oversized to meet peak summer electricity demand driven by high touristic fluxes (Kristoferson et al., 1985), and thus turn out to be oversized for the rest of the year. The high dependence upon remote supply of fuel and the need for a backup storage to cover possible refuelling delays (e.g., due to bad weather conditions) make the operation of these systems very costly and inefficient (Kakazu, 1994; Weisser, 2004; Palone et al., 2017). In addition, balancing energy supply and demand is challenged by the structural lack of flexibility of off-grid systems in modulating the offer and the high seasonal variability of the energy demand (Larsen et al., 2014).
Due to the lack of accessible water sources, potable water, which is typically transported with tank vessels from the mainland, is nowadays produced by desalination technologies, which are in some cases able to meet the entire water demand, though usually consuming large amount of electricity, strongly impacting on the energy system. With an electrical consumption that ranges between 7-14 and 2-6 kWh/m^3 for thermal and membrane based technologies, respectively (Ghalavand et al., 2015), the entire desalination process might account for up to 30% of the total electrical load of a small island. Moreover, high

electrical consumption, combined with a costly and inefficient electricity system, increase water production cost, which varies from 7 to 10 €/m^3, about ten times that on the mainland.

Even if small Mediterranean islands are characterized by a significant RES power potential (i.e., high wind and solar radiation) due to their geographic location, in many cases the development of renewable energy systems has been so far hampered by technical and economical issues. Technical aspects concern the limited size of the electricity grid and, above all, the high load variability between summer and winter that determine difficulties in balancing the electricity services, forcing local electrical companies to reduce the hosting capacity of the grid. Economical issues regard the strong subsidises that local electrical operators unconditionally receive from the national authorities to cover the extra-costs for electricity production. Placed that the lack of scale economies in such small systems inevitably generates much higher costs, it is indisputable that this mechanism does not foster initiatives for improving energy efficiency and the adoption of less-costly renewable sources.
However, these issues have been recently partially overcome: modern renewable technologies are able to provide services to ensure the grid stability and a higher power quality, and national authorities are starting to define strategies for reducing the extra-costs for power generation with the ultimate goal of improving the efficiency and the sustainability of the energy systems.

In this context, EU and single states are promoting specific innovation actions aimed at completely decarbonising small off-grid islands through the introduction of RESs and storage systems, the development of synergies between electricity, heating, cooling water and transport networks, and the increase of the efficiency of the energy system. For example, the political declaration on clean energy for EU Islands of May 2017 aims at accelerating the clean energy transition on more than 2700 islands in Europe, by reducing their dependency on energy imports and embracing more modern and innovative energy systems (EC, 2017).
At the national scale, in February 2017 the Italian Ministry issued a decree providing special incentives for new RES plants in order to reach a 10% of RES share within 2020 and reduce around 5% of electricity consumption for hot water production in the small Italian islands not connected to the national electricity grid. The decree provides also the financing of 2-3 innovative projects, which demonstrate a high reduction of the conventional electricity production (up to 50%).

1.4 Designing hybrid energy systems: state of the art

As already mentioned, a viable and promising solution for achieving sustainability goals is exploiting the high renewable potential of the islands through hybrid energy systems, which combine renewable electricity generation (e.g., PV, wind) with conventional power sources (e.g., diesel generators) and storage technologies. Several studies have recently investigated how to optimally design such hybrid energy systems in order to attain the best system performance (Ekren and Ekren, 2009; Ibrahim et al., 2010; Erdinc and Uzunoglu, 2012). In particular, a widely adopted design method consists in determining type and size of each technology in order to identify a system configuration that is able to meet load requirements by minimizing the present value of costs over a medium-to-long term horizon. The associated optimal design problem consists of a single-objective optimization problem, which can be solved using different methods, ranging from commercial software packages (Rehman et al., 2007; Shaahid and Elhadidy, 2007) to more complex optimization techniques (Koutroulis et al., 2006; Dong et al., 2016; Mohamed and Eltamaly, 2018). Improvement of these methods directly addresses the interconnection between energy and water system by optimally designing both hybrid energy systems and desalination units, evaluating the effects of different system configurations on water production costs (Spyrou and Anagnostopoulos, 2010; Bourouni et al., 2011; Mentis et al., 2016).

Even if the above mentioned methods represent useful tools for supporting the energy transitions of small islands towards more sustainable systems, they usually neglect key aspects and challenges that should be addressed when designing highly renewable hybrid energy systems.

First, the optimal control of the electricity system as well as its interconnection with other energy vectors (e.g., gas, heat) and domains (e.g., water system) allows to attain significant benefits at a very small time scale (e.g., hourly, daily) by fully exploiting the RES power potential and, consequently, increasing RES penetration and reducing operational costs. In this direction, a promising solution focuses on identifying demand side management strategies through the optimal control of flexible loads, such as the one associated to the desalination process. Desalination plant operations are traditionally modelled statically using a fixed electrical load as a surrogate of the actual water demand supplied by the desalination plant through the water distribution network (Kaldellis et al., 2006; Santhosh et al., 2014). This allows to take into account the effects on the electricity system of changes in the water demand at weekly or monthly time scale, but prevents to dynamically manage the desalination plant and the reservoirs composing the water distribution network at an hourly time scale in order

to release water according to the actual demand and, at the same time, allocate water production when it is more convenient (e.g., high renewable power).

Secondly, considering the interdependency between system planning and its operation when designing hybrid energy systems is crucial for identifying solutions that reduce investment costs and allow to obtain better performance over medium-to-long term horizons. As already mentioned, current state-of-the art methods design hybrid energy systems considering pre-defined, static operating rules (Elbaset, 2011; Luna-Rubio et al., 2012) usually bringing to over-dimensioned system configurations. In the context of small Mediterranean islands where small dimensions and tight environmental constraints significantly limit the RES installable capacity, designing optimal solutions that reduce the structural interventions is essential for both decreasing investment costs and reducing the environmental impacts.

As for the third challenge, traditional design methods perform a single-objective optimization for identifying the least cost configuration (i.e., the one that minimizes the present value of costs over a given horizon) (Ter-Gazarian and Kagan, 1992; Mizani and Yazdani, 2009; Anglani and Muliere, 2010). Present value of costs is a widely adopted pure economic metric that consider in an aggregated value all the costs occurring along the project horizon as well as the monetization of environmental and sustainability aspects, such as carbon emissions and energy/water deficits. However, the use of this metric in a single-objective optimization process does not allow to discover the effects of different solutions on different aspects separately, thus preventing to explore trade-offs between potentially conflicting objectives.

Finally, climate change and rapid technological innovation is likely to pose significant challenges to the identification of optimal planning solutions able to guarantee high levels of sustainability over a medium-to-long term horizon. In particular, the performance of hybrid energy systems traditionally designed under average historical conditions (Bhandari et al., 2015) will be strongly affected by the future uncertainty in multiple, co-varying climatic variables (e.g., solar radiation, wind speed, temperature) that represent the main drivers determining RES power potential. Thus, considering this uncertainty in the identification of the optimal hybrid system design is essential to identify solutions that are robust with respect to a wide range of plausible future conditions.

1.5 Thesis motivation and objectives

Driven by the above-mentioned challenges and motivations for the optimal design of off-grid hybrid energy systems, the overall aim of the work done in this thesis is to develop novel methodologies for supporting energy systems transition towards decarbonization, helping decision makers to identify viable solutions at different temporal scales in light of plausible future conditions that might unfold.
In particular, we develop a set of modelling and planning/control optimization tools for optimizing both the design and the operations of off-grid hybrid energy systems, also considering the uncertainty related to future changes in the main external drivers. On one hand, control optimization tools are needed to identify optimal operation strategies, which allow system operators to take optimal decisions at a very small time scale (e.g., hourly) attaining significant benefits through the dynamic operation of water-energy system by fully exploiting the renewable power potential. On the other hand, planning optimization tools are required to optimally design hybrid energy systems, identifying which type and size of technologies to be installed for achieving sustainability goals on a medium-to-long term horizon.

The integration of these tools will allow us to as achieve the following specific research objectives:

- Investigating the benefits of explicitly considering the interdependency between system design and operation with respect to multiple economic, environmental and efficiency objectives.

- Assessing the vulnerability of the hybrid energy systems to the future uncertainty in the main external drivers.

- Identifying solutions that are robust with respect to the deep uncertainty in the main external drivers (i.e., solutions that perform well over a wide range of plausible future conditions).

The innovative aspects of this research are two-fold. First, innovation is present in the methodologies developed for conjunctively optimizing the system design and operation with respect to multiple sustainability objectives, considering the integration of the energy system with the water system in order to maximize the benefits deriving from RES introduction. Secondly, another innovative aspect concerns the identification of the external conditions generating the key vulnerabilities of the system and the use of these conditions for generating robust system designs in an adaptive manner.

1.6 Research method

Figure 1.1 presents the main research stages, performed to achieve the thesis objectives presented in Section 1.5, classified according to the methodological contribution they address. Our methodological contributions, which propose novel advances in the optimal design of hybrid water-energy systems in off-grid contexts, include:

- Joint optimization of water-energy system design and operation with respect to multiple sustainability objectives.
- A novel framework to assess the performance of hybrid energy systems under changes in the main climate drivers.
- A novel active learning algorithm to include future uncertainty in the external drivers within the optimization process for generating robust system designs.

In particular, the first one (i.e., Optimal design and operation of water-energy system) focuses on evaluating the advantages of optimally controlling the water-energy system, exploring the interdependency between system design and operation within the optimization process and considering multiple potentially conflicting objectives to explore trade-offs between different sustainability aspects.

The second one (i.e., Energy system sensitivity to climate change) concentrates on assessing the vulnerability of hybrid energy systems with respect to changes in the main climate drivers (i.e., solar radiation, wind speed, temperature) by proposing a methodological framework for evaluating how historical variability and future uncertainty in these climate variables affect the performance of highly renewable hybrid energy systems, designed under average historical conditions, in terms of different sustainability indicators.

Finally, the third contribution (i.e., Robust system design via active learning) focuses on the challenge of directly including deep uncertainty in future climate drivers within the system design phase for generating robust solutions. This challenge is particularly relevant for our case study as the performance of hybrid energy systems in small Mediterranean islands strictly depends on multiple, deeply uncertain co-varying drivers. This generates a very large number of future scenarios to be included within the optimization process for generating robust solutions, leading to very high, or even intractable, computational costs for solving the robust optimization problem. To address this issue, we develop ROSS (Robust Optimal Scenario Selection), a novel algorithm that uses

Figure 1.1: *Outline of the research developed in this thesis.*

active learning for adaptively selecting the smallest scenario subset to be included into a robust optimization precess. ROSS allows to considerably reduce the computational requirements for the generation of robust solutions with respect to traditional optimization methods and couples scenario discovery with robust optimization for the identification of the most informative regions of the scenario space highlighting the main system vulnerabilities.

Each contribution includes different research stages that are presented more in detail in the following chapters and in the corresponding peer-reviewed publications. Next section summarizes the thesis outline and the content of each chapter.

1.7 Thesis outline

Chapter 2. In Chapter 2, we present the case study used in this thesis to test the effectiveness of the developed methodological frameworks and modelling tools. First, we describe the study site of an off-grid island, namely the Ustica island, which represents a paradigmatic example of off-grid island, where the electricity is generated through carbon intensive diesel generators and water is produced by an energy intensive desalination plant. Due to the very high availability of natural resources (e.g., wind speed, solar radiation), Ustica represents the ideal site for introducing a hybrid energy system and it is thus a very interesting case study for testing our approaches. Then, we present the model of Ustica water-energy system, on which all the performed experiments of this thesis are based.

Chapter 3. In Chapter 3, we address the thesis objective of investigating the benefits of explicitly considering the interdependency between system design and operation with respect to multiple economic, environmental and efficiency objectives by proposing a novel dynamic, multi-objective optimization approach for improving the sustainability of small islands through the introduction of renewable energy sources and the identification of optimal strategies for the desalination plant operations. The main contributions of our approach include: (i) dynamic modelling of desalination plant operations, (ii) joint optimization of system design and operations, (iii) multi-objective optimization to explore trade-offs between potentially conflicting objectives. We test our approach by comparing it with a traditional non-dynamic, least cost optimization approach. Results show the effectiveness of our approach in identifying optimal system configurations, which outperform the traditional design with respect to different sustainability indicators, limiting the structural interventions, the investment costs and the environmental impacts.

The content of this chapter is adapted from Giudici et al. (2019a).

Chapter 4. In Chapter 4, we address the thesis objective of assessing the vulnerability of the hybrid energy systems to the future uncertainty in the main external drivers by proposing a methodological framework to evaluate how the historical variability and the future uncertainty in the climate variables (i.e., solar radiation, wind speed, temperature) affect the performance of highly renewable hybrid energy systems, designed under average historical conditions, in terms of different sustainability indicators. Results show that the performance variability associated to the future scenarios is almost double with respect to the historical one for all the indicators considered. Moreover, the performance of the solutions characterized by high RES and storage capacity is less sensible to changes in the climate drivers with wind speed representing the driver that mainly affects the system performance.
The content of this chapter is adapted from Giudici et al. (2019b), in preparation.

Chapter 5. In Chapter 5, we address the thesis objective of identifying system designs that are robust with respect to the deep uncertainty in the main external drivers by introducing ROSS (Robust Optimal Scenario Selection), a novel algorithm that uses active learning for adaptively selecting the smallest scenario subset to be included into a robust optimization process. ROSS contributes a twofold novelty in the field of robust optimization under deep uncertainty. First, it allows to considerably reduce the computational requirements for the generation of robust solutions with respect to traditional optimization methods. Second, it couples scenario discovery with robust optimization for the identification of the most informative regions of the scenario space highlighting the main system vulnerabilities. We test ROSS on the real case study of robust planning of a hybrid, off-grid energy system, combining diesel generation with renewable energy sources and storage technologies. Results show that ROSS allows to considerably reduce the computational requirements with respect to a traditional robust optimization method, and, in few iterations, identifies very small regions of the scenario space containing the most informative scenarios for generating a robust solution.
The content of this chapter is adapted from Giudici et al. (2019c), under review.

Chapter 6. In Chapter 6, we summarize the achievements of this PhD thesis, providing general conclusions, ideas and opportunities for further research.

2

Study site: Ustica island

Ustica is a small Italian island with an area of 8 km^2 and is located about 50 km north of Sicily in the Mediterranean Sea (Figure 2.1a). It has a resident population of 1,559 inhabitants, which nearly doubles during the summer touristic months.

Electricity is produced entirely by 5 diesel generators with a total installed capacity of 4.6 MW. Household consumption accounts for nearly 70% of the annual electricity demand, with the remaining 30% covered by the desalination plant (Figure 2.1c), built in 2016 to satisfy the entire water demand. The plant is composed of two modules of 35 m^3/h each and is able to produce about 1,600 m^3/d of potable water, which is stored in 5 reservoirs with a total capacity of 11,000 m^3, and released through the water distribution network (Figure 2.1a-b). Due to the high touristic fluxes, electricity and water demand have a high seasonal variability (Figure 2.1c). As a consequence, both the desalination plant and the diesel generators are over-sized to cater to the summer peaking demand and avoid supply deficits.

Even if water and energy supply security is guaranteed, the water-energy system of the island is on the whole highly inefficient and, as a consequence, scarcely sustainable from both environmental and economic points of view. In addition to the high greenhouse gas emissions due to carbon intensive generation technology, the isolation from the mainland impacts considerably on the cost of electricity generation, which is on the order of around 4-5 times the tariff at the national level. Also, the cost of water production is 3 to 4 times higher than that for the nearby Sicily island due to the high cost and the high electricity consumption of the desalination process.

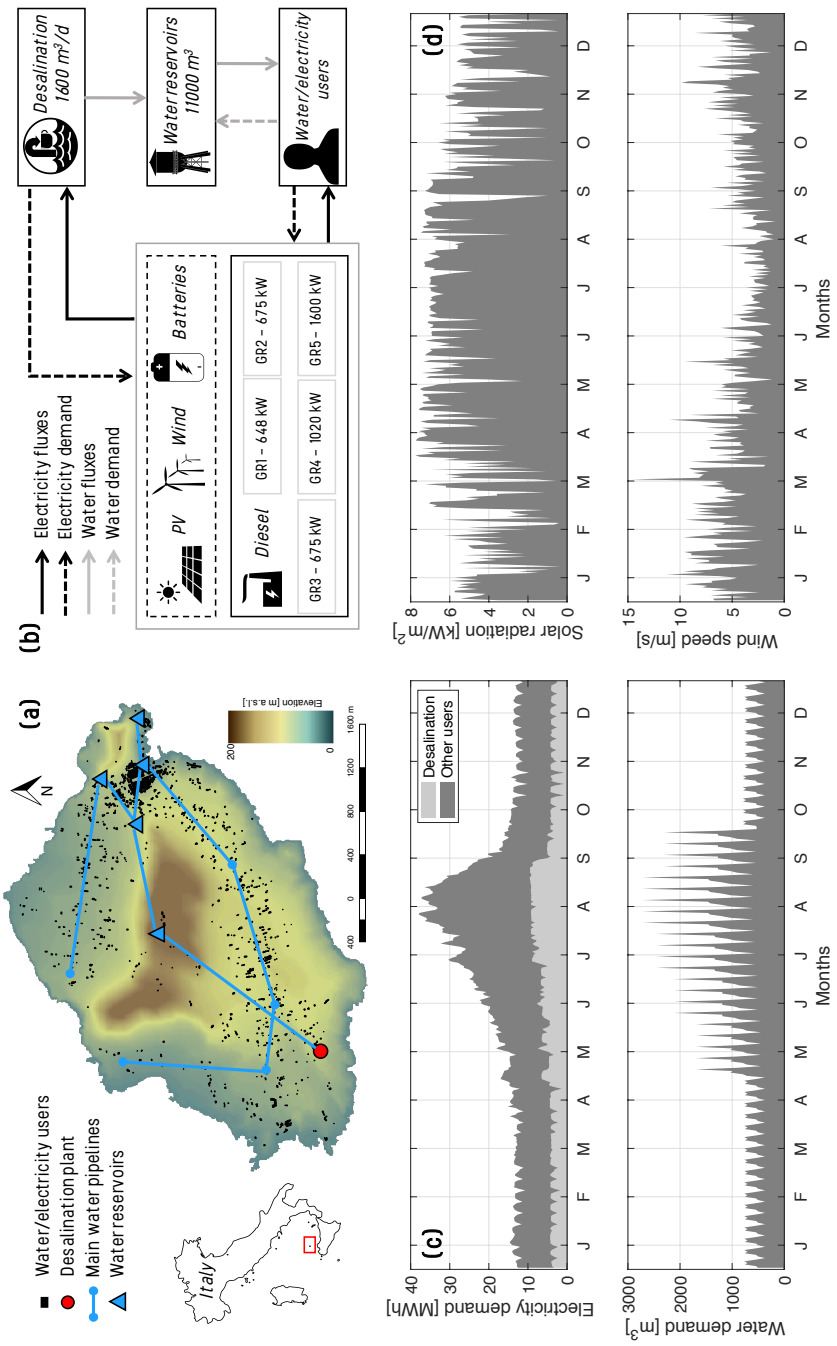

Figure 2.1: *(a) Location and map of Ustica island with the desalination plant, the water reservoirs and the water pipelines highlighted. (b) Schematization of the existing and planned water-electricity system of Ustica. (c) Daily electricity (top panel) and water (bottom panel) demand over a reference year. (d) Daily solar radiation (top panel) and wind speed (bottom panel) over a reference year.*

In order to improve the sustainability of this costly and inefficient system, the design of a hybrid energy system, combining diesel generation with RES and storage (i.e., batteries) technologies, is considered (Figure 2.1b) as a solution to produce clean energy at lower cost. Ustica has, in fact, significant solar and wind power potential (Figure 2.1d): the highest solar radiation is registered during the summer months (top panel), while the wind speed peak is in winter (bottom panel). Despite the high RES potential, both environmental constraints (the whole island is under landscape heritage protection according to the Sicily regional law 29/2015) and the small size of the island strictly limit the maximum installable RES capacity, allowing only roof integrated PV installations and micro wind turbines.

2.1 System model

Water production and distribution, as well as electricity generation, are represented by means of an integrated model (Figure 2.2), which simulates the water-electricity system dynamics using an hourly time step over a 1-year time horizon. At each time step t, the electricity is generated by the planned RES tech-

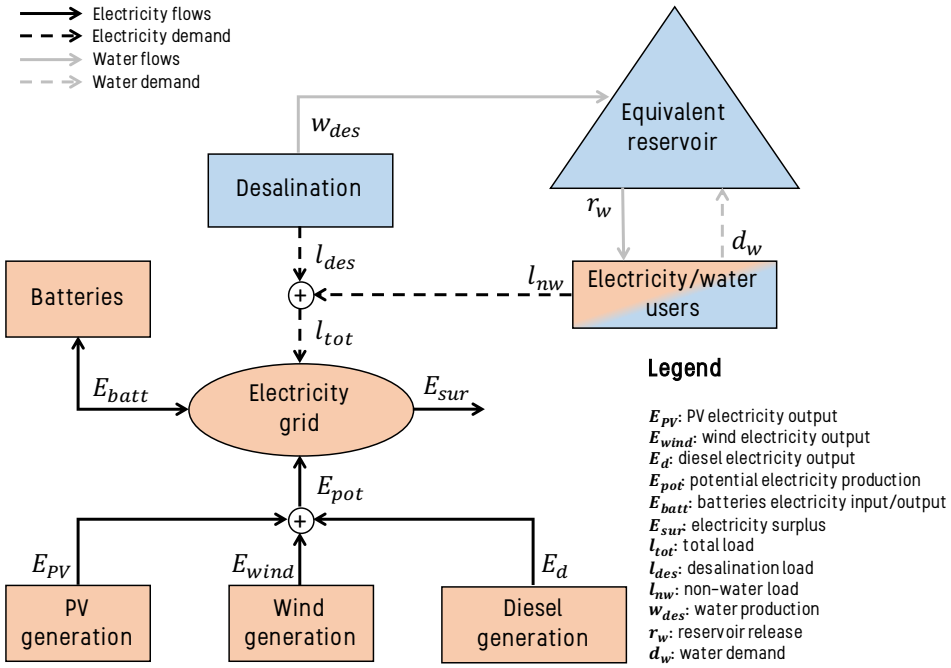

Figure 2.2: *Model schematization of the Ustica water (blue) - electricity (orange) integrated system.*

nologies (i.e., PV and wind) and the 5 existing diesel generators to meet a total load $l_{tot}(t)$ composed of the non-water electrical load $l_{nw}(t)$ and the load of the desalination plant $l_{des}(t)$. The electrical load of the desalination plant $l_{des}(t)$ is estimated as being linearly proportional (i.e., 6 kWh/m^3) to the water production $w_{des}(t)$. Due to the non-programmable nature of RES, sometimes the potential electricity output $E_{pot}(t)$ exceeds the electrical load $l_{tot}(t)$: when this happens, if batteries are installed, they are charged according to their maximum charge and capacity constraints. Then, if a non storable electricity surplus $E_{sur}(t)$ is generated, a RES power curtailment is applied. Conversely, when the electrical load $l_{tot}(t)$ exceeds the potential electricity output, the batteries are discharged according to their maximum discharge and capacity constraints. After having discharged the batteries, if the total load is not met, diesel units are forced to produce electricity in order to ensure the load to be always completely covered. If no batteries are installed, diesel units are forced to entirely cover the difference between $l_{tot}(t)$ and $E_{pot}(t)$.
It is worth noting that this operating strategy (also called "merit order" strategy) is defined a priori and not optimally identified within an optimization process.

2.1.1 PV generation

The PV potential electricity output $E_{PV}(t)$ (kWh) is defined by the following equation:

$$E_{PV}(t) = C_{PV}\rho\frac{G_T(t)}{G_{T,stc}}(1 + \alpha_T(T_c(t) - T_{c,stc})) \tag{2.1}$$

where:

- C_{PV} [kW]: PV rated capacity, namely the PV electricity output under standard test conditions.[1] This will be considered as a design parameter in the optimization experiments presented in the next chapters.
- $\rho = 0.9$ [-]: derating factor. This is a coefficient that quantifies the efficiency of the PV array.
- $G_T(t)$ [kW/m^2]: incident solar radiation at time t.
- $G_{T,stc}$ [kW/m^2]: incident solar radiation under standard test conditions.
- $\alpha_T = -0.4$ [%°C^{-1}]: temperature coefficient. The higher the PV array temperature is, the lower the electricity output is.
- $T_c(t)$ [°C]: PV array operating temperature at time t.
- $T_{c,stc}$ [°C]: PV array temperature under standard test condition.

[1] Standard test conditions consider an incident solar radiation of 1 kW/m^2 and a PV array temperature of 25 °C.

2.1.2 Wind generation

Due to the presence of tight environmental constraints, which limit the wind turbines to few small units, in this model we consider only wind turbines with a rated capacity of 60 kW and a hub height of 36 meters. The wind farm potential electricity output $E_{wind}(t)$ (kWh) is thus calculated as follow:

$$E_{wind}(t) = n_w P_{60}(t) \tag{2.2}$$

where $P_{60}(t)$ is the electricity output of a single wind turbine and n_w is the number of wind turbines installed (design parameter in the optimization experiments). $P_{60}(t)$ is computed using a power curve, typical of the wind turbine, which defines the electricity output as a function of the wind speed at the hub height $v_h(t)$ (m/s):

$$P_{60}(t) = \begin{cases} 0 & \text{if } v_h(t) = 0 \vee v_h(t) \geqslant 26 \\ 0.1072 \cdot v_h(t)^{3.064} + 0.2167 & \text{if } 0 \geqslant v_h(t) < 8 \\ 60 & \text{if } 8 \leqslant v_h(t) < 26 \end{cases} \tag{2.3}$$

The wind speed at the hub height $v_h(t)$ is calculated from the wind speed measured at the anemometer $v_a(t)$ (m/s) using the following empirical formula:

$$v_h(t) = v_a(t)(\frac{z_h}{z_a})^{\beta} \tag{2.4}$$

where $z_h = 36$ m and $z_a = 10$ m are the height of the hub and the anemometer, respectively, and β is an empirical coefficient equal to 0.21 for our case study (Giudici et al., 2019a).

2.1.3 Batteries

In this model, we consider a storage system composed of lithium ion batteries. Each battery has a storage capacity of 100 kWh and it is characterized by the following parameters:

- $v_b = 600$ [V]: nominal voltage.
- $curr_{max} = 83$ [A]: maximum charge/discharge current.
- $\eta_b = 0.9$ [-]: charge and discharge efficiency.
- $s_{min} = 0.1$ [-]: minimum state of charge.

The capacity C_b of the storage system is calculated by multiplying the capacity of a single battery by the number of batteries to be installed n_b (design parameter in the optimization experiments). At each time step, the maximum charge

$c_{max}(t)$ and discharge $d_{max}(t)$ capacity of the storage system is computed as follow:

$$c_{max}(t) = \min(n_b v_b \frac{curr_{max}}{1000\sqrt{\eta_b}}, \frac{C_b - s_b(t)}{\sqrt{\eta_b}}) \tag{2.5}$$

$$d_{max}(t) = \min(n_b v_b \frac{curr_{max}\sqrt{\eta_b}}{1000}, (s_b(t) - C_b s_b(t))\sqrt{\eta_b}) \tag{2.6}$$

where $s_b(t)$ is the state of charge of the storage system. If the potential electricity output $E_{pot}(t)$ is higher than the total load $l_{tot}(t)$, the discharge is equal to zero and the electricity $E_{batt}(t)$ entering the batteries is computed as follow:

$$E_{batt}(t) = \min(c_{max}, \eta_c \min(C_{conv}, E_{pot}(t) - l_{tot}(t))) \tag{2.7}$$

where C_{conv} [kW] and $\eta_c = 0.95$ are the capacity and the efficiency of the converter, respectively. Vice-versa, if electricity is needed to cover the load, the charge is equal to zero and the electricity outgoing from the batteries is computed as follow:

$$E_{batt}(t) = \min(d_{max}, \frac{1}{\eta_c} \min(C_{conv}, l_{tot}(t) - E_{pot}(t))) \tag{2.8}$$

The capacity C_{conv} of the converter is set to 25% of the capacity of the storage system C_b.
Once computed $E_{batt}(t)$, the state of charge of the batteries is updated according to the following equation:

$$s_b(t+1) = \begin{cases} s_b(t) + E_{batt}(t)\sqrt{\eta_b}, & \text{if } (E_{pot}(t) - l_{tot}(t)) > 0 \\ s_b(t) - \frac{E_{batt}(t)}{\sqrt{\eta_b}}, & \text{if } (E_{pot}(t) - l_{tot}(t)) < 0 \end{cases} \tag{2.9}$$

2.1.4 Diesel generation

In this model we assume that the 5 diesel generators are managed to cover the difference between the total electrical load $l_{tot}(t)$ and the sum of the discharge from the batteries $E_{batt}(t)$ and the renewable power potential $E_{RES}(t) = E_{PV}(t) + E_{wind}(t)$. However, to ensure the stability and reliability of the grid and to efficiently operate the generators, the following constraints, provided by the Ustica power company, are considered:

- *Minimum operating power.* When a generator is switched on, its electricity output has to be at least 20% of its nominal capacity.
- *Minimum functioning time.* Each generator, when switched on, has to work for at least 2 hours.
- *Schedule.* This constraint defines the periods when each generator has to be switched on.

- *Operating capacity.* At each time step, the diesel generators, together with the storage system, have to ensure an operating capacity defined as a function of the total electrical load $l_{tot}(t)$, the PV electricity output $E_{PV}(t)$, and the wind electricity output $E_{wind}(t)$:

$$OC(t) = l_{tot}(t) + k_l l_{tot}(t) + k_{PV} E_{PV}(t) + k_w E_{wind}(t) \tag{2.10}$$

  where $k_l = 0.05$, $k_{PV} = 0.25$ and $k_w = 0.5$.

The total diesel electricity output $E_d(t)$ is thus the sum of the electricity output of each diesel generator, which is computed according to the above mentioned strategy and constraints. The fuel requirements to generate $E_d(t)$ are computed based on efficiency curves specific to each diesel generator, provided by the Ustica power company.

2.1.5 Water system

The model of the water system is composed of a desalination plant with a maximum operating capacity of 70 m^3/h, which feeds an equivalent reservoir of 11,000 m^3. The equivalent reservoir (see Figure 2.2) has a storage capacity equal to the sum of the capacities of the existing reservoirs and a maximum release equal to the sum of their maximum releases. The reservoir storage dynamics are modelled with the following mass balance equation:

$$s(t+1) = s(t) + w_{des}(t) - r_w(t) \tag{2.11}$$

where s is the storage of the reservoir, $w_{des}(t)$ is the water produced by the desalination plant and $r_w(t)$ is the release from the reservoir, which is computed as follows:

$$r_w(t) = \min(s(t), d_w(t))) \tag{2.12}$$

where $d_w(t)$ is the water demand. This means that the water demand $d_w(t)$ can be entirely satisfied whenever enough water is stored in the equivalent reservoir. In all the other cases, the entire water volume stored in the reservoir is released and a water supply deficit occurs.

All the analysis and the experiments performed in this thesis are based on the system model presented in this section, which has been implemented considering the technical parameters reported in Table 2.1, and the following simulation parameters, set according to the EU reference scenario 2016 (EC, 2016):

- H [years] = 25: project horizon;
- γ' [%] = 2.5: annual nominal discount rate;
- φ [%] = 1: annual inflation rate;

- C_f [€/l] = 0.54: base fuel cost;
- ΔC_f [%] = 4: annual fuel cost increment.

Table 2.1: *Budget and technical simulation parameters.*

Electricity system				
Component	**Lifetime**	**Capital cost**	**Replacement cost**	**Operational cost**
Photovoltaic (PV)	25 y	1150 €/kW	1150 €/kW	50 €/kW/y
Wind turbines	25 y	3500 €/kW	3500 €/kW	5000 €/unit/y
Batteries	3000 kWh/y	500 €/kWh	500 €/kWh	500 €/kWh/y
Converter	25 y	300 €/kW	300 €/kW	-
Diesel generators	60000 h	400 €/kW	400 €/kW	50 €/kW/h
Electricity grid	-	-	-	950000 €/y
Water system				
Component	**Capacity**	**Max production**	**Max release**	**Initial state**
Desalination plant	-	70 m^3/h	-	-
Equivalent reservoir	11000 m^3	-	300 m^3/h	2000 m^3

The electricity system parameters are directly provided by the Ustica power company and the Italian energy authority (AEEGSI, 2014), while the water system parameters are provided by the Ustica municipality. The lifetime of each technology is expressed in years, except for the batteries. In this case, the lifetime is expressed in terms of throughput, namely the amount of energy that cycles through the storage bank in one year.
It is worth noting that for reducing the computational costs of the performed experiments, the system is explicitly simulated over a 1-year hourly horizon considering a reference year of the main external drivers and assuming that system operation does not change from one year to the next over the project horizon. Details on how the reference year is defined for the natural drivers (i.e., solar radiation, wind speed and temperature) are provided in each of the following chapters. Non-water electrical load and the load of the desalination plant comes from an average year computed from data provided by the Ustica power company for the period 2016-2017. Water demand has been instead reconstructed starting from the load of the desalination plant and the water distribution rules provided by the Ustica municipality.

3

A dynamic, multi-objective approach for identifying optimal system designs and operations

Abstract[1]

Small Mediterranean islands are remote, off-grid communities characterized by carbon intensive electricity systems coupled with high energy consuming desalination technologies to produce potable water. In this chapter, we propose a novel dynamic, multi-objective optimization approach for improving the sustainability of small islands through the introduction of renewable energy sources and the identification of optimal strategies for the desalination plant operations. The main contributions of our approach include: (i) dynamic modelling of desalination plant operations, (ii) joint optimization of system design and operations, (iii) multi-objective optimization to explore trade-offs between potentially conflicting objectives. We test our approach by comparing it with a traditional non-dynamic, least cost optimization approach. Numerical results show the effectiveness of our approach in identifying optimal system configurations, which outperform the traditional design with respect to different sustainability indicators, limiting the structural interventions, the investment costs and the environmental impacts. In particular, the optimal dynamic solutions able to satisfy the whole water demand allow high levels of penetration of renewable

[1] Giudici, F., Castelletti, A., Garofalo, E., Giuliani, M., Maier, H. R., 2019a. Dynamic, multi-objective optimal design and operation of water-energy systems for small, off-grid islands. Applied Energy 250, 605–616

energy sources (up to more than 40%) to be reached, reducing the present value of costs by about 2-3 M€ and the CO_2 emissions by more than 200 tons/y.

3.1 Introduction

Water supply and energy generation are two essential services that any community has to securely provide to succeed in development and sustainability goals (Chester, 2010; Bogardi et al., 2012). Even if traditionally considered as separate and disconnected (Santhosh et al., 2014), water and energy systems are intrinsically coupled (Olsson, 2015). Large amounts of energy are needed for extraction, treatment, conveyance, and distribution of water and wastewater (Pate et al., 2007). Conversely, significant volumes of water are withdrawn and consumed for energy generation processes such as fuel production, thermoelectric cooling, and hydropower generation (Macknick et al., 2012).
This nexus between water and energy (Lubega and Farid, 2014) implies that decisions made in one domain might affect positively or negatively the other, and vice-versa, over different spatio-temporal scales (Scott et al., 2011) and multiple dimensions (e.g., environmental, economic, technological, social) (Hamiche et al., 2016). These implications become amplified when global trends, such as growth in total and per capita demand of both water and energy, climate change, and the increasing pressure of droughts, strengthen the interactions between water and energy systems, negatively impacting their reliability and sustainability (Scott et al., 2015).

In remote, off-grid communities, these issues are further intensified by the unique and specific challenges typical of closed and disconnected systems (Beal et al., 2016) such as geographic isolation, high cost of supply, and highly variable water and energy demand (Kaygusuz, 2011; Mohtar and Lawford, 2016).
As already mentioned in Chapter 1, small islands, such as those found in the Mediterranean Sea, represent a paradigmatic example of remote, off-grid communities, where water supply and electricity generation are strictly interconnected (Singal et al., 2007; Patlitzianas and Christos, 2012), and the distance from the mainland, the lack of potable water sources and the high variability of both water and electricity demand generate a large number of pressing issues (Douglas, 2006; Karagiannis and Soldatos, 2007; Ciriminna et al., 2016). The electricity system relies on stand alone, carbon intensive diesel generators (Duić and Da Graça Carvalho, 2004; Patlitzianas et al., 2007), which are usually sized to meet the peaking summer electricity demand driven by high touristic fluxes (Kristoferson et al., 1985), and thus turn out to be oversized for the rest of the year. The high dependence upon remote supply of fuel and the need for backup storage to cover possible refuelling delays (e.g., due to bad weather con-

ditions) make the operation of these systems very costly and inefficient (Kakazu, 1994; Weisser, 2004; Palone et al., 2017). In addition, balancing electricity supply and demand is challenged by the structural lack of flexibility of off-grid systems in modulating the high seasonal variability of electricity demand (Larsen et al., 2014). The pressure on this unsustainable electricity system is further increased by water supply system operations Voivontas et al. (2003); Kaldellis et al. (2012). The lack of accessible and safe water sources has resulted in the adoption of desalination technologies to produce potable water in many islands (Kaldellis et al., 2004), which in the past was usually transported with tank vessels from the mainland. These technologies are in some cases able to meet the entire water demand, though usually consuming large amounts of electricity (Kalogirou, 2005). With an electrical consumption that ranges between 7-14 and 2-6 kWh/m^3 for thermal and membrane based technologies, respectively (Ghalavand et al., 2015), the entire desalination process might account for up to 30% of the total electrical load of a small island. Moreover, high electrical consumption, combined with a costly and inefficient electricity system, increase water production cost, which varies from 7 to 10 €/m^3, about ten times that on the mainland.

In recent years, several studies have provided guidelines and suggestions to improve the sustainability and efficiency of the water and energy supplies of these remote, off-grid communities. A common approach, widely adopted in the literature, is to optimally design a hybrid energy system, which combines renewable electricity generation (e.g., wind, solar) with conventional power sources (e.g., diesel generators) and storage technologies (Ekren and Ekren, 2009; Ibrahim et al., 2010; Erdinc and Uzunoglu, 2012). Among these latter, several studies explore pumped-storage as a solution to maximize RES penetration and consequently improve the overall sustainability of the water-energy system (Caralis and Zervos, 2007; Papaefthymiou et al., 2010; Chalakatevaki et al., 2017). This well established technology allows the exploitation of RES electricity surplus by pumping water to be stored in an upstream reservoir and released for hydropower when electricity is needed (Koutsoyiannis et al., 2009). Different system configurations are comparatively evaluated in order to identify the one that is able to meet load requirements by minimizing the present value of costs over a given project horizon (Ter-Gazarian and Kagan, 1992; Mizani and Yazdani, 2009; Anglani and Muliere, 2010). The optimal design problem thus consists of a least cost single-objective optimization problem, which can be solved using different methods, ranging from commercial software packages such as HOMER (Rehman et al., 2007; Shaahid and Elhadidy, 2007) to more complex optimization techniques, such as genetic algorithms (Koutroulis et al., 2006; Yang et al., 2009), ant colony (Dong et al., 2016) and particle swarm optimiza-

tion (Hakimi et al., 2007; Mohamed and Eltamaly, 2018).

Other applications directly address the water-energy nexus by optimally designing both desalination and renewable energy units, exploring different simple and hybrid configurations (Spyrou and Anagnostopoulos, 2010; Bourouni et al., 2011) and evaluating their effects on water production costs (Mentis et al., 2016). Although a wide range of studies focuses on the optimal sizing of the electricity and water system components, only few works deal with the optimization of system operations (Santhosh et al., 2014; Clarke et al., 2015). Each electricity system component is in fact usually managed using static, pre-defined operating strategies, which define priority rules for power allocation (Elbaset, 2011; Luna-Rubio et al., 2012). The desalination plant operation is modelled statically using a fixed electrical load as a surrogate of the actual water demand supplied by the desalination plant through the water distribution network (Kaldellis et al., 2006). Since real water distribution networks are usually composed of reservoirs, which can store and delay the movement of water, the above mentioned electrical load can generally provide a good representation of the actual water demand on a monthly or annual time scale, but it is not suitable to capture daily or hourly dynamics. In some cases, the storage capacity of the water distribution network is implicitly modelled considering a deferrable desalination load in order to exploit the renewable electricity surplus generated (Setiawan et al., 2009; Bognar et al., 2012; Segurado et al., 2016).

The main limitations of current state-of-the-art optimal design approaches thus include the lack of an explicit representation of the water system (i.e., the reservoir dynamics are not modelled explicitly), the use of non-dynamic modelling of the desalination plant operation (i.e., fixed operating rule) and the adoption of a single pure economic objective (i.e., present value of costs) to solve the optimization problem, which prevent the consideration of additional sustainability aspects (e.g., RES penetration, CO_2 emissions, reliability of the water supply system).

In order to overcome these limitations, in this chapter we propose a novel dynamic, multi-objective (MO) approach to optimally identify more efficient system configurations. The main contributions of our approach include: (i) dynamic modelling of desalination plant operations to explore the impacts that RES introduction coupled with different demand side management strategies may have on both electricity and water systems, (ii) joint optimization of system design and its operations that allows the interdependency between planning and management to be addressed directly by automatically identifying the most efficient operating policies associated with each optimal system configu-

ration, (iii) multi-objective optimization to explore trade-offs between potentially conflicting objectives, which include, apart from present value of costs, additional aspects related to RES penetration and water supply efficiency. We assess the potential of our approach by means of a comparative analysis with the traditional non-dynamic, single-objective (SO) approach. In particular, we first focus on quantifying the advantages of dynamically modelling the desalination plant operation given a fixed system configuration (i.e., fixed RES capacity). Then, we concentrate on the identification of the optimal system design, showing the benefits of jointly considering the interdependency between system design and operation within the optimization process. In both cases, we also discuss the advantages of considering multiple potentially conflicting objectives rather than focusing on a single pure economic one.

3.2 Methods and Tools

We compare our dynamic MO approach (Figure 4.1b) with a traditional non-dynamic SO optimization (Figure 4.1a) to identify the optimal installable RES capacity on Ustica island. Both methods adopt a simulation-based optimization scheme, where the integrated model presented in Chapter 2 is repeatedly run for different values of the decision variables until the optimal solution, or the set of Pareto optimal solutions, is found.
The traditional SO approach is characterized by a single planning decision variable, namely the PV capacity C_{PV}, which is defined within the following feasibility set: $C_{PV} \in [0, C_{PV,max}]$, where $C_{PV,max} = 4000$ kW is the maximum PV installable capacity. For our specific case study, this value is large enough to allow all the feasible planning solutions to be explored within the optimization phase.
Our MO approach adds an additional control variable $w_{des}(t)$, which defines the desalination plant water production at each time step as a function (called control policy) of different inputs (see section 3.2.2 for further details). This control variable can vary within the following feasibility set: $w_{des}(t) \in [0, C_{des}]$, where $C_{des} = 70\ m^3/h$ is the maximum capacity of the desalination plant. It is worth noting that, due to the strong limitations associated with the maximum installable RES capacity discussed in Chapter 2, in this work we do not consider the number of wind turbines n_w as a planning decision variable but we fixed $n_w = 4$ for both the approaches analyzed. This allows the wind potential of the island to be exploited respecting the environmental constraints. In addition, in order to better assess the benefits of operating the desalination plant as a non-conventional storage technology, we do not consider the introduction of batteries in our analysis.

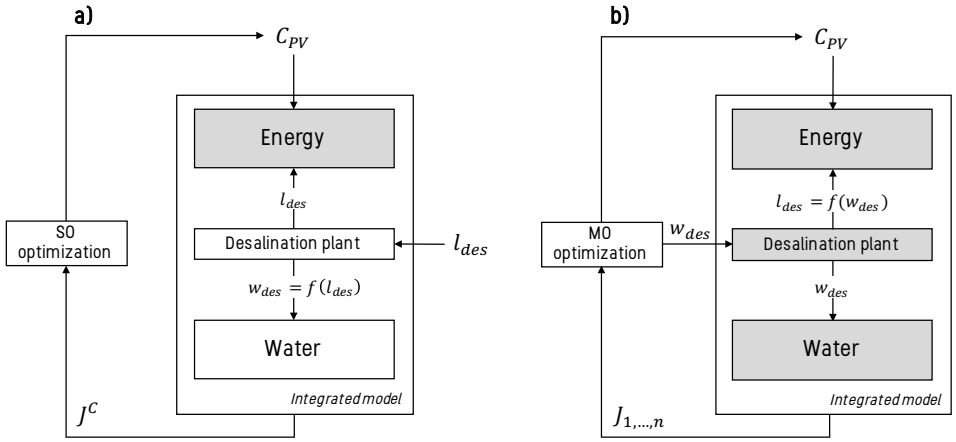

Figure 3.1: *Schematization of the non-dynamic, single-objective (a) and the dynamic, multi-objective (b) optimization approaches. Grey boxes within the system model box represent the system components active in the optimization process.*

3.2.1 Non-dynamic, single-objective optimization approach

The non-dynamic, single-objective optimization approach optimizes the electricity system configuration (i.e., PV capacity) with respect to the present value of costs only, considering a pre-defined static operating strategy for the desalination plant (i.e., a fixed observed electrical load $l_{des}(t)$). This strategy reflects the historical management of the desalination plant, which has been operated for the only purpose of satisfying water demand. The optimization problem is thus characterized by the following objective function (to be minimized), in which all costs occurring at each hour t throughout the simulation horizon are aggregated on a yearly basis y:

$$J^C = C^{cap} + \sum_{y=1}^{H} \delta(y)(C^{grid} + C^{oper}(y) + C^{rep}(y) + C^{sal}(y)) \qquad (3.1)$$

where H is the number of years of the simulation horizon, C^{cap} are the capital costs, C^{grid} are the costs for the management of the electricity grid, and $C^{oper}(y)$, $C^{rep}(y)$, $C^{sal}(y)$ are the operational, replacement and salvage costs at year y, respectively. All costs, except the capital ones, are discounted using the following time varying coefficient:

$$\delta(y) = \frac{1}{(1+\gamma)^y} \qquad (3.2)$$

where γ is the real discount rate, calculated as a function of the nominal discount rate γ' and the inflation rate φ. The capital costs occur at the beginning of

the simulation horizon and represent the investment to install the power technologies, the replacement costs occur when a technology has to be substituted, and the salvage costs are negative costs which are incurred at the end of the simulation horizon, when one or more technologies have not reached the end of their lifetime. It is worth noting that the lifetime of the RES technologies is completely independent from their actual electricity production, since we suppose their wear does not depend on the hours of operation. This dependence is instead considered for diesel generators, the management of which strongly affects costs. Finally, the operational costs take into account both the cost to produce 1 kWh of electricity and the cost of maintenance of each power technology. Moreover, diesel generator costs also include the cost of fuel.
The single-objective optimization problem is formulated as follow:

$$C_{PV}^{*} = \arg\min_{C_{PV}} J^{C} \tag{3.3}$$

where C_{PV} (kW) is the PV capacity and J^{C} is defined by 5.2.
We solve problem 3.3 using an exhaustive search within the feasibility set of the C_{PV} decision variable, which has been sampled with a 100 kW discretization step. It is worth noting that, for our specific case study, this discretization step is sufficiently fine to allow significant changes in the objective function to be captured.

3.2.2 Dynamic, multi-objective optimization approach

The dynamic, multi-objective optimization approach conjunctively optimizes both the planning (i.e., PV capacity) and the management (i.e., desalination plant operation) of the integrated water-electricity system. The desalination plant is controlled using a closed-loop control policy p, which determines the control decision variable $w_{des}(t)$ as follows: $w_{des}(t) = p(I(t))$, where $I(t)$ is an input vector, which has to include at least the state of the system $s(t)$ (i.e., the storage of the equivalent reservoir in our case). It is worth noting that optimizing a closed-loop control policy instead of performing an open loop optimization of the sequence of controls over the simulation horizon allows to both reduce the number of parameters to be optimized and ensure adaptability with respect to the uncertainty in the external drivers (e.g., wind speed, solar radiation, water and electricity demand). The dependence upon the state of the system provided by the closed-loop control policy allows the control variable to be modulated based on changes in the state of the system due to changes in the external drivers. Further details on the generation of the closed-loop optimal policy are provided at the end of this section.
This dynamic, multi-objective approach considers multiple, potentially conflicting objectives beyond the total cost:

1. **Present value of costs (J^C)** (to be minimized). This is the same as that adopted in the SO optimization, even if here it is influenced by both the planning variable C_{PV} and the control variable $w_{des}(t)$, as changes in water production significantly affect the total electrical load and consequently power generation.

2. **Electricity surplus (J^E)** (to be minimized), defined as the mean annual difference between the total potential electricity output $E_{pot}(t)$ (MWh) and the total electrical load $l_{tot}(t)$ (MWh) as defined by the following equation:

$$J^E = \frac{1}{H} \sum_{t=1}^{T} (E_{pot}(t) - l_{tot}(t)) \tag{3.4}$$

   where H and T are the number of years and hours of the simulation horizon, respectively.
   Since the electrical load has to be always covered according to the model constraints, the difference between the potential electricity output and the total load represents a RES surplus that is higher than or equal to zero at each time step. Minimizing this surplus through the control of the electrical load corresponds to maximizing the RES penetration exploiting the RES power potential.

3. **Water deficit (J^W)**, defined as the mean annual squared water deficit ($(m^3/s)^2$/year), i.e.:

$$J^W = \frac{1}{H} \sum_{t=1}^{T} (d_w(t) - r_w(t))^2 \tag{3.5}$$

   where $r_w(t)$ (m^3/s) is the release from the equivalent reservoir and $d_w(t)$ (m^3/s) is the water demand. Since the release is always set equal to the water demand, a deficit can occur only when the demand is higher than water availability (i.e., reservoir storage). The squared power penalizes high deficits occurring in a single time step and allows high-impact shortage water events to be avoided (Hashimoto et al., 1982). To minimize this objective, the desalination plant has to be managed in order to ensure that enough water is available to satisfy the demand.

The MO optimization problem is thus formulated as follow:

$$C^*_{PV}, p^* = \arg \min_{C_{PV}, p} |J^C J^E J^W| \tag{3.6}$$

Within the optimization process, the operating policy p provides the control $w_{des}(t)$, which determines the amount of water the desalination plant has to produce at each time step t. Given $w_{des}(t)$, the simulation model computes

the electrical load of the desalination plant $l_{des}(t)$ using a linear function with angular coefficient equal to 6 kWh/m^3, as defined in Chapter 2.
We solve the optimization problem given in 3.6 using an evolutionary multi-objective direct policy search approach (EMODPS) (Giuliani et al., 2016). This approach transforms the optimal control problem into a planning one by parameterizing the control policy p_θ with $\theta \in \Theta$ within a pre-defined class of functions and exploring the parameter space through multi-objective evolutionary algorithms (Coello Coello et al., 2007; Deb, 2011; Maier et al., 2019), in order to identify a set of Pareto approximate policies (Quinn et al., 2017; Salazar et al., 2017). Using this approach, the planning and management optimization problem given in 3.6 can be solved by jointly evolving solutions in a complex search space formed by the parameters θ of the control policy and the planning decision variable C_{PV} within a single optimization process.
In this work, we adopt the multi-objective evolutionary algorithm Borg MOEA (Hadka and Reed, 2013) and we parameterize the operating policy by means of a universal approximating network, namely the Gaussian radial basis functions (Busoniu et al., 2011), in order to ensure high flexibility of the control policy structure. We provide further details about the optimization setup in the next section.

3.3 Experiment settings

Within the dynamic MO approach, the operating policy p_θ of the desalination plant is parameterized by means of a weighted sum of non-linear Gaussian radial basis functions, which determine the control $w_{des}(t)$ at each time step as follows:

$$w_{des}(t) = \beta + \sum_{i=1}^{N} w_i \varphi_i(I(t)) \tag{3.7}$$

where N is the number of basis function $\varphi(\cdot)$, β is the linear parameter associated with the control variable $w_{des}(t)$, and w_i is the non-negative weight of the i-th basis function ($w_i \geqslant 0, \forall i$). Each single basis function is defined as follows:

$$\varphi_i(I(t)) = \exp\left[-\sum_{j=1}^{M} \frac{[(I(t))_j - c_{j,i}]^2}{b_{j,i}^2}\right] \tag{3.8}$$

where M is the number of policy inputs $I(t)$, c_i and b_i are the M-dimensional center and radius vectors of the i-th basis function. In particular, the centers must lie within the input bounded space and the radii must be strictly positive. The parameters vector used to parameterized the control policy is defined as $\theta = [c_{j,i}, b_{j,i}, w_i, \beta] \in \mathbb{R}^{n_\theta}$ where $i = 1, \ldots, N$, $j = 1, \ldots, M$. In this

work, we condition the control policy upon the following four input variables: hour of the day, day of the week, week of the year, and time-varying storage of the equivalent reservoir. In this way, we can capture all the dynamics affecting the system at different temporal scales, namely water, electricity demand and RES power variability. Considering N = 9 and M = 4, the total number of parameters to be optimized is equal to 101 (i.e., 100 parameters of the control policy and 1 planning parameter representing the PV capacity C_{PV}). It is worth noting that this approach allows the number of variables to be optimized to be reduced significantly compared with optimizing the sequence of control variables step-by-step within an open loop optimization process, as the parameters of the control policy are completely independent from the length of the simulation horizon considered.
The reference year of the external drivers used to perform the optimizations comes from an averge year computed from historical data. In particular, incident solar radiation comes from experimental measurements conducted by the Italian company RSE S.p.A for the period 2011-2015 in Catania (Sicily). Wind speed at the anemometer and temperature are provided by measurements registered at a meteorological station located in Ustica for the period 2011-2015.

The results of the comparison between the traditional and our approach are visualized in terms of optimization objectives (i.e., present value of costs, electricity surplus and water deficit) and system trajectories (e.g., RES power, water production, reservoir storage). Moreover, in order to evaluate the solutions with respect to other sustainability aspects not directly included in the optimization process, we also compute these additional indicators:

1. **RES penetration** (%). This indicator represents the percentage of the total electrical load covered by RES power over the entire project horizon.
2. **Fuel consumption** (liters/y). This indicator is calculated through specific efficiency curves, which define the fuel consumed by each diesel generator as a function of its electricity output.
3. **CO_2 emissions** (tons/y). This indicator is computed by multiplying the total fuel consumption for an empirical coefficient, which defines the CO_2 emissions per liter of fuel consumed.

3.4 Numerical results

The main goal of this work is to numerically quantify the advantages of using a dynamic MO approach (see section 3.2.2) to optimize the RES planned capacity of remote, off-grid islands with respect to adopting a traditional non-dynamic SO approach (see section 3.2.1). More precisely, we want to assess the benefits

of (i) dynamically modelling the desalination plant operation through an explicit representation of the whole water supply system, (ii) jointly considering the interdependency between system design and its operation within the optimization process, (iii) considering multiple, potentially conflicting, optimization objectives. In doing so, we first focus on a pre-defined system design in order to assess the advantages of dynamically modelling the desalination plant operation (section 3.4.1), and then we concentrate on the identification of the optimal RES planned capacity, exploring the benefits of considering the interdependency between planning and management within the optimization phase (section 3.4.2).

3.4.1 Dynamic vs non-dynamic water-energy system operations

To quantitatively assess the advantages of dynamically modelling the desalination plant operation, we compare our dynamic MO approach with the non-dynamic SO one for a pre-defined system design (i.e., 1200 kW of PV). In this case, we generate the dynamic solutions by solving the problem given in 3.6 for $C_{PV} = 1200$ kW, and the non-dynamic solution by simulating the system, for the same PV capacity, using a fixed observed electrical load to represent the desalination plant operation.

Figure 3.2 shows the Pareto optimal dynamic solutions (circles) and the non-dynamic one (diamond) in the space of the objectives. The x-axis represents the objective J^C, the y-axis shows the objective J^E, and the color corresponds to the value of the objective J^W. The arrows identify the direction of preference of each objective. The ideal solution would be a blue point in the bottom left corner of the figure. The non-dynamic solution is able to satisfy the entire water demand but is dominated by almost all dynamic solutions with respect to the other objectives. More precisely, all dynamic solutions have a lower cost and about 90% of them are also characterized by lower electricity surplus. The non-dynamic solution reflects, in fact, the historical management of the system. In particular, since the electricity system was entirely composed of diesel generators and, consequently, the electricity cost was constant in time, the desalination plant has been operated only for the purpose of satisfying the water demand.
The dynamic solutions explore the whole range of variability of the objectives as a consequence of changes in the desalination plant operation. The optimal policies outline a clear conflict between the objectives as high cost solutions present low electricity surplus and low water deficit. This trade-off can be explained by analyzing three different alternative solutions: the extreme solution that minimizes the cost (best cost solution) and two solutions that minimize the electricity surplus but present different values of water deficit (best surplus so-

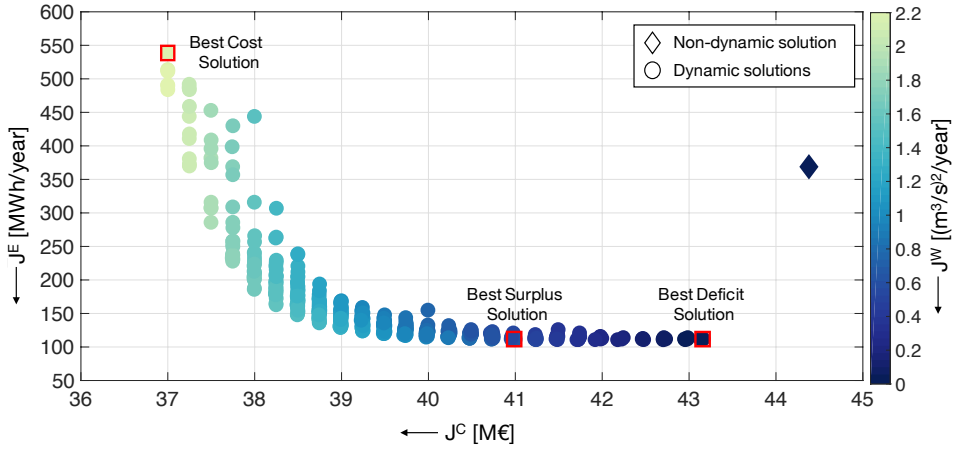

Figure 3.2: *Visualization in the space of the optimization objectives of the non-dynamic and the dynamic solutions obtained by fixing the PV capacity to 1200 kW. Dark blue points represent solutions with low water deficit. Light green points represent solutions with high water deficit. Squares are the solutions analysed in Figure 3.3.*

lution and best deficit solution).

Figure 3.3 visualizes these operating policies projecting the control decision $w_{des}(t)$ (i.e., water production) as a function of the hours of the day with the colors illustrating how the control decision changes depending on RES power. Blue points refer to time periods when electricity is produced by diesel generators only, whilst yellow points indicate hours of the day when RES power is equal to or higher than the electricity needed to operate the desalination plant at its maximum capacity (i.e., 420 kWh). Top and bottom panels refer to winter (November - April) and summer (May - September) periods, respectively.
To minimize the present value of costs (best cost solution), the desalination plant is operated to reduce water production and, consequently, the total electrical load in both winter and summer. This prevents the system from entirely satisfying the water demand, causing the highest water deficit. Moreover, the RES power cannot be exploited, leading to the highest electricity surplus. It is worth noting that water production is not always zero, but assumes higher values only when high RES power allows water to be produced without increasing the costs (i.e., no diesel generation). The best surplus solution minimizes the electricity surplus by modulating the desalination plant operation in order to exploit RES power. The maximum feasible water production is thus observed in the middle hours of the day (from 9 am to 4 pm), when the high solar potential significantly increases the PV electricity output. A higher overall water production

leads to a lower water deficit with respect to the best cost solution. However, the consequent higher load results in an increase in present value of costs due to the operating capacity constraint, which forces the diesel generators to be activated proportionally to the total electrical load and the RES power output (see Chapter 2 for details). All alternatives that represent a lower water deficit than

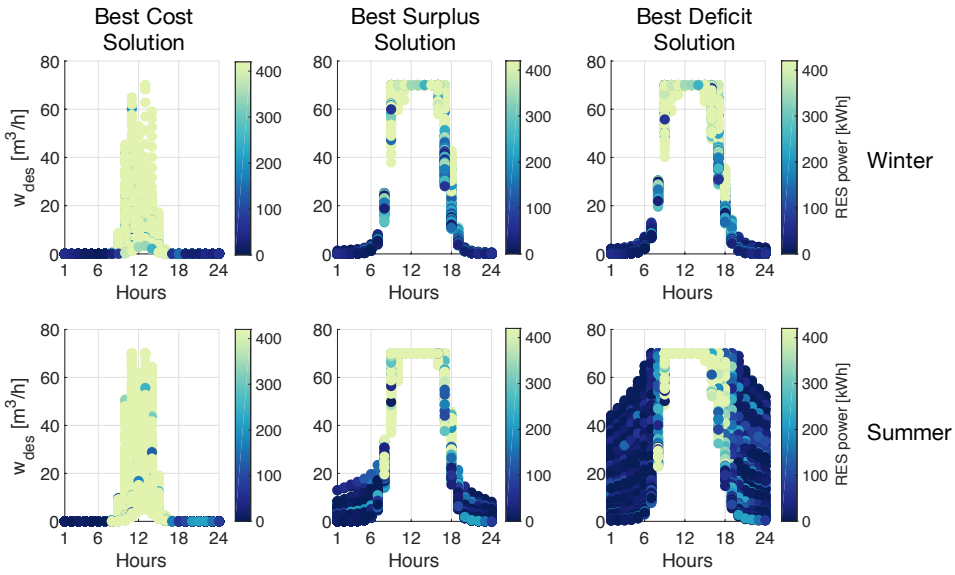

Figure 3.3: *Policy visualization of the three dynamic solutions highlighted in Figure 3.2. The control decision (i.e., water production) is projected as a function of the hours of the day with the color illustrating how the control decision changes depending on the RES power. Blue points refer to hours when electricity is produced by diesel generators only, whilst yellow points indicate hours when RES power is equal to or higher than the electricity needed to operate the desalination plant at its maximum capacity.*

the best surplus solution are characterized by the same electricity surplus and an increasing present value of costs: the desalination plant already operates at its maximum capacity in the middle hours of the day preventing the high RES power to be fully exploited; water is thus produced in other periods, relying on diesel generators to satisfy the water demand. In particular, when analyzing the operating policy that minimizes the water deficit (best deficit solution), two different operating strategies can be observed: in winter (top panel) a lower water demand allows production in the middle hours of the day only, relying on available storage capacity to satisfy the demand at every time step; in summer (bottom panel), the higher water demand forces the system to increase water production also when RES power is not available, with a consequent increase in operating costs.

In order to better understand the advantages of dynamically controlling desalination, the best deficit solution is directly compared to the non-dynamic solution in terms of water system trajectories, as both are able to satisfy the entire water demand. Figure 3.4a-c shows the temporal dynamics of water production (a), storage of the equivalent reservoir (b), and release from the equivalent reservoir (c) on daily time scale over a reference year. It is worth noting that the

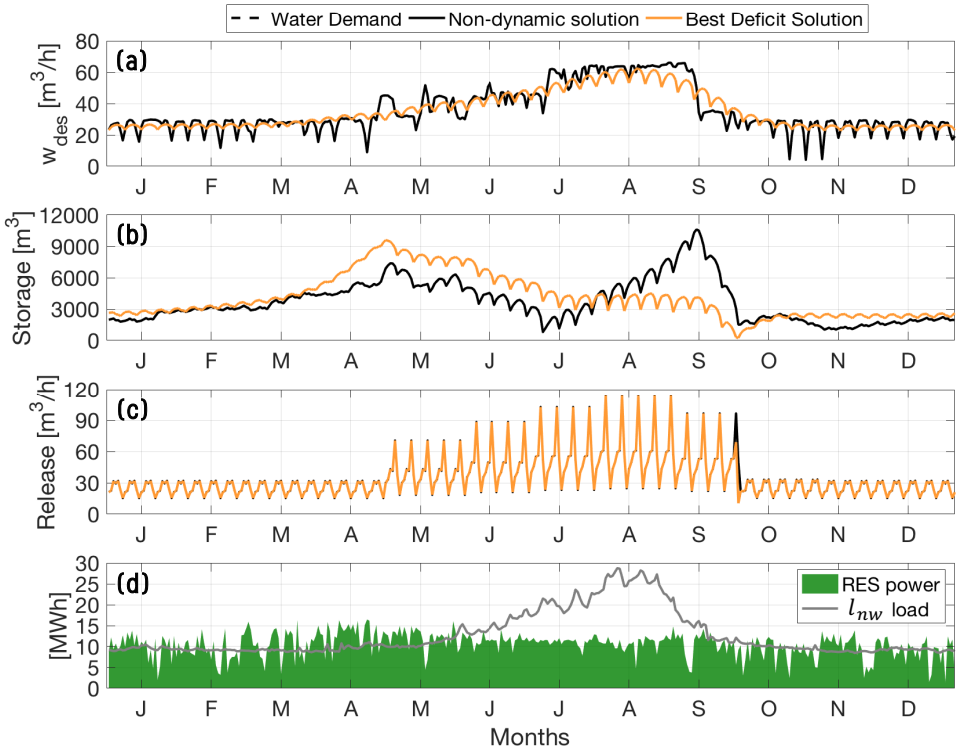

Figure 3.4: *Daily trajectories of water production (a), storage of the equivalent reservoir (b), release from the equivalent reservoir (c), non-water electrical load* l_{nw} *and RES power (d) over a reference year.*

best deficit solution modulates water production in order to fill up the reservoir at the beginning of the summer season (April/May), exploiting the storage to satisfy the high water demand during the summer months (Figure 3.4a-b). This operating strategy almost completely satisfies the water demand (Figure 3.4d) in each period of the year by reducing both the electricity surplus and present value of costs with respect to the non-dynamic solution (Figure 3.2). The lower base electrical load observed in winter (Figure 3.4d) allows the RES power to be exploited, operating the desalination plant as a non-conventional storage technology in order to both satisfy the water demand and fill the reser-

voir. In particular, the storage significantly increases from March to May (Figure 3.4b), when the RES power peak is registered. The water stored in these months contributes to partially cover the summer water demand, which can be thus satisfied by reducing water production from the desalination plant in the months when the non-water electrical load l_{nw} entirely exploits the RES power (from June to September) (Figure 3.4d).
The non-dynamic solution highlights a completely different operating strategy. In this case, the water demand is the only driver of desalination plant operation. The storage peak is observed at the end of the summer season (Figure 3.4b) and a significant increase in water production is recorded during the months with higher water demand (July and August) (Figure 3.4a).

A quantitative comparison between the best deficit solution and the non-dynamic solution is finally performed in terms of different sustainability indicators (Table 3.1). The first two indicators represent the optimization objectives adopted

Table 3.1: *Sustainability indicators computed for the non-dynamic solution and the best deficit solution.*

	Non-dynamic Solution	**Best Deficit Solution**
Present value of costs (M€)	44.4	43.2
Electricity surplus (MWh/y)	368.8	111.9
Fuel consumption ($l*10^6$/y)	1.1	1.0
CO_2 emissions (tons/y)	2909	2739
RES penetration (%)	33.7	37.6

to identify the dynamic solutions. The best deficit solution outperforms the non-dynamic solution reducing the present value of costs of 1.2 M€ and the electricity surplus of about 257 MWh/year (more than 80% of the electricity surplus obtained by the non-dynamic solution). Focusing on the other sustainability indicators defined in section 5.3, the best deficit solution is able to reduce the fuel consumed of 100,000 liters per year and the CO_2 emissions of 170 tons/year. Finally, exploiting the RES power significantly increases the RES penetration from 33.7% to 37.6%.

3.4.2 Interdependency between water-energy system design and operations

In this section, our dynamic MO approach is compared to the non-dynamic SO one in order to assess the advantages of exploring the interdependency between system design and its operations to identify the optimal installable PV capacity. We generate the dynamic solutions by solving the problem given in 3.6, and the non-dynamic solution by solving the problem given in 3.3.

Figure 3.5 shows the dynamic (circles) and the non-dynamic (diamond) optimal solutions in the space of the optimization objectives. Arrows identify the direction of preference of each objective and the marker size represents the value of the planning decision (i.e., PV capacity). The traditional approach optimizes the

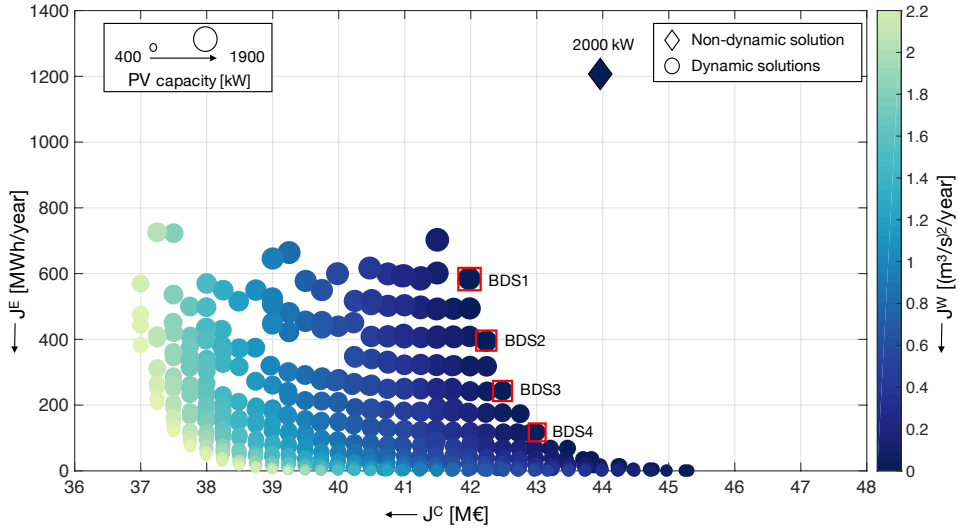

Figure 3.5: *Visualization in the space of the optimization objectives of the dynamic solutions (circles) and the non-dynamic solution (diamond). The marker size illustrates the value of the planning decision (i.e., PV capacity) and the circles highlighted in red represent 4 dynamic solutions we directly compare to the non-dynamic solution. Dark blue points represent solutions with low water deficit. Light green points represent solutions with high water deficit.*

PV capacity by minimizing the present value of costs (J^C) over the project horizon. As discussed in the previous section, this approach simulates the system using the historical desalination plant operation, which always satisfies the entire water demand (i.e., zero deficit) regardless of the PV capacity installed. This non-dynamic system operation leads to an oversized optimal design, which underperforms compared with the dynamic solutions with respect to both present value of costs and electricity surplus. In particular, all dynamic solutions obtain lower electricity surplus and more than 90% of them also show lower present value of costs.

Our approach is in fact able to capture the interdependency between planning and management, automatically generating alternative closed-loop operating policies for each Pareto optimal PV capacity, which explore the trade-off between the optimization objectives, by modulating the desalination plant operation (see section 3.4.1).

The dynamic solutions show that present value of costs (J^C) decreases with an

increase in installed PV capacity. This can be explained by the fact that present value of costs considers, in addition to the capital costs, also the operational costs of the system: a significant reduction in operational costs due to higher RES power production (and consequently lower diesel generation) is able to compensate for an increase in capital costs associated with installing higher PV capacity. However, the lower the present value of costs, the higher the electricity surplus (J^E). The increasing electricity surplus associated with higher PV capacity demonstrates, in fact, that the RES contribution towards the total electrical load decreases with an increase in PV capacity. Over 1900 kW, almost all the increasing RES power would be surplus and the small operational cost reduction would not be able to compensate for the capital cost increase, generating dominated solutions (not shown). It is worth noting that the dynamic solution characterized by the maximum PV capacity (1900 kW) is lower than the optimal non-dynamic PV capacity (2000 kW). Moreover, focusing on the dynamic solutions that minimize the water deficit (blue circles), a strong reduction of both present value of costs and electricity surplus is observed by installing a significantly lower PV capacity.

Table 3.2 directly compares the non-dynamic solution with 4 dynamic best deficit solutions (BDS1-4), characterized by different PV optimal capacities, in terms of sustainability indicators. It is worth noting that all the dynamic solutions reduce the present value of costs and the electricity surplus and almost all of these solutions also show lower fuel consumption and CO_2 emissions. In particular, the dynamic solution characterized by 1800 kW of PV significantly outperforms the non-dynamic solution reducing the present value of costs by 2 M€ and the CO_2 emissions by about 220 tons/y. Moreover, it attains a slightly higher RES penetration with a lower PV capacity.

Table 3.2: *Comparison between the non-dynamic solution and 4 dynamic solutions that minimize the water deficit (BDS) in terms of sustainability indicators.*

	Non-dynamic Solution	**BDS1**	**BDS2**	**BDS3**	**BDS4**
PV capacity (kW)	2000	1800	1600	1400	1200
Present value of costs (M€)	44.0	42.0	42.2	42.5	43.0
Electricity surplus (MWh/y)	1207	584.9	394.7	244.0	117.9
Fuel consumption ($l*10^6$/y)	0.96	0.88	0.92	0.95	1.00
CO_2 emissions (tons/y)	2606	2389	2487	2583	2717
RES penetration (%)	41.0	41.2	40.0	37.9	35.5

The ability of the dynamic MO approach to automatically identify the best operating policies associated with each system design leads to optimal solutions that allow structural interventions to be limited, consequently reducing investment costs and environmental impacts.

As already mentioned in Chapter 2, all the solutions presented in this work are obtained simulating the system according to specific technical and economical parameters. However, even if the parameters characterizing each technological component (e.g., investment costs, RES efficiency) can be considered strongly reliable for our specific case study, some economical parameters are highly uncertain.
In order to assess the effects of this uncertainty on the system performance, we perform a sensitivity analysis focusing on the optimal solution that minimizes the present value of cost covering the entire water demand (BDS1 in Figure 3.5). More precisely, we estimate how the present value of cost of BDS1 solution changes according to different values of the real discount rate γ and the fuel cost C_f. In particular, we consider perturbations of these parameters within feasible ranges provided by Kaldellis (2010) and Steinbach and Staniaszek (2015).
Results show that increasing the real discount rate from 1.5% (benchmark) to 3% and 6% leads to a decrease of the present value of cost from 42 M€ (benchmark) to 35.3 M€ (-16% with respect to the benchmark) and 26.2 M€ (-38% with respect to the benchmark), respectively.
Focusing on the fuel cost, a decrease/increase of its value from 0.54 €/l (benchmark) to 0.3/0.7 €/l brings to a reduction/increase of the present value of cost from 42 M€ (benchmark) to 35/46.8 M€ (-17/+11% with respect to the benchmark).
These results suggest that the performance of the solutions is strongly sensitive to changes in the main economical parameters. Thus, considering the uncertainty associated to these parameters within the decision making process is crucial to identify more robust solutions.

3.5 Conclusions

In this chapter, we propose a novel dynamic, multi-objective approach to conjunctively optimize the capacity of renewable energy sources and desalination plant operation for the integrated water-electricity system of small off-grid islands. The advantages of using this novel approach are evaluated by means of a comparative analysis with a traditional non-dynamic, single-objective approach, which determines the least cost optimal design (i.e., renewable sources capacity) of the hybrid electricity system investigated using a fixed observed load to model desalination plant operation. The comparative analysis is performed for the real case study of the Italian Ustica island.

Results obtained for a pre-defined planning configuration (i.e., 1200 kW of PV) show that the optimal dynamic solutions outperform the non-dynamic solution obtained by simulating the system using a fixed observed desalination load

with respect to almost all sustainability indicators considered. In particular, the dynamic solution that minimizes the water deficit entirely satisfies the water demand reducing the present value of costs by 1.2 M€ and the electricity surplus by about 257 MWh/year (more than 80% of the electricity surplus obtained by the traditional approach), and significantly increasing RES penetration.

Results of the joint optimization of system design and operation show that all planning and management dynamic alternatives outperform the optimal least cost non-dynamic solution in terms of electricity surplus and more than 90% of them also show lower present value of costs. For example, the dynamic solution characterized by 1800 kW of photovoltaic reduces the present value of costs by 2 M€ and the CO_2 emissions by about 220 tons/y. At the same time, this solution also slightly increases RES penetration, while installing a lower photovoltaic capacity. These results demonstrate that optimal system management leads to more acceptable planning solutions, which achieve higher system performance by reducing the structural interventions (lower renewable sources capacity), the investment costs and the environmental impacts. However, it should be noted that the performance of the obtained solutions is significantly affected by the uncertainty associated to the main economical parameters (i.e., real discount rate, fuel cost).

Further research efforts will focus on testing our dynamic, multi-objective approach on more complex systems considering additional power sources (e.g., wind turbines) and energy storage technologies (e.g., batteries) within the optimization process. In addition, a more detailed and comprehensive sensitivity analysis might be performed in order to consider the uncertainty in all the techno-economical simulation parameters. Moreover, synthetic generators of the main external drivers might be developed to enlarge the observed dataset in order to consider the inter-annual variability of the main natural and socio-economic variables within the optimization process.

4

Exploring the effects of climate change on the performance of hybrid energy systems

Abstract[1]

Designing hybrid energy systems that combine traditional power generation with renewable energy sources and storage technologies represents a viable and promising solution for improving the sustainability of remote off-grid systems, such as the small Mediterranean islands. However, in the future, the performance of these system will be strongly affected by uncertainty in climate conditions, posing a big challenge in the identification of the best system design able to guarantee high levels of sustainability over a medium-to-long term horizon. In this chapter, we propose a methodological framework to assess the vulnerability of hybrid energy systems with respect to changes in the main climate drivers (i.e., solar radiation, wind speed, temperature). More precisely, we aim at evaluating how the historical variability and the future uncertainty in the climate variables affect the performance of highly renewable hybrid energy systems, designed under average historical conditions, in terms of different sustainability indicators. Numerical results show that the performance variability associated to future scenarios is almost double with respect to the historical one for all the indicators considered. Moreover, the performance of the solutions

[1] Giudici, F., Castelletti, A., Garofalo, E., Maier, H. R., 2019b. Exploring the effects of climate change and technological innovation on the robust design of off-grid hybrid energy systems. Nature Energy (in preparation)

characterized by high RES and storage capacity is less sensitive to changes in the climate drivers with wind speed representing the driver that mainly affects the system performance.

4.1 Introduction

Small Mediterranean islands represent a paradigmatic example of remote off-grid systems facing a large number of sustainability issues, mainly due to their distance from the mainland, the lack of accessible water sources, and the high seasonal variability of both water and electricity demand. Energy security is generally reliant on carbon intensive diesel generators, which are usually oversized to meet peak summer electricity demand driven by high touristic fluxes. Potable water is often produced by energy intensive desalination technologies, which strongly impact on the electricity system, increasing air pollution and greenhouse gas emissions. In addition, the high dependence upon the remote supply of fuel and the need for backup storage to cover possible refuelling delays contribute to increasing operational costs and the overall inefficiency of these systems.

In order to improve the economic and environmental sustainability of small islands, hybrid energy systems, combining traditional power generation (e.g., diesel) with RES (e.g., PV, wind) and storage technologies (e.g., batteries), provide a potentially viable solution for reducing costs and carbon emissions (Ekren and Ekren, 2009; Ibrahim et al., 2011; Erdinc and Uzunoglu, 2012). In particular, as reported by Sawle et al. (2018), coupling PV and wind generation through PV-wind based hybrid systems represents a good option to maximize RES production and thus reducing costs and emissions. These technologies rely in fact on complementary natural resources: wind peaks are usually observed during the night and in winter, whilst solar radiation is higher during the day and in spring and summer months. In addition, the introduction of batteries coupled to PV technologies is considered a well-establish solution to fully exploit the RES power potential by storing electricity surpluses during the day for using them during the night hours (Shaahid and El-Amin, 2009; Merei et al., 2013). Even if storage systems are usually characterized by very high costs of installation, they allow to significantly reduce the operational costs on a medium-to-long term horizon, increasing RES penetration and reducing the carbon emissions.

Traditionally, the optimal configuration of the hybrid energy system is obtained by identifying the size of each technologies that minimizes the present value of costs over a given horizon under average historical conditions of the main

climate drivers (i.e., wind speed, solar radiation, temperature) (Bhandari et al., 2015). However, the well recognised uncertainty associated to these external drivers might strongly affect the performance of the optimal configuration, posing significant challenges to the identification of hybrid energy systems able to guarantee high levels of sustainability over a medium-to-long term horizon. In particular, the optimal solution designed under average historical conditions may be not robust when re-evaluated under future changing scenarios. In recent years, several studies have been focused on assessing the future variability of climate drivers and analysing how future changes in these drivers may affect the RES power potential over different spatial scales (Pašičko et al., 2012; Stanton et al., 2016). In particular, the impacts of climate change on wind production have been assessed for the European countries either by directly estimating future projection of wind resource, or by assessing the impact of future changing conditions on the operation and maintenance of wind farms as well as on the design of wind turbines (Pryor and Barthelmie, 2010; Nolan et al., 2012; Carvalho et al., 2017). Climate change effects on PV and solar power generation are instead evaluated by analysing future projections of solar radiation and developing simulation models for better estimating changing in PV efficiency due to extreme weather events or changes in temperature and cloud cover transmissivity (Jerez et al., 2015; Fant et al., 2016). Even if several works focus on understanding the impacts of climate change on future RES power potential, only few studies concentrate on assessing the effects of such changes on the system performance (i.e., sustainability indicators) through a comprehensive analysis aiming at exploring and identifying the main system vulnerabilities (Schaeffer et al., 2012; van Vliet et al., 2012).

In order to address this aspect, in this chapter we propose a methodological framework to assess the vulnerability of hybrid energy systems with respect to changes in the main climate drivers (i.e., solar radiation, wind speed, temperature). More precisely, we aim at evaluating how the historical variability and the future uncertainty in the climate variables affect the performance of highly renewable hybrid energy systems, designed under average historical conditions, in terms of different sustainability indicators. Moreover, we also concentrate on exploring the key variables that have a more significant impact on the system performance in order to identify the more interesting drivers to include in the system design phase in order to generate robust planning solutions.

4.2 Methods and Tools

In this chapter, we propose a methodological framework (Figure 4.1) to evaluate the effects that historical variability and future uncertainty in the main climate

drivers (i.e., solar radiation, wind speed, temperature) may have on the performance of highly renewable hybrid energy systems, which combine conventional power generation (e.g., diesel) with RES (e.g., PV, wind) and storage technologies (e.g., batteries). First, we optimally design a hybrid energy system considering average historical conditions (Section 4.2.1). Secondly, starting from historical data, we generate stationary scenarios of the main climate drivers through the implementation of different synthetic generators in order to enlarge the historical dataset and fully capture the historical drivers variability (Section 4.2.2). Then, we generate future climate scenarios starting from the climate projections provided by EURO-CORDEX[2] in order to analyse how the main climate drivers change in future (Section 4.2.3). Finally, we re-evaluate the optimal system designs under historical and future scenarios for assessing how changes in the climate drivers affect the system performance in terms of different sustainability indicators (Section 4.2.5).

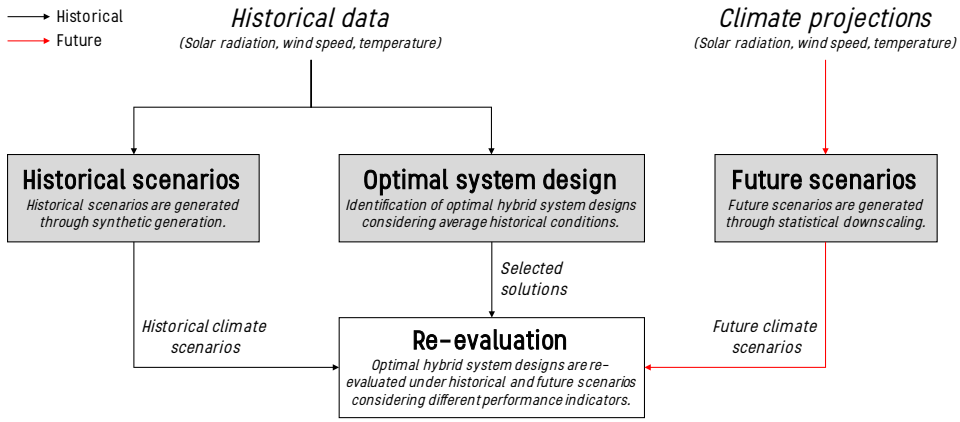

Figure 4.1: *Methodological framework for assessing the effects of historical and future climate variability on the performance of hybrid energy systems designed under average historical conditions. Grey boxes represent the tools for generating the optimal system designs and the scenarios used to re-evaluate the system.*

4.2.1 Optimal system design

We identify optimal system designs by solving a multi-objective optimization problem with respect to two objectives considering average historical conditions of the climate drivers. The first objective, to be minimized, is the present value of costs, defined as in Chapter 3. The second objective, to be maximized, is the RES penetration, defined as the percentage of electrical load covered by

[2] www.euro-cordex.net

renewable power over the project horizon. The decision variables are PV capacity, number of wind turbines and number of batteries to be installed. In this work, we do not optimize the desalination plant operations but we consider the historical ones. Like for the experiments performed in Chapter 3, we solve the optimization problem by means of a simulation-based optimization approach using the evolutionary multi-objective algorithm Borg MOEA (Hadka and Reed, 2013).

4.2.2 Historical scenario generation

For each of the three climate variables considered (i.e., solar radiation, wind speed and temperature), a different synthetic generator has been implemented in order to fully capture the historical variability of the external drivers. Synthetic generators are tools that aim to obtain an amount of data, starting from a limited set of historical data. They are particularly useful when dealing with climate drivers, as long and continuous series that capture the full variability of the processes are often not available. Synthetic data can have, hourly, daily, or monthly scale and preserve the statistics of the starting series. In the following, the synthetic generators adopted for the different climate variables are presented.

Solar radiation Hourly radiation data can be synthetically generated through stochastic techniques, such as autoregressive models (Aguiar and Collares-Pereira, 1992) or Markov chains approaches (Bright et al., 2015). Markov chains are usually preferred as they generally reproduce better some of the basic characteristics of the occurrence probability of solar radiation data. Since solar radiation is a complex process, which depends upon many external factors (e.g., cloud dynamics, atmospheric losses and transport of airborne pollutants), synthetic generators work with the clearness index k_t, defined as the ratio between the radiation at surface and the radiation at TOA (Top Of Atmosphere). In fact, this dimensionless variable can be generalized for different areas and can be easily de-trended (Poggi et al., 2000). A Markovian process is a mathematical representation of a stochastic process, whereby transitions from one state to the next are directed by discrete probabilities taken from the statistics of real world processes and under the assumption that the future state depends only on the last n states. Considering a higher number of states (i.e., higher Markov chain order) improves the accuracy of the generated data, but also increases the computational cost.
In this analysis, a first order Markov chain is considered and the historical series is discretized in k states (or classes). Given the process in state i at time $t-1$, the probability that it will be in state j at time t is determined by the transition

probability p_{ij}:

$$p_{ij} = \frac{n_{ij}}{\sum_{j=1} n_{ij}} \tag{4.1}$$

where n_{ij} represents the number of transitions from state i to state j observed in the historical discretized series. These frequencies are converted into probabilities by dividing them by the total number times in which state i has transitioned towards any of the k states. The probability transition matrix P of size $k * k$ is thus created as follows:.

$$P = \begin{bmatrix} p_{1,1} & p_{1,2} & \cdots & p_{1,k} \\ p_{2,1} & p_{2,2} & \cdots & p_{2,k} \\ \vdots & \vdots & \vdots & \vdots \\ p_{k,1} & p_{k,2} & \cdots & p_{k,k} \end{bmatrix}$$

Its values range between 0 and 1. Higher values occur on the diagonal of the matrix and, in general, all the transition probabilities are around the diagonal (i.e., transitions from one state to another are rare when the states are far each other). Once the matrix P has been computed, the generation phase starts: the first state is randomly chosen from the classes of the discretized series and the subsequent states are determined according to the probability transition matrix, until the desired length of the generated series is reached. The result is a dimensionless series of classes. In order to obtain a series of real data, this series is multiplied by the class step, generating the discretized series SG_d, in which each element corresponds to the upper boundary of the interval of the corresponding class. From this series a random quantity multiplied by the step length (sl) is substracted for generating the synthetic series SG:

$$SG = SG_d - rand(0,1) * sl \tag{4.2}$$

In this work, hourly clearness index is synthetically generated considering daylight hours only, while darkness hours are attained at the end of the generation phase depending on the considered month. Hourly k_t is finally multiplied by radiation at TOA for generating the solar radiation series.

Wind speed Since wind is a continuous process in real world, wind speed data at any time is strongly correlated to previous data (Shamshad et al., 2005). Methods based on Markov chains are extremely suitable for modeling this kind of processes and are thus the most commonly adopted for generating synthetic series of wind speed (Aksoy et al., 2004). The synthetic generator here implemented follows the same method developed for generating solar radiation data. However, in this case, we consider each month of the year independently, by determining 12 different probability transition matrices in order to accurately reproduce the seasonal pattern.

Temperature The most commonly adopted approaches for generating synthetic series of air temperature are based on Fourier series, Auto Regressive Moving Average (ARMA) models (Magnano et al., 2008) or non-parametric methods (Sharif et al., 2007). In this work, we adopt a non-parametric method, namely the K-Nearest Neighbour (K-NN) resampling approach. Non-parametric generators employ the nearest neighbor bootstrap resampling technique (Lall and Sharma, 1996) to reproduce the autocorrelation in generated time series without assuming a parametric generating process. Since K-NN approach works with daily time series, first we transform our historical hourly time series in a daily one. Secondly, we divide the historical series into overlapping blocks of d data and the most recent block is compared to all historical blocks to find the first k nearest neighbors according to a distance measures, namely the Euclidean distance. The k nearest neighbors are then sorted according to the distance measure and associated to a probability $P(j)$ that is inversely proportional to the rank j:

$$P(j) = \frac{\frac{1}{j}}{\sum_{j=1}^{k} \frac{1}{j}} \tag{4.3}$$

Finally, the generated value is the one that succeeds the sampled nearest neighbor according to $P(j)$. The blocks are then recomputed accounting for the generated value and the process restarts and continues until the desired series length is reached. Since temperature is a strong autocorrelated process, a block length d=6 is chosen, while k is calculated as the square root of the length n of the historical record (Lall and Sharma, 1996). At the end, the generated daily time series is disaggregated in an hourly time series by means of a disaggregation method (see Section 4.2.4 for details).

4.2.3 Future scenario generation

Future climate scenarios of solar radiation, wind speed and temperature are provided by the EURO-CORDEX project[3]. The aim of this project is to generate realistic climate change projections by simulating the physical processes of atmosphere, oceans and land surface through a modeling chain composed of Global Circulation Models (GCMs) and Regional Circulation Models (RCMs). These models are fed by Radiative Concentration Pathways (RCPs), which describe how Greenhouse Gas (GHG) concentrations will evolve in the future according to different emission scenarios. In particular, RCPs define how the radiative forcing values change with respect to pre-industrial age by considering different assumptions about patterns of economic and demographic growth, technology development and future energy consumption (Moss et al., 2010). In particular, the Intergovernmental Panel on Climate Change (IPCC) (IPCC,

[3] www.euro-cordex.net

2014) identify 4 RCPs namely RCP 2.6, RCP 4.5, RCP 6 and RCP 8.5 (Hijioka et al., 2008), which correspond to different increase in the radiative forcing estimated at the end of the century with respect to the pre-industrial values (i.e., +2.6, +4.5, +6 and +8.5 W/m^2). RCPs feed GCMs, which simulate the physical processes at the global scale defining the boundary conditions for RCMs. These latter work on an higher resolution providing a more detailed description of the orography, the land use and the local circulation phenomena. Simulation results are climate projections at different spatial and temporal scales. In particular, depending on the combinations of GCMs and RCMs, the time resolution ranges between one hour to six months, while the spatial resolution from 0.11 degrees (EUR-11, about 12.5 km) to 0.44 degrees (EUR-44, about 50 km). The simulation horizon includes two periods: the control period (1971-2005), where the models are fed with observed inputs and the simulation period (2006-2100), where climate models are fed by RCPs. In this work, we consider 5 combinations of GCMs and RCMs, fed by 3 different RCPs, namely RCP 2.6, RCP 4.5, RCP 8.5, with a spatial resolution of 0.11 degrees (Table 4.1). Since some combinations do not provide projections until 2100 for all the variables of interest, we consider the simulation period 2006-2095 as the longer common period between model combinations. For each combination of RCP, GCM and RCM, we thus obtain daily time series of solar radiation, wind speed and temperature for the period 1971-2095.

Table 4.1: *Climate scenarios from EURO-CORDEX project. Scenarios are generated using different combinations of GCMs and RCMs forced with different RCPs.*

GCM	RCM	RCP	Spatial resolution
ICHEC	CCLM4	2.6; 4.5; 8.5	0.11 deg
ICHEC	RCA4	2.6; 4.5; 8.5	0.11 deg
MPI	RCA4	2.6; 4.5; 8.5	0.11 deg
MOHC	RCA4	2.6; 4.5; 8.5	0.11 deg
MOHC	RACMO22E	2.6; 4.5; 8.5	0.11 deg

Statistical downscaling To resolve the mismatch between the resolution of the climate projections and the resolution of the observed variables at the local scale (i.e., Ustica island), a statistical downscaling technique (i.e., Quantile Mapping) (Boé et al., 2007) is applied for each of the three climate variables considered. Quantile Mapping technique is based on the identification of a transfer function f which maps the cumulative density function of a predictor onto the cumulative density function of a predictand. In our case, the predictor is the climate model output over the control period, and the predictand is the observed time series. The method consists in two distinct phases:

- **Calibration phase**: the transfer function f between the climate model output over the control period C and the observed time series O is calibrated:

$$O = f(C) \tag{4.4}$$

- **Projection phase**: the calibrated function f is applied to the climate model output over the simulation period, called forecast (F), removing the bias. A linear interpolation is applied between two percentiles. The result of the operation is the downscaled time series (F'):

$$F' = f(F) \tag{4.5}$$

The calibration phase can be done yearly, seasonally or monthly, as the model error might differ during the year. In this work, a time-dependent correction function calibrated for each day of the year is applied on a seasonal basis.
The results of the downscaling phase are local scale daily time series of the three climate variable considered over the period 1971-2095. In order to obtain hourly time series, we apply the disaggregation methods presented in Section 4.2.4.

4.2.4 Temporal disaggregation

In this work, different disaggregation methods are implemented to generate hourly time series from daily ones. The methods adopted for the three climate variable considered are reported in the following.

Solar radiation Disaggregation methods for solar radiation can be mathematical, linear, polynomial, heuristic or Artificial Neural Networks (Khatib and Elmenreich, 2015). A mathematical method based on the cosine function and the average daily radiation is developed. It works on a monthly basis and imposes zero values during the hours of darkness. During daylight hours the solar radiation $G(h)$ at hour h is calculated as follows:

$$G(h) = k * rand(a, b) \cos(\frac{\pi}{12}(h - c)) + e * G(d) \tag{4.6}$$

where $G(d)$ is the average daily radiation $[W/m^2]$, a, b, c, e are parameters that depend upon the considered month and the considered daylight hour, k is a constant depending upon the day of the month that determines the increasing/decreasing speed of solar radiation within the month. In Table 4.2 the values of the hourly dependent parameters are reported for the month of January, as an example.

	8 am	9 am	10 am	11 am	12 am	1 pm	2 pm	3 pm	4 pm
a	0.6	0.6	0.6	0.6	0.6	0.6	0.6	0.6	0.6
b	1	1	1	1	1	1	1	1	1
c	12	12	12	12	12	12	12	12	12
e	0.2	0.45	0.7	1	1	1	1	0.7	0.5

Table 4.2: *Hourly dependent disaggregation parameters for the month of January.*

Wind speed Disaggregation methods for wind speed are based on equations that consider cosine function or random uniform distributions, given the daily average wind speed (Debele et al., 2007). The method adopted in this work calculates the wind speed $WS(h)$ at hour h using the following equation:

$$WS(h) = \begin{cases} rand(a,b) * (1 - (\frac{|h-c|}{15})) * WS(d)\cos(\frac{\pi}{12}(h-c)) + k * WS(d) & 8 \leqslant h \leqslant 20 \\ rand(a,b) * WS(d)\cos(\frac{\pi}{12}(h-c)) + k * WS(d) & else \end{cases} \tag{4.7}$$

where $WS(d)$ is the daily average wind speed and a=0, b=0.3, c=15, k=1 are constant parameters.

Temperature We adapt the method proposed by Debele et al. (2007) to estimate hourly temperature from daily mean temperature. Hourly temperature $T(h)$ is thus generated using the following equation:

$$T(h) = k * rand(a,b)\cos(\frac{\pi}{12}(h-c)) + T(d) \tag{4.8}$$

where $h \in (1-24)$, $T(d)$ is the average daily temperature, a, b, c, k are constants that depend upon the month considered (Table 4.3).

	Jan	Feb	Mar	Apr	May	Jun	Jul	Aug	Sep	Oct	Nov	Dec
a	0	0	0	0	0	0	0	0	0	0	0	0
b	1	1	1	1	1	1	1	1	1	1	1	1
c	15	15	15	15	15	15	15	15	15	15	15	15
k	0.6	0.6	0.7	0.85	1	1.1	1.25	1.2	1	0.85	0.6	0.45

Table 4.3: *Temperature disaggregation parameters.*

4.2.5 System re-evaluation

Solutions obtained from the planning optimization presented in Section 4.2.1 are re-evaluated, first, under the historical synthetic scenarios (see Section 4.2.2) to assess the system vulnerability with respect to the historical variability in the main climate drivers and, then, under future scenarios (see Section 4.2.3) to evaluate the robustness of the system with respect to the future uncertainty in

the climate variables. During this phase the system model presented in Chapter 2 is repeatedly run considering different scenarios. Results are then analysed considering the following sustinability indicators:

- **Present value of costs** [M€]. This indicator is one of the objectives used in the planning optimization phase;
- **RES penetration** [%]. This indicator is one of the objectives used in the planning optimization phase;
- **Fuel consumption** [liters/year]. This indicator is computed as a function of the electricity output of each diesel generator;
- **CO_2 emissions** [tons/year]. This indicator is computed by multiplying the total fuel consumption for an empirical coefficient.

4.3 Experiment settings

Optimal system designs (Section 4.2.1) are generated considering average historical conditions of the climate variables, computed from hourly time series provided by the re-analysis dataset MERIDA (MEteorological Reanalysis Italian DAtaset) (Lacavalla et al., 2017) over the period 2001-2017 (17 years). These data are also used as input to the synthetic generators (Section 4.2.2) for producing hourly time series of 100 years, and are adopted as historical observations for performing the statistical downscaling of the climate projections (Section 4.2.3). Since the system model presented in Chapter 2 requires the incident solar radiation as input, the global solar radiation provided by the MERIDA dataset and the future projections are transformed in incident solar radiation following the method proposed by Duffie and Beckman (2013) and considering a slope for the PV panels equal to 30° with respect to the horizontal.

4.4 Numerical results

4.4.1 Identification of the optimal system design

Figure 4.2 shows the Pareto optimal solutions in the space of the optimization objectives. The x-axis represents the present value of costs, the y-axis the RES penetration and the color shows the PV capacity (Figure 4.2a), the number of wind turbines (Figure 4.2b) and the number of batteries (Figure 4.2c). We can observe a clear trade-off between the two objectives: the lower the present value of costs the lower the RES penetration. This is due to the need of increasing the installed RES capacity in order to achieve higher RES penetrations. In this way, an higher RES power allows to reduce diesel generation for covering the load,

thus increasing the RES penetration and reducing operational costs. However, the operational cost reduction does not compensate the higher investment costs leading to higher present value of costs. The highest increase in RES penetration (from 60% to 80%) is obtained for a very small increase in the present value of costs (from 42 M€ to 44 M€) and is associated to a rapid increase of the PV capacity (from 1500 kW to 2500 kW) and the number of batteries (from 2 to 50). The number of wind turbines remains instead fixed to about 20 units. These results suggest that coupling PV to storage technologies is the most efficient way for exploiting RES potential and reducing operational costs. The very high renewable power produced during the day can be in fact stored in the batteries and used during the night for covering the load and thus reducing diesel generation.

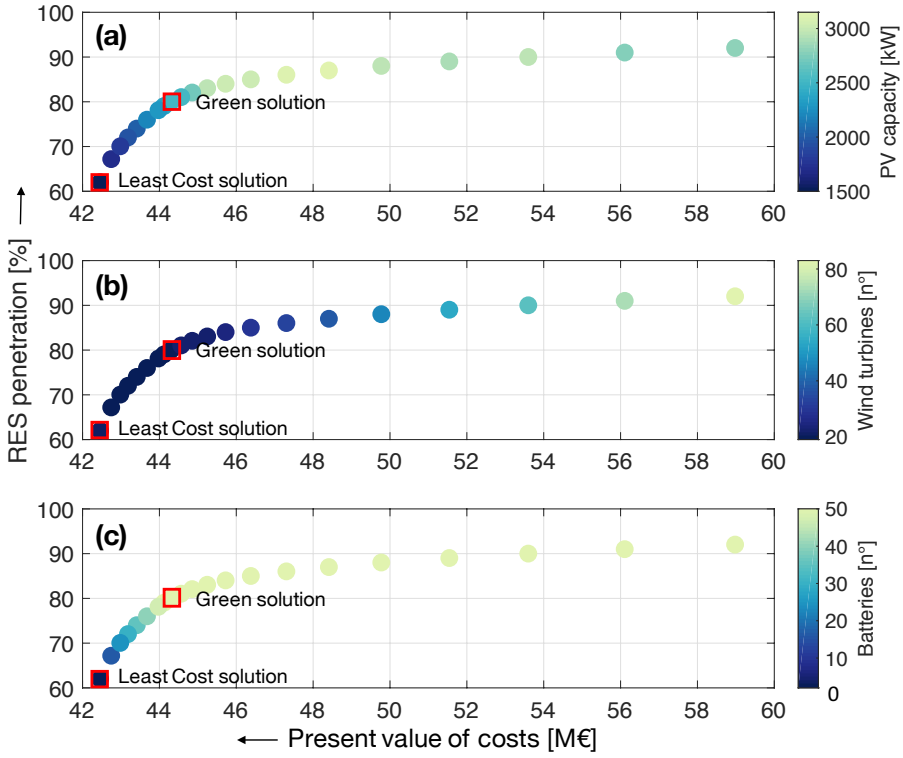

Figure 4.2: *Pareto-optimal system designs in the space of the optimization objectives. Red squares highlight the solutions considered in the re-evaluation analysis. The color of each point represents the PV capacity (a), the number of wind turbines (b) and the number of batteries (c) to be installed.*

In order to further increase RES penetration, also the number of wind turbines has to be necessarily increased. However this causes a significant increase

in the present value of costs. In particular, for a small increase in the RES penetration of 10% (from 80% to about 90%), the present value of costs increases of about 15 M€ (from 44 M€ to 59 M€).
In order to assess the performance of the solutions under the uncertainty in the climate variables, we select two different designs (red squares in Figure 4.2) as the more representative of the trade-off between present value of costs and RES penetration. More precisely, we focus on the solution that minimizes the present value of costs (42.2 M€), called Least Cost solution, which installs 1550 kW of PV, 21 wind turbines and 2 batteries, and a compromise solution that presents a very high RES penetration (80%) and a slightly higher present value of costs (44.1 M€), called Green solution, which installs 2200 kW of PV, 19 wind turbines and 40 batteries.

4.4.2 Analysis of historical and future climate scenarios

Figures 4.3-4.5 show the mean annual values of solar radiation (Figure 4.3), wind speed (Figure 4.4) and temperature (Figure 4.5) over the period 1971-2095 estimated by the CORDEX scenarios in Table 4.1 for three different RCPs, namely RCP 2.6, RCP 4.5 and RCP 8.5.

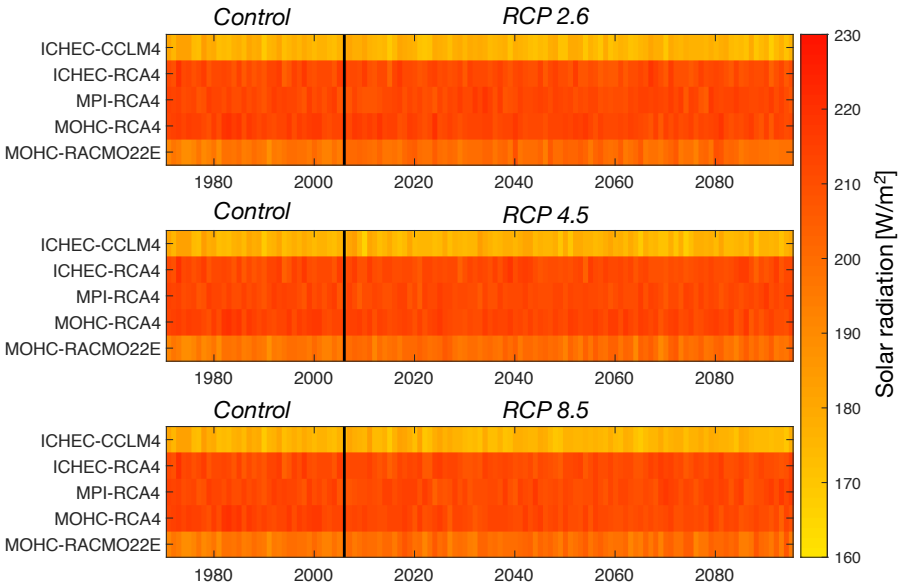

Figure 4.3: *Mean annual values of solar radiation over the control period (1971-2005) and the simulation period (2006-2095) provided by 5 EURO-CORDEX models for 3 different RCPs.*

For all the variables considered, we can clearly observe how different combinations of GCMs and RCMs produce different results. In particular, the scenarios characterized by the RCM RCA4 present higher solar radiation and lower wind speed and temperature.
This discrepancy between the estimated values of different model combinations clearly suggests the need of adopting a downscaling technique in order to remove these biases and generate reliable local scale projections.
Focusing on the temporal variability, we can observe that all the scenarios considered highlight a clear trend of temperature increase from the beginning of the control period (1971) to the end of the century (Figure 4.5). Temperature increases form 14 to 23 °C with higher values associated to the RCP 8.5. Conversely, solar radiation and wind speed do not present any clear trend (Figure 4.3,4.4). However, these variables show a very high inter-annual variability, independently from the period and RCP considered, with values that can strongly differ from one year to another reflecting the unpredictable behaviour typical of these variables. In particular, solar radiation is characterized by values that range from 160 to 230 W/m^2 (Figure 4.3) and wind speed presents mean annual values that vary from 5 m/s to 10 m/s (Figure 4.4).

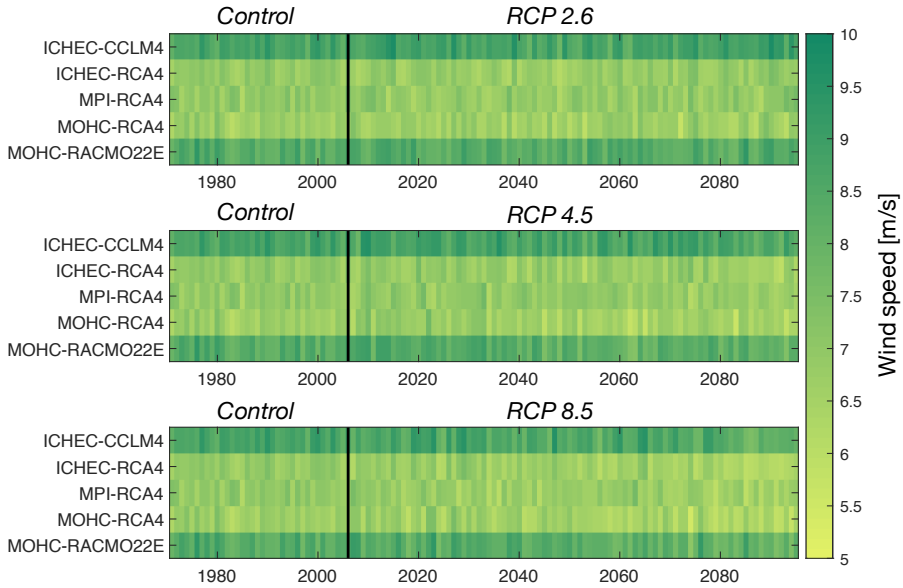

Figure 4.4: *Mean annual values of wind speed over the control period (1971-2005) and the simulation period (2006-2095) provided by 5 EURO-CORDEX models for 3 different RCPs.*

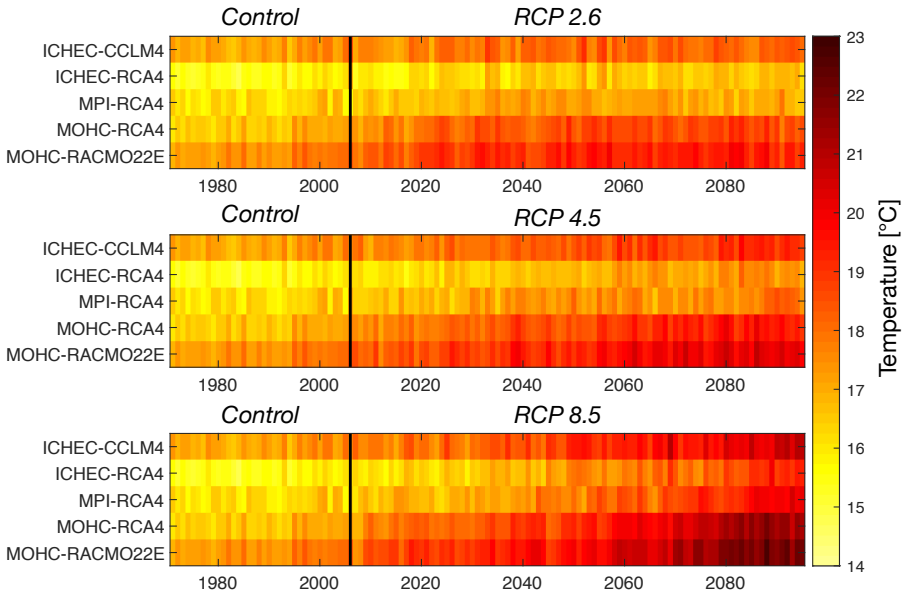

Figure 4.5: *Mean annual values of air temperature over the control period (1971-2005) and the simulation period (2006-2095) provided by 5 EURO-CORDEX models for 3 different RCPs.*

The downscaled future scenarios are shown in Figure 4.6 compared to the historical synthetically generated scenarios. The x-axis represents the wind speed, the y-axis the incident solar radiation and the color shows the temperature: blue points refer to low temperature values instead red points represent high temperature values. Each circle represents a specific year over the period 2006-2095 estimated by a specific model combination for a given RCP, instead each diamond refers to one of the 100 synthetically generated years preserving the statistics of the historical observations. We can observe that historical scenarios show very low temperature, high solar radiation and average wind speed with a very low variability associated to all the variables considered. In particular, temperature does not exceed 20 °C, solar radiation ranges from 263.9 to 266.2 W/m^2 and wind speed varies from 4.8 to 5.7 m/s. Future scenarios are instead characterized by a very high variability, with temperature that varies from 18 to 25 °C, solar radiation from 259 to 268 W/m^2 and wind speed from 4.2 to 6 m/s. By analysing the future scenarios, we can observe that the values assumed by one of the variables are not conditioned by the values assumed by the others. This means that no correlation exits between the variables considered and all the possible combinations of solar radiation, wind speed and temperature within their range of variability constitute plausible future conditions.

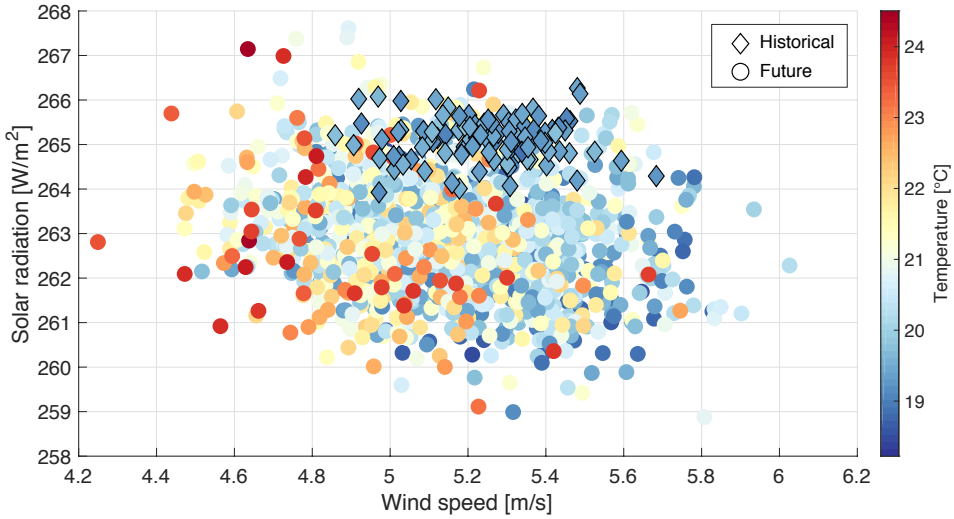

Figure 4.6: *Historical (diamonds) and future (circles) scenarios. Each point represents the mean annual value of wind speed, solar radiation and temperature for a specific scenario. Blue points refer to low temperatures, whilst red points represent high temperatures.*

4.4.3 Re-evaluation of the system performance under historical and future climate variability

In this section, we assess how historical and future climate variability analysed in Section 4.4.2 affects the performance of the Least Cost and the Green solutions identified in Section 4.4.1.

Figure 4.7 shows the box plots of the performance of the Least Cost and the Green solutions when re-evaluated under historical (grey) and future (blue) climate scenarios. In particular, Figure 4.7a refers to the present value of costs, Figure 4.7b shows the RES penetration, Figure 4.7c and Figure 4.7d represent the fuel consumption and the CO_2 emissions, respectively. Not surprisingly, the re-evaluation under both historical and future climate variability confirms that the Green solution shows a slightly higher present value of costs but a significantly higher RES penetration associated to lower fuel consumption and lower CO_2 emissions with respect to the Least Cost solution. However, the performance of both the Least Cost and the Green solutions is strongly affected by the variability in the climate drivers. In particular, it is worth noting that the variability associated to the future scenarios is almost double with respect to the historical one for all the performance indicators considered. More precisely, even if the performance associated to the best possible scenario remains almost the same when considering historical and future conditions, the average performance and the one associated to the worst possible scenario significantly

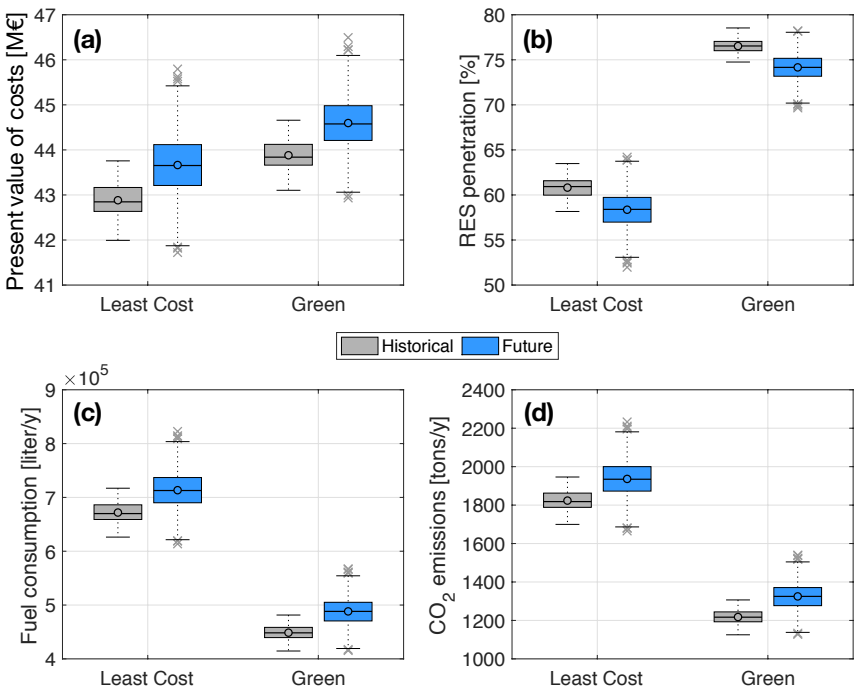

Figure 4.7: *Box-plots representing the performance in terms of present value of costs (a), RES penetration (b), fuel consumption (c), CO_2 emissions (d) of the Least Cost and the Green solutions re-evaluated under historical (grey) and future (light blue) climate scenarios.*

degrades in the future. In other words, future climate conditions will likely negatively affect the performance achieved by the optimal solutions when re-evaluated under historical climate variability, posing great challenges for the identification of the best solutions over a medium-to-long term horizon. Another interesting aspect concerns the different effects that climate variability causes on the Least Cost and the Green solution. This latter shows, in fact, less variable performance indicators compared to the Least Cost solution when considering both historical and future climate variability.

This result suggests that the solutions characterized by higher RES and storage capacity are less sensitive to changes in the climate drivers. On one hand, high RES capacity often allows to produce more power than the one needed to cover the load. In these cases, changes in the natural resource affect the system performance only when the resulted RES power potential becomes lower than the load, causing the diesel generators to be activated. On the other hand, high storage capacity filters the uncertainty in the climate drivers, and consequently in the RES power potential, by storing and redistributing energy in time.

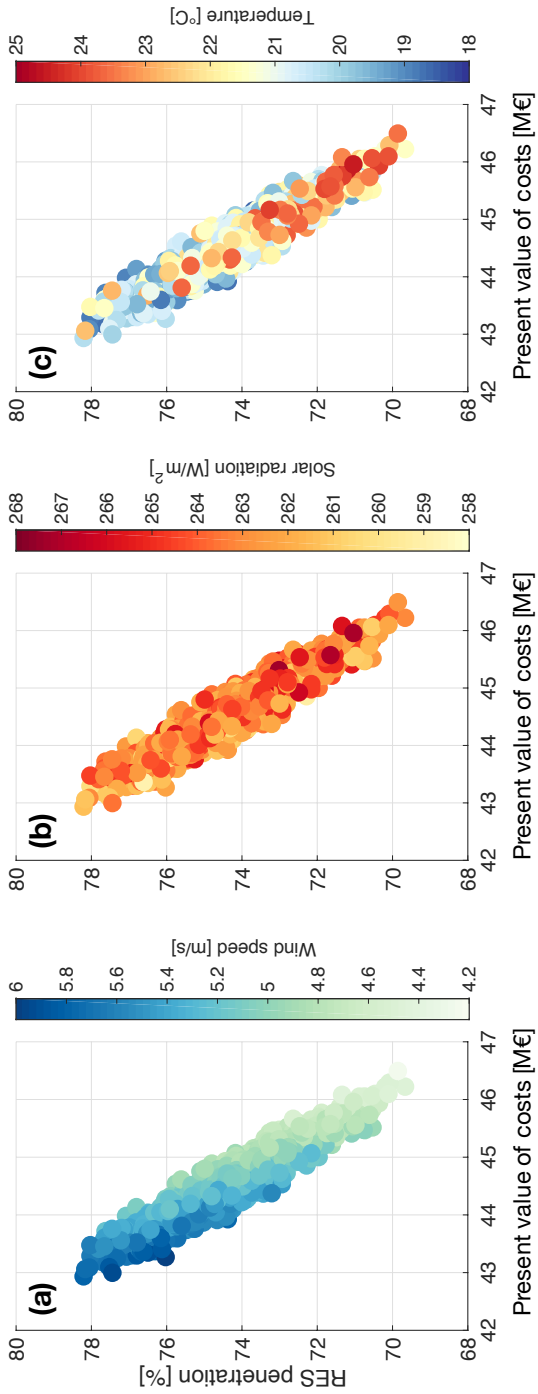

Figure 4.8: *Performance of the Green solution over the future scenarios in terms of present value of costs and RES penetration with the color representing wind speed (a), solar radiation (b) and temperature (c).*

In order to identify the climate drivers that mainly affect the system performance, we focus on the Green solution showing in the space of the optimization objectives, namely the present value of costs and the RES penetration, the re-evaluation over the future scenarios with the color representing the values assumed by the climate variables (Figure 4.8). In particular, Figure 4.8a shows the wind speed, Figure 4.8b the solar radiation and Figure 4.8c the temperature. It is worth noting that wind speed is the climate variable that mainly drives the system performance. In particular, the higher the wind speed, the higher the RES penetration and the lower the present value of costs. This is not surprising as a higher wind speed allows to increase the RES power to cover the load reducing the use of diesel generators and, consequently, decreasing the costs. System performance is instead completely insensitive to changes in solar radiation as its variability (about +/-2% of the average value) is negligible with respect to the very high variability of wind speed (about +/-15% of the average value), and only slightly sensitive to the temperature. In particular, the higher the performance (i.e., low present value of costs and high RES penetration) observed, the lower the temperature, as the efficiency of PV panels decreases for high temperature values (see Chapter 2 for further details). Finally, we can observe that changes in the climate variables and, more precisely, in the wind speed, cause different effects on the RES penetration for fixed present value of costs (see Appendix A for further details).

4.5 Conclusions

In this chapter, we propose a methodological framework to evaluate the effects that historical variability and future uncertainty in the main climate drivers (i.e., solar radiation, wind speed, temperature) may have on the performance of highly renewable hybrid energy systems, combining conventional power generation (e.g., diesel) with RES (e.g., PV, wind) and storage technologies (e.g., batteries). First, we optimally design a hybrid energy system considering average historical conditions and we select the system configuration that minimizes the present value of costs, called Least Cost solution, and a compromise solution that presents a very high RES penetration and a slightly higher present value of costs, called Green solution. Then, we re-evaluate the selected optimal system designs under historical and future scenarios of the main climate variables.

Results show that the system performance variability associated to the future scenarios is almost double with respect to the historical one for all the indicators considered. In particular, these latter significantly degrade when computed over the future conditions, especially if focusing on the average and the worst case scenario. Moreover, the performance of the solution characterized

by higher RES and storage capacity (i.e., Green solution) is less sensitive to changes in the climate drivers, as a lower performance variability with respect to the Least Cost solution is observed. Finally, numerical results show that wind speed is the climate variable that mainly drives the system performance: the higher the wind speed, the higher the RES penetration and the lower the present value of costs. In conclusions, the performed analysis shows that the performance of the optimal hybrid energy systems designed under average historical conditions is very sensitive to the future climate conditions and will likely degrade on a medium-to-long term horizon. These results suggest the need of directly considering future climate conditions within the design phase in order to generate solutions that are robust with respect to the deep uncertainty in the climate drivers. This aspect will be extensively discussed in Chapter 5.

Further research efforts will focus on exploring, in addition to climate change, future technological (e.g., cost and efficiency of different technologies) and socio-economic (e.g., energy demand, electricity prices) scenarios in order to assess the vulnerability of the hybrid energy systems with respect to a large set of co-varying plausible future conditions. Moreover, a complete robustness analysis might be performed for assessing how the robust solutions change when considering different robustness metrics, which reflect different levels of risk aversion of the decision maker.

5

An active learning approach for identifying the smallest subset of informative scenarios for robust planning

Abstract[1]

Deep uncertainty in future climate, socio-economic and technological conditions poses a great challenge to medium-long term decision making. Recently, several approaches have been proposed to identify solutions that are robust with respect to a large ensemble of deeply uncertain future scenarios or states of the world. In this chapter, we introduce ROSS (Robust Optimal Scenario Selection), a novel algorithm that uses an active learning algorithm for adaptively selecting the smallest scenario subset to be included into a robust optimization process. ROSS contributes a twofold novelty in the field of robust optimization under deep uncertainty. First, it allows the computational requirements for the generation of robust solutions to be considerably reduced with respect to traditional optimization methods. Second, it couples scenario discovery with robust optimization for the identification of the most informative regions of the scenario space, highlighting the primary system vulnerabilities. We test ROSS on the real case study of robust planning of an off-grid hybrid energy system,

[1] Giudici, F., Castelletti, A., Giuliani, M., Maier, H. R., 2019c. An active learning approach for identifying the smallest subset of informative scenarios for robust planning under deep uncertainty. Environmental Modelling & Software (Under Review)

combining diesel generation with renewable energy sources and storage technologies. Results show that ROSS enables computational requirements to be reduced between 23% to 84% compared with traditional robust optimization methods, depending on the complexity of the robustness metrics considered. It is also able to identify very small regions of the scenario space containing the most informative scenarios for generating a robust solution.

5.1 Introduction

Changes in future climatic and socio-economic conditions, as well as rapid technological innovation, represent sources of uncertainty that significantly influence medium-long term decision making in different fields (e.g., water management, infrastructure planning, energy systems design) (Harrison et al., 2015; Maier et al., 2016). Identifying planning solutions or management strategies for complex environmental systems can thus be extremely challenging, as the consequences of a decision, in terms of system performance, strongly depend on the external uncertain conditions that will actually unfold in the future (Uusitalo et al., 2015; McPhail et al., 2018). When information on the probability of occurrence of future uncertain conditions is available, and the uncertainty can be described using a stochastic model, the problem is defined as decision making under risk (French, 1986). When, instead, such probability of occurrence is unknown and a set-membership description of the uncertain future conditions is the only available information, the problem is classified as decision making under deep uncertainty (Lempert and Schlesinger, 2000; Lempert, 2002; Dessai et al., 2009).

Several approaches have been proposed to support decision making under deep uncertainty (see Herman et al. (2015) and Maier et al. (2016) for a review). The most widely adopted approaches include Robust Decision Making (RDM) (Lempert, 2002; Lempert et al., 2003; Bryant and Lempert, 2010; Hall et al., 2012), Decision Scaling (Brown et al., 2012; Moody and Brown, 2013; Ghile et al., 2014; Poff et al., 2015) and Many-Objective Robust Decision Making (MORDM) (Kasprzyk et al., 2013; Herman et al., 2014; Paton et al., 2014). All these approaches aim at evaluating the robustness of different planning or management alternatives over an ensemble of plausible future scenarios, called states of the world, focusing on understanding and retrieving the future conditions for which a given alternative fails or not.
Following the taxonomy proposed by Herman et al. (2015), these approaches can be classified based on the methods adopted for (i) identifying alternatives (e.g., pre-specified (Tingstad et al., 2014) or optimally generated (Quinn et al., 2018)), (ii) sampling states of the world (e.g., top-down (Mahmoud et al., 2009)

or bottom-up (Nazemi and Wheater, 2014) methods), (iii) quantifying robustness measures (e.g., regret or satisficing measures (Lempert and Collins, 2007)), and (iv) identifying key uncertainties through sensitivity analysis (e.g., scenario discovery (Bryant and Lempert, 2010; Singh et al., 2014)). Irrespective of which of the above approaches is used, the following sequential steps have to be performed: (i) generation of alternative solutions or policies, (ii) sampling of plausible future states of the world, and (iii) robustness analysis. Since the above robustness analysis is conducted on pre-defined solutions, there is no guarantee the most robust solutions are identified.

Robust optimization (RO) methods overcome this issue by identifying solutions that maximize robustness over a range of plausible future states of the world. This is achieved by combining robustness calculations and formal optimization processes, identifying solutions that perform satisfactorily over a wide range of deeply uncertain states of the world. However, this requires the performance of each alternative to be simulated at each of these states, making the optimization process computationally demanding or even intractable, especially when the number of scenarios increases from tens to several thousand (Roach et al., 2016). This is the reason why most studies that combine robustness assessment and the use of formal optimization for alternative generation perform the robustness assessment after the completion of the optimization process (Kasprzyk et al., 2013; Paton et al., 2014; Beh et al., 2015), with only few studies including robustness as an explicit objective in the optimization problem (Basupi and Kapelan, 2015; Giuliani and Castelletti, 2016; Zeff et al., 2016). To overcome the computational issues of RO methods, some studies use computationally efficient metamodels (Castelletti et al., 2012b) as surrogates of the hi-fidelity, computationally expensive simulation models that are generally used in the calculation of robustness values within the optimization process (Yan and Minsker, 2011; Broad et al., 2015; Beh et al., 2017). These metamodels are usually black-box models that map future uncertain conditions and decision variables onto robustness values. While their use can increase the computational efficiency of the optimization process significantly, their black-box nature means that the underlying system dynamics are not able to be represented explicitly (Castelletti et al., 2011, 2012a), making it difficult to obtain insight into the plausible future conditions that are likely to result in system failure. An alternative approach to increasing the computational efficiency of robust optimization methods is to adopt sampling techniques to extract a smaller scenario subset to be included in the robustness calculation. While consideration of a smaller number of scenarios reduces computational requirements, it also introduces the possibility that the robustness of the solution identified in the optimization process is significantly different from the one resulting from the consideration of the entire

scenario space.

In order to overcome the shortcomings of previous studies incorporating robustness as an optimization objective outlined above, we introduce ROSS (Robust Optimal Scenarios Selection), a novel algorithm that uses an active learning algorithm (Cohn et al., 1996) to identify the smallest scenario subset for which the robustness of the optimized solution is similar (or even equal) to that obtained by re-evaluating that solution over the entire scenario space, thereby increasing computational efficiency by reducing the number of scenarios over which solution performance has to be evaluated. Active learning is a particular case of machine learning as part of which the learning algorithm is directly responsible for acquiring its training data-set through (i) experiments on the real systems or (ii) running simulations of generative models to obtain the desired outputs for new, unknown inputs. In our case, the active learning principles are applied for filtering an existing data-set (i.e., scenario space) in order to select a concise sub-set of sufficiently informative scenarios for generating robust solutions.
ROSS contributes a twofold novelty in the field of robust optimization under deep uncertainty. First, it allows to considerably reduce the computational requirements for the generation of robust solutions with respect to traditional optimization methods. Second, it couples scenario discovery with robust optimization for the identification of the most informative regions of the scenario space, highlighting the main system vulnerabilities for solutions that maximize system robustness.

In order to demonstrate the utility of ROSS, we apply it to the robust planning of a hybrid energy system for the Ustica island, Italy (see Chapter 2 for further details on the case study). This case study is ideally suited to demonstrate the capabilities of ROSS, as it is focused on the optimal design of a hybrid energy system, including different types of renewable energy, which is subject to deep uncertainties associated with future changes in a number of climatic variables (e.g., solar radiation, wind speed, temperature). In addition, due to the very high number of future scenarios, the consideration of robustness as an optimization objective is computationally demanding.
We first assess the ability of ROSS of iteratively identifying the regions of the scenario space that contain the most informative scenarios for generating a robust solution. Then, we evaluate the computational advantages of ROSS with respect to a traditional robust optimization method, which considers the entire scenario space within the optimization process. As highlighted by different studies (Giuliani and Castelletti, 2016; Kwakkel et al., 2016; McPhail et al., 2018), defining the robustness of a solution constitutes itself a meta-problem (i.e., de-

ciding how to decide (Schneller and Sphicas, 1983)) as it strictly depends on the attitude of the decision makers in facing and reacting to future uncertain conditions. To address this aspect, we repeat our analysis for multiple robustness metrics, and explore how the most informative regions of the scenario space and the resulting robust solution change according to the robustness metrics selected, highlighting the relative influence of different uncertain drivers on the robustness of the solution.

5.2 Methods and tools

ROSS (Robust Optimal Scenarios Selection) is an active learning algorithm designed to identify the smallest scenario subset for generating robust solutions (Figure 5.1).

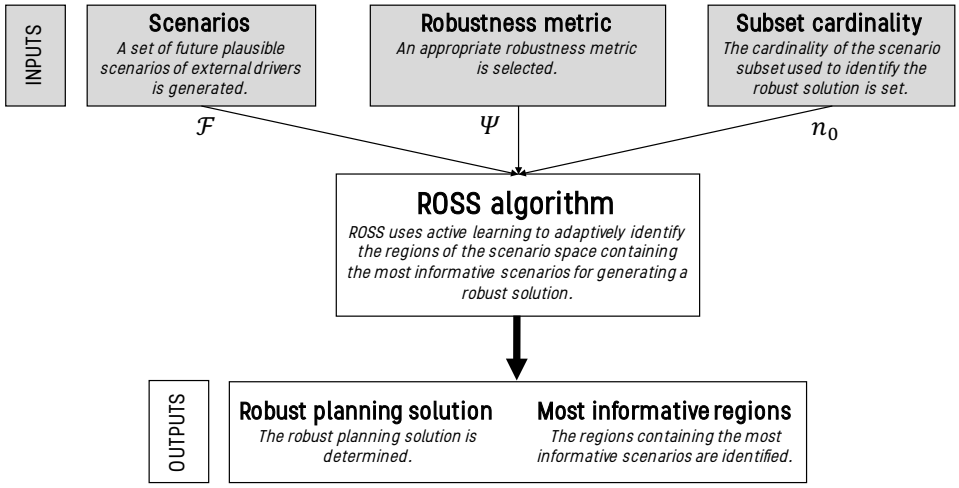

Figure 5.1: *Methodological framework. External inputs to ROSS algorithm are highlighted in grey.*

The main inputs to the algorithm are a set of future plausible scenarios $\mathcal{F}$, a robustness metric Ψ (readers should refer to McPhail et al. (2018) for an overview of the most adopted robustness metrics) used to calculate the performance of an alternative over the scenarios in $\mathcal{F}$, and the cardinality n_0 of the scenario subset to be included in the optimization process.
As a rule of thumb, n_0 is defined, according to the robustness metric selected, as the minimum number of scenarios needed to mathematically compute the robustness metric (see Section 5.3.3 for further details). However, for complex dynamic systems affected by a large set of co-varying uncertain factors, this number could be too small for identifying a robust solution. In this case n_0 has

to be increased iteratively and the algorithm relaunched until a robust solution is found. As outputs, ROSS delivers the robust planning solution and the regions of the scenario space containing the most informative scenarios (i.e., the scenarios that have the largest influence on robustness values).

5.2.1 Robust Optimal Scenario Selection

ROSS adopts an active learning (AL) algorithm that iteratively moves a Gaussian distribution function, defined on the scenario space $\mathcal{F}$, towards the regions containing the most informative scenarios. These are the scenarios for which the robustness of the optimized solution is similar (ideally equal) to that obtained when robustness is calculated over the entire scenario space. The algorithm (Algorithm 1) starts by initializing a nk-variate Gaussian distribution d, where $n = n_0$ is the cardinality of the scenario subset and k is the dimension of the scenario space $\mathcal{F}$. Then, n points are extracted according to the distribution d, which correspond to a single nk-dimensional sample from d. To ensure these sampled points align with members of the scenario space, we perform a nearest neighbour search in the scenario space with respect to the Euclidean distance between the candidate points and the scenarios in $\mathcal{F}$. The n selected scenarios constitute the scenario subset $\hat{\mathcal{F}}(n)$ for which a robust solution a^* is identified via a formal robust optimization process using the selected robustness metric Ψ as an objective. The degree of similarity between the robustness values calculated over the selected scenario subset and over the entire scenario space is then calculated using the following metric:

$$R[\%] = -\frac{|r_{opt}(a^*|\hat{\mathcal{F}}(n)) - r_{reval}(a^*|\mathcal{F})|}{r_{reval}(a^*|\mathcal{F})} \cdot 100 \tag{5.1}$$

where $r_{opt}(a^*|\hat{\mathcal{F}}(n))$ is the robustness of the optimal solution a^* calculated over the scenario subset $\hat{\mathcal{F}}(n)$ and $r_{reval}(a^*|\mathcal{F})$ is the robustness of the optimal solution a^* calculated over the entire scenario space $\mathcal{F}$. The score R, to be maximized, quantifies the absolute difference in percentage between the robustness of the optimized solution calculated over the scenario subset extracted from the Gaussian distribution d and the one computed over the entire scenario space $\mathcal{F}$. The lower this difference, the higher the score. When the score R equals zero, the two robustness calculations match and the solution optimized over the scenario subset is also robust with respect to the entire scenario space.
In order to assess the ability of the Gaussian distribution d to identify the most informative scenarios, the above mentioned steps (i.e., scenario sampling, nearest neighbour search, robust optimization, score computation) are repeated for N_{exp} times. We thus obtain a set $\Phi = (\hat{\mathcal{F}}(n), R)$ of N_{exp} elements, each composed of n scenarios and the corresponding R score. To identify the scenarios

Algorithm 1 ROSS (Robust Optimal Scenario Selection)

Inputs
- Robust planning optimization $= solution\_identification(\cdot)$,
- Evaluation method $= score(\cdot)$,
- Scenario space $\mathcal{F}$,
- Cardinality n_0 of the scenario subset,
- Algorithm parameters (M, N_{exp}, p, k).

Initialization
- Set $n = n_0$,
- Initialize an nk-variate Gaussian distribution d.

Active Learning (AL) iterations: repeat until M is reached.
for $i = 1$ to N_{exp}
- S_i: sampling of n points according to d,
- $\hat{\mathcal{F}}(n)_i$: nearest neighbour search of n scenarios in $\mathcal{F}$ closest to S_i,
- $a_i^* = solution\_identification(\hat{\mathcal{F}}(n)_i)$,
- $R_i = score(a_i^*)$.

end

$\Phi = (\hat{\mathcal{F}}(n), R)$ in descending order w.r.t. R
$\Phi' =$ first pN_{exp} elements of Φ
$d \leftarrow$ maximum likelihood distribution over Φ'

that allow the highest score to be obtained, Φ is ordered descendingly with respect to the evaluation score R and its first pN_{exp} elements are selected and included in Φ'. Then, the scenarios composing Φ' are used to update the distribution d. This corresponds to computing the nk-variate average vector and the $nk \times nk$ co-variance matrix for the scenarios in Φ'.
The AL procedure iterates until a maximum number of iterations M is reached or when the 0.1 quantile of the N_{exp} scores reaches zero. In the latter case, we can claim that ROSS is at convergence, as 90% of the pN_{exp} extraction from d identifies scenarios that allow the maximum R score value to be obtained, namely zero.
The purpose of the AL algorithm thus consists of evolving the parameters (i.e., mean, variance) of a nk-variate Gaussian distribution d so as to maximize its capability of extracting scenarios that allow high R score values to be obtained. If ROSS does not achieve convergence within M iterations, the number of scenarios included in the robust optimization process is too small for identifying a robust solution. In this case, the subset cardinality n_0 has to be increased and the algorithm relaunched.
It is worth noting that the AL parameters N_{exp} and p are strictly dependent

on the dimension nk of the distribution d, as this latter is updated considering pN_{exp} elements of Φ. In addition, the convergence of the distribution d towards the optimal regions of the scenario space is driven by the ratio p/N_{exp}. Once p is defined, the number of experiments N_{exp} has to be selected balancing the convergence speed and the ability to explore the entire scenario space.

5.3 Experiment settings

5.3.1 Formulation of the optimization problem

We focus on identifying the configuration of the hybrid energy system a^* that minimizes the objective function $J(a)$ over a given simulation horizon. The optimization problem is formulated as follows:

$$a^* = arg\min_{a}[J(a)] \tag{1}$$

where $J(a)$ represents the present value of costs and is calculated as follows:

$$J(a) = C^{cap}(a) + \sum_{y=1}^{H} \delta(y)(C^{grid} + C^{oper}(y,a) + C^{rep}(y,a) + C^{sal}(y,a)) \tag{5.2}$$

where all costs occurring at each hour t throughout the simulation horizon are aggregated on a yearly basis y. H is the number of years of the simulation horizon, $C^{cap}(a)$ are the capital costs, C^{grid} are the costs for the management of the electricity grid, and $C^{oper}(y,a)$, $C^{rep}(y,a)$, $C^{sal}(y,a)$ are the operational, replacement and salvage costs at year y, respectively. All costs, except the capital ones, are discounted using the following time varying coefficient:

$$\delta(y) = \frac{1}{(1+\gamma)^y} \tag{5.3}$$

where γ is the real discount rate, calculated as a function of the nominal discount rate γ' and the inflation rate φ:

$$\gamma = \frac{\gamma' - \varphi}{1+\varphi} \tag{5.4}$$

The capital costs occur at the beginning of the simulation horizon and represent the investment to install the power technologies, the replacement costs occur when a technology has to be substituted, and the salvage costs are negative costs which are incurred at the end of the simulation horizon, when one or more technologies have not reached the end of their lifetime. Finally, the operational costs take into account both the cost to produce 1 kWh of electricity, the cost of

maintenance of each power technology, and the cost of fuel. It is worth noting that present value of costs is dependent on both the configuration of the hybrid energy system a and the climatic conditions (i.e., wind speed, solar radiation, temperature), which significantly affect the RES power potential and, consequently, the electricity generation costs. In particular, we assume an electricity generation cost associated to RES equal to zero.
The decision variables a of Problem 1 are the PV capacity C_{PV} and the number of wind turbines n_w to be installed, defined within the following feasibility sets: $C_{PV} \in [100, 2000]$ and $n_w \in [1, 20]$. The upper bound of the feasibility sets is determined considering the small size of the island and the tight environmental constraints, which strictly limit the maximum installable RES capacity. In this work, we do not consider the number of batteries as a decision variable but we fixed the capacity of the storage system equal to the PV capacity. Even if this simplification prevents to exactly identify the optimal number of batteries to be installed, it constitutes a reasonable and conservative assumption (i.e., empty batteries could entirely store the hourly maximum PV power production) to ensure the PV electricity surplus generated in the central hours of the day to be stored in the batteries for covering the required load during the night. In addition, it allows to significantly reduce the size of the decision space, by avoiding to explore bad or even unfeasible solutions (i.e., high number of batteries and low PV capacity).
We solve Problem 1 using an exhaustive search within the feasibility set of the decision variables over 1-year evaluation period, assuming that external drivers do not change from one year to another during the simulation horizon. To do this, we sample the feasibility set of C_{PV} with a 100 kW discretization step, which is sufficiently fine to allow significant changes in the objective function to be captured (Giudici et al., 2019a). Using this discretization, the cardinality of the search space is equal to 400. The optimization is performed using the simulation model presented in Chapter 2 considering the observed desalination load l_{des} to simulate the operation of the desalination plant.

5.3.2 Scenarios

In this work, we generate climate scenarios of wind speed, solar radiation and temperature using an hybrid approach (Matrosov et al., 2013; Roach et al., 2016), which combines top-down (Haasnoot et al., 2013; Herman and Giuliani, 2018) and bottom-up (Culley et al., 2016; Shepherd et al., 2018) methods by first estimating future conditions from climate models and then enlarging the range of plausible future scenarios in order to stress-test the system of interest.
We first consider climate projections generated by five different EURO-CORDEX scenarios (see Chapter 4 for details). Since our model simulates the system over a reference year, we consider each projected year as a single scenario. Then,

we enlarge the mean annual variability of wind speed and solar radiation for stress testing our system under more variable conditions, in order to identify potential vulnerabilities. In particular, we enlarge the variability of solar radiation by +/-2% and the variability of wind speed by +/-10%. These values have been arbitrarily selected to capture more extreme conditions than the ones predicted by the EURO-CORDEX climate projections, but which are still feasible and reliable for our specific case study. We focus on these two variables as the most uncertain and the ones that are most likely to significantly affect planning decisions, as solar radiation and wind speed are the main drivers determining PV and wind power potential for a given installed capacity (see Chapter 2 for further details).
At the end of the scenario generation procedure, we obtain 3125 scenarios of hourly values of wind speed, solar radiation and temperature, composing the scenario space $\mathcal{F}$ considered in ROSS. Wind speed is clearly the driver with the largest variability, with mean annual values that range between 3.4 and 7 m/s. Solar radiation ranges between 253.8 and 272.7 W/m^2 and temperature values vary from 18.2 to 24.5 °C.

5.3.3 Robustness metrics

When dealing with robust optimization, the system performance of a candidate solution is strongly affected by the scenario considered. The objective function in Equation 5.2 thus depends on both the decision variables a and the climate scenario $w \in \Xi$. To filter the uncertainty associated to multiple climate scenarios, we consider different robustness metrics $\Psi_{\Xi}[\cdot]$, which capture different risk aversion degrees of the decision maker. The robustness metrics we consider are the following:

- *maximin*. This metric identifies the alternative a^* that attains the best performance in the worst case:

$$a^* = \arg\min_{a}(\max_{\Xi} J(a, w)) \tag{5.5}$$

  This metric, usually associated with a pessimistic point of view, allows to select the alternative that guarantees to obtain at least a certain minimum performance level independently from which scenario will realize in the future (Wald, 1950).

- *maximax*. This metric identifies the alternative a^* that attains the best performance in the best case:

$$a^* = \arg\min_{a}(\min_{\Xi} J(a, w)) \tag{5.6}$$

This metric, usually associated with an optimistic point of view, selects the alternative assuming that the best future conditions will realize (Wald, 1950).

- *Hurwicz*. This metric, called optimism-pessimism rule, combines the first two metrics, identifying the alternative a^* that attains the best weighted sum of the performance obtained in the worst case and in the best case:

$$a^* = \arg\min_{a}(\alpha \max_{\Xi} J(a, w) + (1 - \alpha) \min_{\Xi} J(a, w)) \tag{5.7}$$

  where $0 \leqslant \alpha \leqslant 1$ is a weight that specifies the relative importance associated to the realization of the worst or best future scenario. Depending on the choice of the weight α, which is strictly related to the level of risk aversion of the decision maker, this metric can be associated to a more or less pessimistic or optimistic point of view. In this work, we consider $\alpha = 0.66$ (Hurwicz, 1953).

- *Laplace*. This metric, called principle of insufficient reason, selects the alternative a^* that attains the best expected performance over the n future scenarios:

$$a^* = \arg\min_{a}(\frac{1}{n}\sum_{i=1}^{n} J(a, w_i)) \tag{5.8}$$

  This metric suggests a risk neutral aversion of the decision maker and assumes that each future scenario could realize with the same probability (Laplace, 1951).

- *mean-variance*. This metric tries to balance the expected performance and its variability over future scenarios, identifying the alternative a^* such that:

$$a^* = \arg\min_{a}(\frac{1}{n}\sum_{i=1}^{n} J(a, w_i) \cdot \underset{\Xi}{var}(J(a, w))) \tag{5.9}$$

  This metric is based on the assumption that an optimal robust solution is one whose performance is not very sensitive to the scenario that will realize in future (Hamarat et al., 2014). However, the main disadvantages of this metric are that it is not always monotonically increasing (Ray et al., 2014) and positive and negative deviations from the mean are treated equally (Takriti and Ahmed, 2004).

5.3.4 ROSS parameterization

We implement ROSS (see Section 5.2.1) for our case study using the following parameters: $M = 20$; $N_{exp} = 100$; $p = 0.1$; $k = 3$. These parameters

have been set taking into account the specific characteristics of our case study and indications reported at the end of Section 5.2.1 by means of a sensitivity analysis. In contrast, the parameter n_0, which identifies the cardinality of the scenario subset, is set according to the robustness metric selected. It is worth noting that for the maximin, maximax and Hurwicz metrics the cardinality n_0 defines exactly the minimum number of scenarios to search for, following their intrinsic formulation. In particular, for the maximin and maximax metrics, n_0 is equal to 1, as both require system performance to be evaluated for the worst and the best scenario, respectively. For the Hurwicz metric, n_0 is equal to 2, as it requires system performance to be evaluated for a weighted sum of the worst and the best scenario. For the Laplace and mean-variance metrics, n_0 is set equal to 2, as this represents the minimum number of scenarios needed to mathematically compute the metrics. Even though, in theory, this value of n_0 could be too small for identifying a robust solution and would therefore have to be increased iteratively until such a robust solution is found (see Section 5.2), this is not the case of our specific case study.

5.4 Computational experiments

ROSS is run for each of the five robustness metrics considered using the settings defined in the Section 5.3.
The computational experiments are performed on a personal computer with a 2.5 GHz Intel Core i5-3210M processor with 2 cores and 8 GB system RAM.
First, we assess the ability of ROSS to identify the most informative sub-regions of the scenario space by analysing the evolution of the R score and the Gaussian distribution d throughout the M AL iterations (Section 5.5.1). At each AL iteration, ROSS calculates N_{exp} different R scores corresponding to the N_{exp} scenario subset extractions from the same Gaussian distribution d. Since the best and the worst scores are strongly affected by outliers, we assume that ROSS is at convergence as soon as the 0.1 quantile of the scores (i.e., value under which only 10% of the scores lies) reaches zero (see Section 5.2.1).
Secondly, we assess the advantages of using ROSS in terms of computational requirements, by comparing it with a traditional robust optimization method (i.e., benchmark method), which evaluates all candidate solutions over the entire scenario space (Section 5.5.2). Since, for our case study, we determine the optimal solution using an exhaustive search within the feasibility set of the decision variables, the computational requirements are calculated in terms of system simulations multiplying the number of scenarios included in the robust optimization process (i.e., 3125) by the number of candidate solutions in the search space, namely 400 (see Section 5.3.1), resulting in a total of 1,250,000 simulations. With ROSS, this number depends on the metric considered and is

calculated by multiplying the number of AL iterations needed to reach the convergence by the subset cardinality n_0 and the number of extraction N_{exp}. At each AL iteration, ROSS solves N_{exp} robust optimization problems considering n scenarios.
Finally, in order to identify the key drivers that mostly influence system robustness, we explore how the most informative regions of the scenario space and the resulting robust solution change according to the robustness metric selected by comparing the different Gaussian distributions at convergence (Section 5.5.3).

5.5 Numerical results

5.5.1 Ability to identify the most informative sub-regions of the scenario space

Numerical results show that best and worst scores, as well as the 0.1 quantile of the N_{exp} scores, rapidly increase with the number of AL iterations, leading ROSS to reach convergence in a small number of AL iterations (12 maximum) for all the robustness metrics considered (Figure 5.2). This means that ROSS effectively moves towards the regions of the scenario space $\mathcal{F}$ containing the most informative scenarios for generating a robust solution. In particular, convergence is reached earlier for the maximin and maximax metrics (Figure 5.2a,b), which are characterized by a subset cardinality of $n_0 = 1$ and, consequently, a Gaussian distribution with $nk = 3$ dimensions only. The other metrics (Figure 5.2c-e) are characterized by a subset cardinality of $n_0 = 2$ and, thus, a Gaussian distribution with $nk = 6$ dimensions. Due to the higher dimensions of the Gaussian distribution, convergence is reached later in these cases.
Another interesting aspect related to algorithm convergence concerns the value the worst score (grey lines in Figure 5.2) assumes in the first AL iterations. As can be seen, this is strongly dependent on the metric considered and indicates the degree to which the robustness of the optimal solution is sensitive to the scenario subset considered. For example, if we consider the Laplace metric (Figure 5.2d), the worst score at the first AL iteration is about -5%, meaning that, independently from the scenarios extracted, the robustness of the optimal solution computed over that scenarios does not differ too much from the one computed over the entire scenario space. On the contrary, for the mean-variance metric (Figure 5.2e), the worst score at the first AL iteration is about -230%. In this case, the difference between the robustness of the optimal solution calculated for the scenario subset and the one computed for the entire scenario space is highly sensitive to the scenarios extracted, making the identification of the most informative regions of the scenario space more challenging. This different behavior is related to both the system dynamics of our specific case study and the intrinsic formulation of the robustness metric. In particular, the mean-variance metric

has a more complex formulation compared with the Laplace one, as it evaluates the robustness of a solution considering a combination of the average performance and the performance dispersion over the entire scenario space, making it difficult to identify a smaller number of scenarios able to generate a robustness value that is similar to the one obtained considering the entire scenario space.

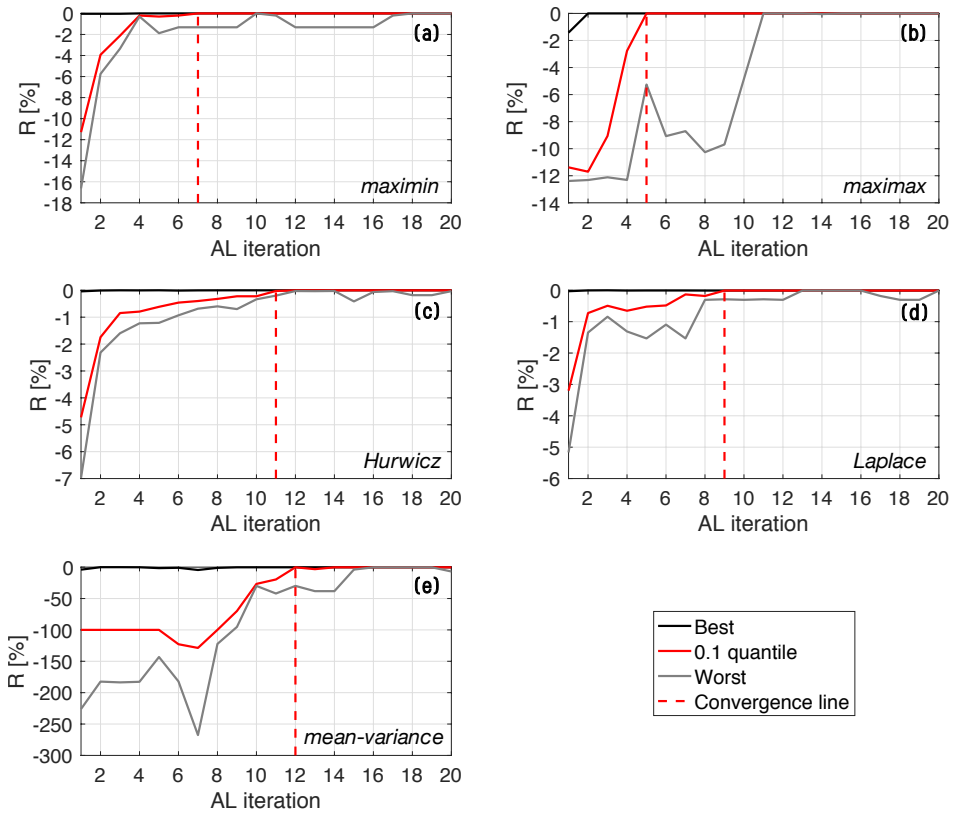

Figure 5.2: *Evolution of the score* R *throughout the AL iterations for the five metrics considered. Black, grey and red lines represent the best, worst and 0.1 quantile score among the* N_{exp} *extractions of* n *scenarios to be included in the optimization process for each AL iteration.* n *is equal to 1 for the maximin and the maximax metrics (a,b) and to 2 for the Hurwicz, Laplace and mean-variance metrics (c,d,e). The red dashed line identifies the AL iteration at convergence.*

The rapid increase in R score towards convergence is driven by the evolution of the multivariate Gaussian distribution d, according to which the scenarios to be included in the optimization process are extracted. Results show that the Gaussian distribution rapidly shrinks in the most informative regions of the scenario space: the mean identifies the most interesting regions and the variance tends to decrease throughout the AL iterations (Figure 5.3). In particular,

Figure 5.3a refers to the maximin metric and Figure 5.3b to the Hurwicz metric (see Appendix B for the other metrics). For illustrative purposes, we show the Gaussian distribution projected in the space of wind speed and solar radiation, the two drivers that mostly influence system performance. Each grey point represents a plausible scenario and each black circle represents two dimensions of the multivariate Gaussian distribution, corresponding to the two variables (i.e., wind speed and solar radiation) characterizing a scenario, with the center representing the mean and the radius three times the standard deviation (i.e, 99.7% of extraction probability is included in the circle). The upper and bottom panels refer to the first AL iteration and the AL iteration at convergence, respectively. The middle panels show an intermediate AL iteration.

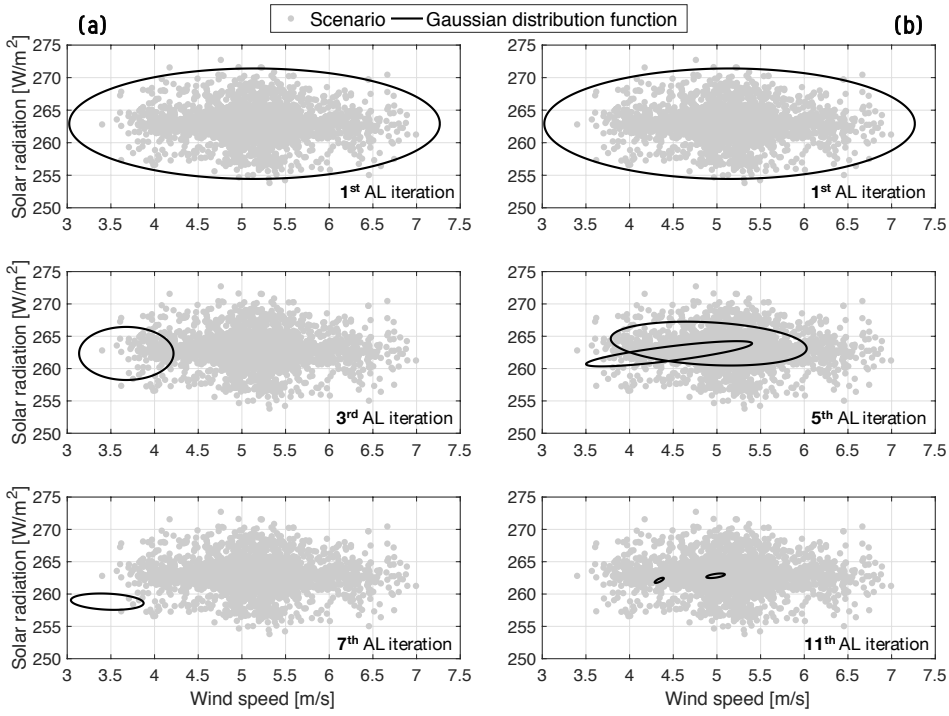

Figure 5.3: *Evolution of the Gaussian distribution projected in the space of wind speed and solar radiation for the maximin (a) and Hurwicz (b) metrics. Each grey point represents a future scenario and the black circles the Gaussian distribution functions.*

It is worth noting that for the maximin metric, there is only one circle evolving towards convergence, as the cardinality of the scenario subset is equal to 1 (Figure 5.3a). For the Hurwicz metric, there are two circles, as the cardinality of the scenario subset is equal to 2. We can observe that at the first AL iteration, the Gaussian distribution is initialized, covering the entire scenario space, so

that there is no need to precondition the algorithm to evolve towards particular regions of the scenario space. For the same reason, the two circles of the Hurwicz metric completely overlap. It is interesting to note that the variance of the Gaussian distribution at convergence for the maximin metric is higher compared with that of the Hurwicz metric. This is mainly due to the fact that, in this case, the distribution moves outside the scenario space, where no scenarios exist. As a consequence, irrespective of which point is extracted from that distribution, the nearest neighbour search (see Section 5.2.1) always identifies the same small number of scenarios included in the circle representing the distribution.

5.5.2 Increases in computational efficiency

Numerical results show that the computational efficiency gain obtained using ROSS ranges from 23% to 84%, depending on the complexity of the robustness metric and the cardinality n_0 of the scenario subset. This result suggests that in all cases, ROSS succeeds in considerably reducing the computational requirements of solving robust optimization problems by selecting the most informative scenarios to consider within the optimization process.
Table 5.1 shows the computational requirements (see Section 5.4 for details on the calculations) for each metric considered and the corresponding computational efficiency gain calculated as the percentage reduction in required system simulations with respect to the benchmark method.

Table 5.1: *Subset cardinality n_0, computational requirements in terms of number of system simulations (SS), and computational efficiency gain as percentage reduction of SS with respect to the traditional robust optimization method for the robustness metrics considered.*

Robustness metric	**Subset cardinality** (n_0)	**Computational requirements** (SE)	**Computational efficiency gain** (%)
maximin	1	280,000	78
maximax	1	200,000	84
Hurwicz	2	880,000	30
Laplace	2	720,000	55
mean-variance	2	960,000	23

The total computational time of ROSS ranges from 2.77 h for the maximax metric (84% of reduction) to 13.33 h for the mean-variance metric (23% of reduction), compared with approximately 17 h for the benchmark method. Such computational efficiency gains become more significant when considering applications on more complex systems characterized by a higher number of scenarios and where simulation-based optimization techniques are adopted

to find the robust solutions, such as the growing number of studies relying on evolutionary algorithms to solve robust optimization problems (Watson and Kasprzyk, 2017; Trindade et al., 2017, 2019).

5.5.3 Ability to identify key drivers and robust solutions for different robustness metrics

In order to explore how the most informative regions of the scenario space change according to the robustness metric selected, we show the Gaussian distribution at convergence projected in the space of wind speed and solar radiation for the five metrics considered (Figure 5.4). The Gaussian distribution circles and the corresponding most likely extracted points are represented with different colors according to the robustness metric.
We can observe that the distribution associated with the maximin metric (purple circle), which aims at selecting the best solution in the worst case, identifies a region characterized by low wind speed and low solar radiation. In our case, these conditions represent the worst possible conditions, as they significantly reduce the renewable power potential and increase the cost for electricity production. The robust solution can be thus determined by evaluating the system performance over one of the scenarios included in the purple circle.
Not surprisingly, the distribution associated with the maximax metric (green circle), which focuses on determining the best solution in the best case, identifies a region characterized by high wind speed and high solar radiation. These conditions allow the highest renewable power potential to be attained and, consequently, lower cost for electricity production.
The most informative regions associated with the Laplace metric (yellow circles) include scenarios with average values of wind speed and solar radiation, coherent with the metric definition. This result shows that the average system performance evaluated over the entire scenario space is almost equal to that evaluated over a small scenario subspace characterized by average future conditions. This behaviour suggests a direct correlation between the values of wind speed and solar radiation and system performance in terms of net present cost.
If we consider the Hurwicz metric, the solution that performs better over a weighted combination of worst and best case can be obtained by extracting scenarios from two regions (red circles) that present average values of solar radiation and average and low values of wind speed. One of these regions almost overlaps the one identified by the Laplace metric: the scenarios that are most likely to be extracted by both Laplace and Hurwic metrics are represented as orange points. The other region is instead located between maximin and Laplace, as the highest weight (i.e., 0.66) is associated with the worst case (see Section 5.3.3). We can observe that in this case, the two scenarios to be included in the

optimization process are extracted from the two regions of the scenario space that present different values of wind speed, but almost the same values of solar radiation. This suggests that wind speed is the driver that most influences system performance for a given RES installed capacity.
Finally, the regions identified for the mean-variance metric (blue circles), which aims to select the solution that performs better on average and, at the same time, has a low variance if re-evaluated over the entire scenario space, present medium-low values of solar radiation and average values of wind speed. In particular, unlike the Laplace metric, which focuses on average performance only, in this case the two regions are further apart in order to capture the variability of wind speed, which is the driver that most affects the system performance of a given solution.

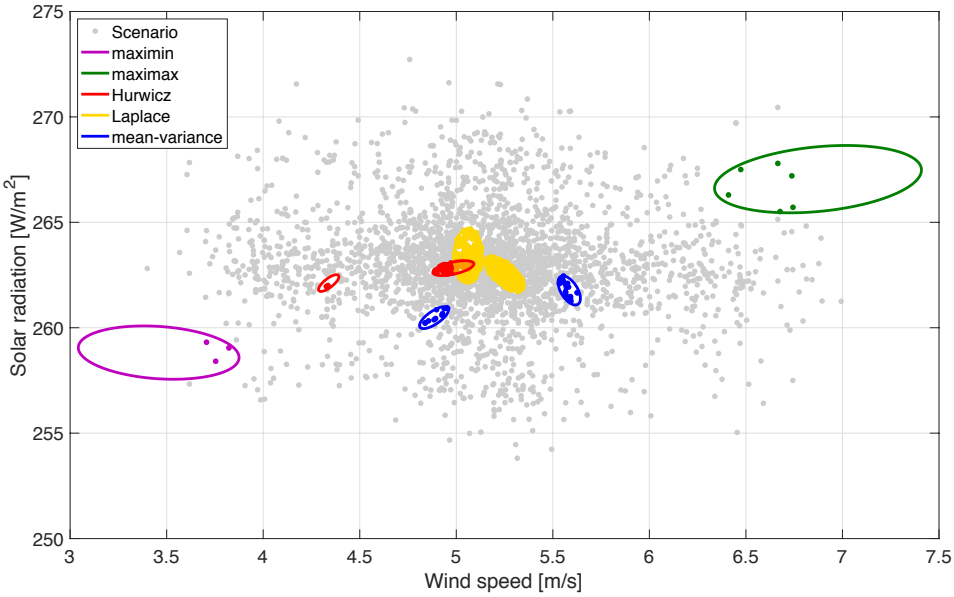

Figure 5.4: *Gaussian distribution, projected in the space of wind speed and solar radiation, at convergence with the associated most likely extracted scenarios for the five metrics considered. Each color represents a different metric. The orange scenarios are identified by both Laplace and Hurwicz metric.*

In conclusion, the robust solutions obtained for the different robustness metrics are reported in Table 5.2, in terms of PV capacity C_{PV} and number of wind turbines n_w. As expected, the maximin and mean-variance metrics result in the installation of the minimum number (i.e., 1) of wind turbines. The first metric (i.e., maximin) focuses on the worst scenario, which is characterized by very low values of wind speed. As a consequence, installing a higher number of wind

turbines would cause an increase in the capital costs without having any benefit associated with higher renewable energy production. The second metric (i.e., mean-variance) focuses on minimizing the variability of the solution performance when re-evaluated over the entire scenario space. In this case, the variability in renewable power generation due to the high variability in wind speed would increase with the number of wind turbines installed, leading to highly variable solution performance. Conversely, the maximax metric results in the installation of the maximum number (i.e., 20) of wind turbines, in order to fully exploit the high values of wind speed associated with the best scenario. In contrast, the Hurwicz and Laplace metrics result in the selection of an intermediate number of wind turbines (10 for Hurwicz and 12 for Laplace). In particular, the solution associated with the Hurwicz metric is characterized by a slightly lower number of wind turbines, as it assigns a higher weight to the worst scenario.
In contrast, the robust solution in terms of PV capacity is selected in a completely different way: the maximin and mean-variance metrics result in the installation of the maximum allowable PV capacity (i.e., 2000 kW), whereas the maximax metric results in the installation of a very low PV capacity (i.e., 900 kW). Both the Hurwicz and Laplace metrics result in the installation of a medium-high PV capacity, namely 1700 kW and 1600 kW, respectively. This is mainly due to the relative low marginal cost of PV with respect to that of the wind turbines and the very small variability of solar radiation when compared with that of wind speed. Focusing, for example, on the maximin metric, since only 1 wind turbine is installed, the capital cost of an increasing PV capacity can be easily compensated by a higher renewable power, which contributes to cover the electricity load by significantly reducing the operational costs. On the contrary, for the maximax metric, the high values of wind speed associated with the best scenario are completely exploited through the installation of 20 wind turbines. In this case, even if a high solar radiation is registered, the capital cost of an increasing PV capacity is too high with respect to the benefit in terms of renewable power production. Most of the potential renewable power would be in fact surplus without contributing to cover the electricity load.

Table 5.2: *Robust solution in terms of PV capacity (C_{PV}) and number of wind turbine (n_w) obtained considering the five different robustness metrics.*

Robustness metric	**Robust solution C_{PV}** [kW]	**Robust solution n_w** [-]
maximin	2000	1
maximax	900	20
Hurwicz	1700	10
Laplace	1600	12
mean-variance	2000	1

5.6 Conclusions

In this chapter, we propose ROSS (Robust Optimal Scenario Selection), a novel algorithm to identify the smallest scenario subset to be included in the optimal generation of robust solutions under deep uncertainty. Once the space of deeply uncertain scenarios, the robustness metric and the cardinality of the scenario subset have been defined, ROSS uses an active learning algorithm to adaptively identify the regions of the scenario space that include scenarios for which the robustness of the optimized solution is similar (or even equal) to that obtained by re-evaluating that solution over the entire scenario space.
We tested ROSS on the robust planning of a hybrid energy system on the Ustica island, Italy. The problem consists in the identification of the least cost photovoltaic (PV) and wind capacity under deep uncertainty in the main climatic variables affecting the system, namely wind speed, solar radiation and temperature.

Results show that ROSS rapidly reaches convergence (maximum 12 iterations for the more complex mean-variance metric) by identifying the regions of the scenario space containing the most informative scenarios for generating a robust solution. This results in a computational efficiency gain varying from 23% (man-variance metric) to 84% (maximax metric) compared with a traditional robust optimization approach, which is achieved by solving multiple optimization problems considering small scenario subsets. The regions identified at the end of the active learning procedure highlight the deeply uncertain future conditions that mostly influence the system robustness. Depending on the robustness metric considered, these regions are characterized by different values of the uncertain drivers.

By abstracting from this specific case study, ROSS has the ability to significantly improve existing state-of-the-art robust optimization methods with respect to two important aspects. First, ROSS allows the high computational requirements associated with the inclusion of robustness within the optimization process to be reduced significantly, by selecting a small scenario subset as the most informative for generating robust solutions. Second, ROSS identifies the key uncertain drivers to which system performance is most sensitive, as well as the values of the drives over which this occurs, in an adaptive manner using active learning. In the past, the exploration of system vulnerabilities has been conducted through a sensitivity analysis in the scenario discovery phase of most of the approaches dealing with deep uncertainty (e.g., RDM, MORDM). However, this is generally performed a-posteriori for pre-specified solutions.
Our algorithm radically changes this by directly including scenario discovery within the robust optimization process. Through a single run of the algorithm,

the regions of the scenario space that highlight system vulnerabilities are identified and exploited for generating robust solutions. These improvements can lead to significant advantages, especially when complex dynamic systems, where decisions are affected by a large ensemble of deeply uncertain co-varying factors, are involved. In these cases, system non-linearity as well as unpredictable behaviours pose great challenges in predicting how the system would perform in response to uncertain changing conditions and, consequently, in identifying system vulnerabilities and robust solutions.

Further research efforts will focus on testing ROSS for (i) solving robust joint planning and management optimization problems where the optimal system design strictly depend on the adopted control strategy, and vice-versa, and (ii) analysing more complex systems characterized by a large set of climate, socio-economic and technological uncertain and potentially interdependent drivers.

6

Conclusions and future research

6.1 Summary

Hybrid energy systems combining renewable electricity generation (e.g., PV, wind) with conventional power sources (e.g., diesel generators) and storage technologies constitute a viable and promising solution for improving the sustainability of remote off-grid islands by driving them towards complete decarbonization. Traditionally, such hybrid energy systems are designed identifying the system configuration that is able to meet load requirements by minimizing the present value of costs over a medium-to-long term horizon.

These state-of-the-art optimal design methods are useful tools for supporting the energy transitions of small islands towards more sustainable systems, yet they usually neglect key aspects and challenges that should be addressed when designing highly renewable hybrid energy systems. These include (i) the optimal control of the electricity system as well as its interconnection with other energy vectors (e.g., gas, heat) and domains (e.g., water system); (ii) the interdependency between system planning and its operation; (iii) the presence of multiple, potentially conflicting, objectives reflecting economic, environmental and other sustainability aspects; (iv) deep uncertainty in climate, technological and socio-economic conditions that may affect the system performance in the future.

Driven by the above-mentioned challenges, the overall aim of the work done in this thesis is to develop novel methodologies for supporting energy systems transition towards decarbonization, helping decision makers to identify viable

solutions at different temporal scales in light of plausible future conditions that might unfold. In particular, we develop a set of modelling and optimization tools to achieve the following specific research objectives:

- Investigating the benefits of explicitly considering the interdependency between system design and operation with respect to multiple economic, environmental and efficiency objectives.
- Assessing the vulnerability of the hybrid energy systems to the future uncertainty in the main external drivers.
- Identifying solutions that are robust with respect to the deep uncertainty in the main external drivers (i.e., solutions that perform well over a wide range of plausible future conditions).

According to this research objectives, the novel contributions of this thesis are the following:

- A novel dynamic, multi-objective approach for conjunctively optimizing the design and the operation of hybrid energy systems by focusing on the interconnection between electricity generation and water supply. The main contributions of our approach include: (i) dynamic modelling of desalination plant operations to explore the impacts that RES introduction coupled with different demand side management strategies may have on both electricity and water systems, (ii) joint optimization of system design and its operations that allows the interdependency between planning and management to be addressed directly by automatically identifying the most efficient operating policies associated with each optimal system configuration, (iii) multi-objective optimization to explore trade-offs between potentially conflicting objectives, which include, apart from present value of costs, additional aspects related to RES penetration and water supply efficiency. We test our approach by comparing it with a traditional non-dynamic, least cost optimization approach.
- A novel methodological framework to assess the vulnerability of hybrid energy systems with respect to changes in the main climate drivers (i.e., solar radiation, wind speed, temperature). More precisely, we evaluate how historical variability and future uncertainty in the climate variables affect the performance of highly renewable hybrid energy systems, designed under average historical conditions, in terms of different sustainability indicators.
- ROSS (Robust Optimal Scenario Selection), a novel algorithm that uses active learning for adaptively selecting the smallest scenario subset to be included into a robust optimization precess. ROSS contributes a twofold

novelty in the field of robust optimization under deep uncertainty. First, it allows to considerably reduce the computational requirements for the generation of robust solutions with respect to traditional optimization methods. Second, it couples scenario discovery with robust optimization for the identification of the most informative regions of the scenario space highlighting the main system vulnerabilities. We test ROSS for the robust planning of a hybrid energy system by comparing it with a traditional robust optimization method.

6.2 Take-home messages

Overall, we think that the methods proposed and developed in this research, as well as its findings, constitute important progress for the efficient design of highly renewable hybrid energy systems to lead off-grid communities towards a complete decarbonization, and considerably advance existing state-of-the-art planning optimization approaches in the field, by proposing a set of modelling and optimization tools for supporting decision makers in shaping the energy transition to more sustainable systems.

Besides the specific findings of each methodological contribution of this research, which are extensively discussed at the end of each chapter, we can here provide a list of general conclusions and take-home messages:

- Optimally controlling the flexible loads through the identification of efficient demand side management strategies is essential for achieving better system performance. In small islands, dynamically modelling the nexus between water production and electricity generation allows to identify efficient operating policies that operate the desalination plant as a non-conventional storage technology, in order to fully exploit RES power potential and, consequently, increase RES penetration and significantly reduce operational costs.
- Considering the interdependency between system design and its operations within the planning optimization phase leads to more efficient system configurations that considerably reduce the structural interventions, yet obtaining better system performance in terms of different sustainability indicators with respect to traditional design methods that consider pre-defined, static rules for operating the system. Obtaining smaller, less costly, yet more effective system configurations is extremely important in small islands where small dimensions and tight environmental constraints usually limit the RES installable capacity.
- Future uncertainty in the main climate drivers could strongly affect the

system performance of hybrid energy systems by significantly reducing the RES power potential over a medium-to-long term horizon. Considering such uncertainty when designing hybrid energy systems is thus a key point for identifying robust solutions that allow to guarantee high level of sustainability in the future. In this way, based on the level of risk aversion of the decision maker, a system configuration that performs well over a wide range of uncertain future conditions can be selected and the key drivers that highlights the main system vulnerabilities can be identified.

6.3 Future research recommendations

Starting from the main findings of this thesis, follow-up research should focus on the following aspects:

- Adopting the developed tools for evaluating the potential economic and environmental benefits of introducing novel renewable energy sources such as off-shore wind turbines and technologies exploiting energy from waves.
- Developing more sophisticated multi-energy models that, in addition to the interconnection between the electricity and the water systems, are able to accurately represent synergies and interdependencies between different energy vectors (e.g., heat, gas, electric vehicles) in order to both estimate the impacts of different economic and environmental policies and identify optimal planning and management solutions for complex multi-energy systems.
- Considering uncertainty in technological innovation (i.e., cost and efficiency of the technologies) by assessing the robustness of different hybrid system designs with respect to a large set of co-varying climate and technological future conditions, evaluating system performance according to different robustness metrics, which reflect different levels of risk aversion of the decision maker.
- Testing the developed methodological approaches on more complex systems as, for example, groups of interconnected islands for exploring the benefits of considering multiple, off-grid systems as a unique highly intra-connected system.
- Coupling the developed modelling approaches with higher spatial resolution tools (e.g., household scale) for assessing the actual feasibility of the optimal solutions based on system topography, building locations and volumes, as well as microgrid connection issues.

A

Appendix A

In the study presented in Chapter 4, we show that changes in the climate variables and, more precisely, in the wind speed, cause different effects on the RES penetration for fixed present value of costs. To understand these effects we analyse how the replacement cost and the fuel consumption change according to the scenarios considered.

Figure A.1 shows the performance of the Green solution (i.e., optimal solution that maximizes the RES penetration) over the future scenarios in terms of present value of costs (x-axis) and RES penetration (y-axis), with the color representing the cost for substituting the technologies when they reach the end of their life (Figure A.1a) and the fuel consumed during the project horizon (Figure A.1b). It is worth noting that for a fixed present value of costs the highest RES penetration is achieved with low fuel consumption and high replacement costs. This means that the higher RES potential is fully exploited through the use of the batteries, which needed to be replaced due to the higher number of charge/discharge cycles (see Chapter 2 for details). The economical advantages of reducing diesel generation are thus compensated by an increase in the costs for replacing the storage technologies. Conversely, the lowest RES penetration is achieved with high fuel consumption and low replacement costs. In this case, a lower RES potential is compensated by a higher diesel generation, causing higher fuel consumption and higher power generation costs. As a consequence, the use of batteries decreases and a reduction in the number of charge/discharge cycles leads to a decrease in the costs for replacing the storage technologies.

These results suggest the importance of considering environmental and sustainability aspects, in addition to the economical ones, for better designing hybrid energy systems, especially in context of future uncertainty in the main cli-

mate drivers.

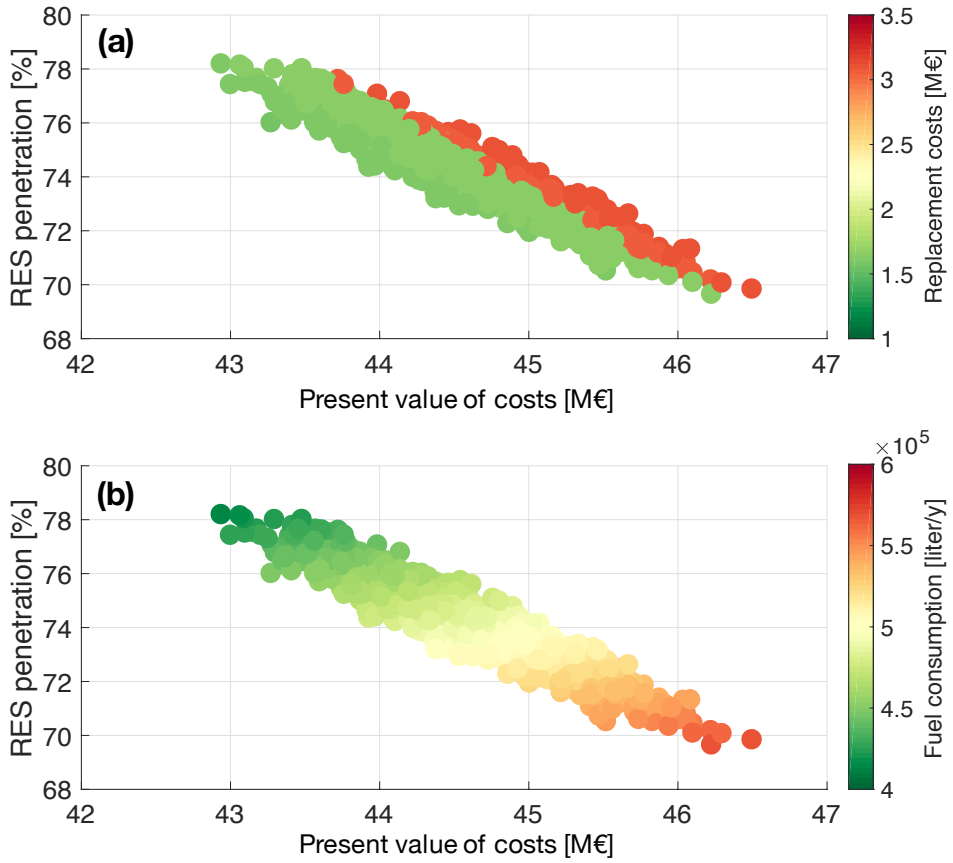

Figure A.1: *Performance of the Green solution over the future scenarios in terms of present value of costs and RES penetration with the color representing the replacement costs (a) and the fuel consumption (b).*

B

Appendix B

In the study presented in Chapter 5, we show the evolution of the Gaussian distribution function throughout the active learning (AL) iteration for the maximin and Hurwicz metrics.

Figures B.1-3 show the evolution of the Gaussian distribution functions projected in the space of wind speed and solar radiation throughout the AL iterations for the maximax (Figure B.1), Laplace (Figure B.2), and mean-variance (Figure B.3) metrics. Each grey point represents a plausible scenario and each black circle represents two dimensions of the multivariate Gaussian distribution, corresponding to the two variables (i.e., wind speed and solar radiation) characterizing a scenario, with the center representing the mean and the radius three times the standard deviation (i.e, 99.7% of extraction probability is included in the circle). The upper and bottom panels refer to the first AL iteration and the AL iteration at convergence, respectively. The middle panels show an intermediate AL iteration.

As for the metrics presented in Figure 5.3, the Gaussian distribution rapidly shrinks in the most informative regions of the scenario space: the mean identifies the most interesting regions and the variance tends to decrease throughout the AL iterations. It is worth noting that for the maximax metric, there is only one circle evolving towards convergence, as the cardinality of the scenario subset is equal to 1 (Figure B.1). For the Laplace and mean-variance metrics, there are two circles, as the cardinality of the scenario subset is equal to 2 (Figures B.2 and B.3).

It is interesting to note that, as for the maximin metric (Figure 5.3a), the variance of the Gaussian distribution at convergence for the maximax metric is higher compared with that of the other metrics (Figure B.1). This is mainly due to the

fact that, also in this case, the distribution moves outside the scenario space, where no scenarios exist. As a consequence, irrespective of which point is extracted from that distribution, the nearest neighbour search always identifies the same small number of scenarios included in the circle representing the distribution.

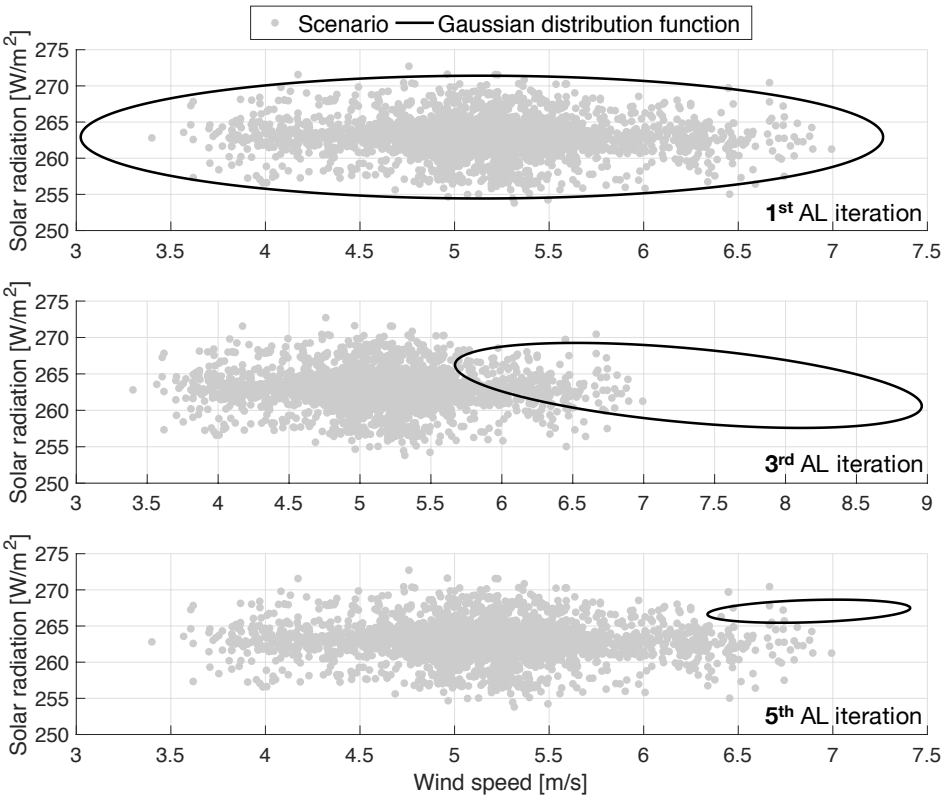

Figure B.1: *Evolution of the Gaussian distribution projected in the space of wind speed and solar radiation for the maximax metric. Each grey point represents a future scenario and the black circles the Gaussian distribution function.*

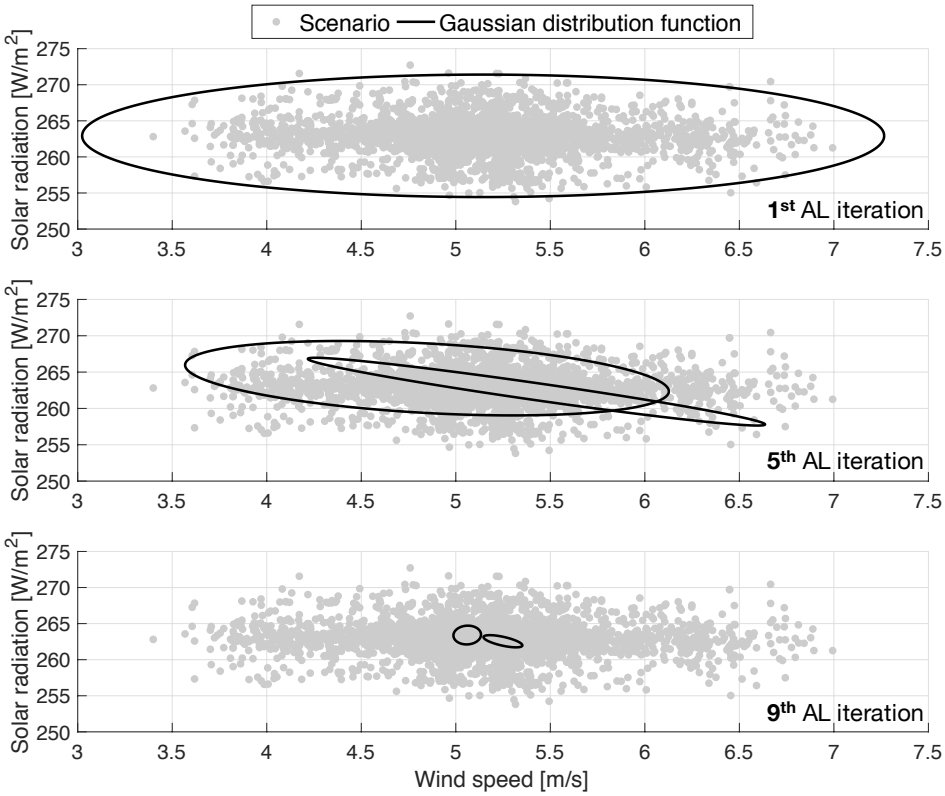

Figure B.2: *Evolution of the Gaussian distribution projected in the space of wind speed and solar radiation for the Laplace metric. Each grey point represents a future scenario and the black circles the Gaussian distribution function.*

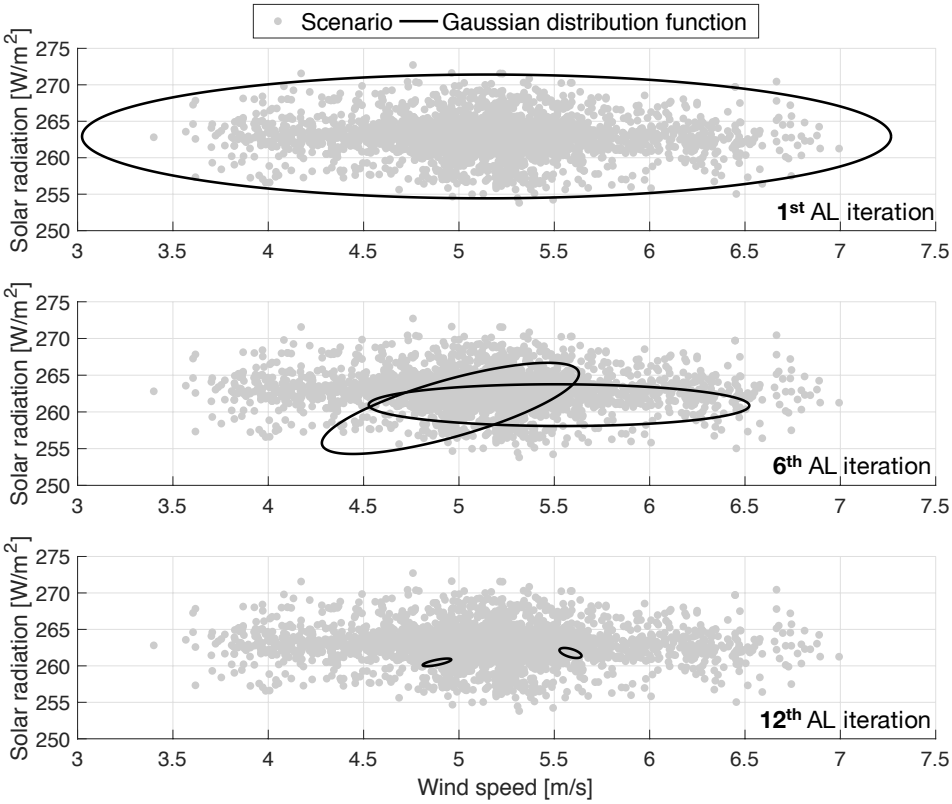

Figure B.3: *Evolution of the Gaussian distribution projected in the space of wind speed and solar radiation for the mean-variance metric. Each grey point represents a future scenario and the black circles the Gaussian distribution function.*

Bibliography

Aguiar, R., Collares-Pereira, M., 1992. TAG: a time-dependent, autoregressive, Gaussian model for generating synthetic hourly radiation. Solar energy 49 (3), 167–174.

Aksoy, H., Toprak, Z. F., Aytek, A., Ünal, N. E., 2004. Stochastic generation of hourly mean wind speed data. Renewable energy 29 (14), 2111–2131.

Anglani, N., Muliere, G., 2010. Analyzing the Impact of Renewable Energy Technologies by means of Optimal Energy Planning Tools for the energy management of local and imported resources. International Conference on Environment and Electrical Engineering (EEEIC), 1–5.

Autoritá di Regolazione per Energia Reti e Ambiente (AEEGSI), 2014. Documento per la consultazione 598/2014/R/EEL. Orientamenti per la riforma delle integrazioni tariffarie per le imprese elettriche minori non interconnesse. Tech. rep.

Basupi, I., Kapelan, Z., 2015. Flexible Water Distribution System Design under Future Demand Uncertainty. Journal of Water Resources Planning and Management 141 (4).

Beal, C. D., Gurung, T. R., Stewart, R. A., 2016. Modelling the impacts of water efficient technologies on energy intensive water systems in remote and isolated communities. Clean Technologies and Environmental Policy 18 (6), 1713–1723.
URL "http://dx.doi.org/10.1007/s10098-016-1241-9

Beh, E. H. Y., Maier, H. R., Dandy, G. C., 2015. Adaptive, multiobjective optimal sequencing approach for urban water supply augmentation under deep uncertainty. Water Resources Research 51 (3), 1529–1551.
URL https://agupubs.onlinelibrary.wiley.com/doi/abs/10.1002/2014WR016254

Beh, E. H. Y., Zheng, F., Dandy, G. C., Maier, H. R., Kapelan, Z., 2017. Robust optimization of water infrastructure planning under deep uncertainty using metamodels. Environmental Modelling & Software 93, 92–105.
URL http://www.sciencedirect.com/science/article/pii/S1364815217303018

Bhandari, B., Lee, K.-T., Lee, G.-Y., Cho, Y.-M., Ahn, S.-H., jan 2015. Optimization of hybrid renewable energy power systems: A review. International Journal of Precision Engineering and Manufacturing-Green Technology 2 (1), 99–112.
URL https://doi.org/10.1007/s40684-015-0013-z

Boé, J., Terray, L., Habets, F., Martin, E., 2007. Statistical and dynamical downscaling of the Seine basin climate for hydro-meteorological studies. International Journal of Climatology: A Journal of the Royal Meteorological Society 27 (12), 1643–1655.

Bogardi, J. J., Dudgeon, D., Lawford, R., Flinkerbusch, E., Meyn, A., Pahl-Wostl, C., Vielhauer, K., Vörösmarty, C., 2012. Water security for a planet under pressure: Interconnected challenges of a changing world call for sustainable solutions. Current Opinion in Environmental Sustainability 4 (1), 35–43.

Bognar, K., Blechinger, P., Behrendt, F., 2012. Seawater desalination in micro grids: An integrated planning approach. Energy, Sustainability and Society 2 (1), 1–12.

Bourouni, K., Barek, T. B. M., Taee, A. A., 2011. Design and optimization of desalination reverse osmosis plants driven by renewable energies using genetic algorithms. Renewable Energy 36 (3), 936–950.
URL http://dx.doi.org/10.1016/j.renene.2010.08.039

Bright, J. M., Smith, C. J., Taylor, P. G., Crook, R., 2015. Stochastic generation of synthetic minutely irradiance time series derived from mean hourly weather observation data. Solar Energy 115, 229–242.

Broad, D. R., Dandy, G. C., Maier, H. R., 2015. A systematic approach to determining metamodel scope for risk-based optimization and its application to water distribution system design. Environmental Modelling & Software 69, 382–395.
URL http://www.sciencedirect.com/science/article/pii/S1364815214003417

Brown, C., Ghile, Y., Laverty, M., Li, K., 2012. Decision scaling: Linking bottom-up vulnerability analysis with climate projections in the water sector. Water Resources Research 48 (9).
URL https://agupubs.onlinelibrary.wiley.com/doi/abs/10.1029/2011WR011212

Bryant, B. P., Lempert, R. J., 2010. Thinking inside the box: A participatory, computer-assisted approach to scenario discovery. Technological Forecasting and Social Change 77 (1), 34–49.

Busoniu, L., Ernst, D., De Schutter, B., Babuška, R., 2011. Cross-entropy optimization of control policies with adaptive basis functions. IEEE Transactions on Systems, Man, and Cybernetics, Part B: Cybernetics 41 (1), 196–209.

Caralis, G., Zervos, A., 2007. Analysis of the combined use of wind and pumped storage systems in autonomous Greek islands. IET Renewable Power Generation 1 (1), 49.

Carvalho, D., Rocha, A., Gómez-Gesteira, M., Santos, C. S., 2017. Potential impacts of climate change on European wind energy resource under the CMIP5 future climate projections. Renewable energy 101, 29–40.

Castelletti, A., Antenucci, J. P., Limosani, D., Quach Thi, X., Soncini-Sessa, R., 2011. Interactive response surface approaches using computationally intensive models for multiobjective planning of lake water quality remediation. Water Resources Research 47 (9).

Castelletti, A., Galelli, S., Ratto, M., Soncini-Sessa, R., Young, P. C., 2012a. A general framework for dynamic emulation modelling in environmental problems. Environmental Modelling & Software 34, 5–18.

Castelletti, A., Galelli, S., Restelli, M., Soncini-Sessa, R., 2012b. Data-driven dynamic emulation modelling for the optimal management of environmental systems. Environmental Modelling & Software 34, 30–43.
URL http://www.sciencedirect.com/science/article/pii/S1364815211002015

Chalakatevaki, M., Stamou, P., Karali, S., Daniil, V., Dimitriadis, P., Tzouka, K., Iliopoulou, T., Koutsoyiannis, D., Papanicolaou, P., Nikos Mamassis, A., 2017. Creating the electric energy mix in a non-connected island. Energy Procedia 125, 425–434.
URL http://dx.doi.org/10.1016/j.egypro.2017.08.089

Chester, L., 2010. Conceptualising energy security and making explicit its polysemic nature. Energy Policy 38 (2), 887–895.
URL http://dx.doi.org/10.1016/j.enpol.2009.10.039

Ciriminna, R., Pagliaro, M., Meneguzzo, F., Pecoraino, M., 2016. Solar energy for Sicily's remote islands: On the route from fossil to renewable energy. International Journal of Sustainable Built Environment 5 (1), 132–140.
URL http://dx.doi.org/10.1016/j.ijsbe.2016.04.003

Clarke, D. P., Al-Abdeli, Y. M., Kothapalli, G., 2015. Multi-objective optimisation of renewable hybrid energy systems with desalination. Energy 88, 457–468.
URL http://dx.doi.org/10.1016/j.energy.2015.05.065

Coello Coello, C. A., Lamont, G. B., Veldhuizen, D. a. V., 2007. Evolutionary Algorithms for Solving Multi-Objective Problems. Genetic and Evolutionary Computation Series. Springer US, Boston, MA.
URL http://link.springer.com/10.1007/978-0-387-36797-2

Cohn, D. A., Ghahramani, Z., Jordan, M. I., 1996. Active learning with statistical models. Journal of artificial intelligence research 4, 129–145.

Culley, S., Noble, S., Yates, A., Timbs, M., Westra, S., Maier, H. R., Giuliani, M., Castelletti, A., 2016. A bottom-up approach to identifying the maximum operational adaptive capacity of water resource systems to a changing climate. Water Resources Research 52 (9), 6751–6768.
URL https://agupubs.onlinelibrary.wiley.com/doi/abs/10.1002/2015WR018253

Deb, K., 2011. Multi-objective Optimisation Using Evolutionary Algorithms: An Introduction. Springer London, London, pp. 3–34.
URL https://doi.org/10.1007/978-0-85729-652-8{_}1

Debele, B., Srinivasan, R., Parlange, J. Y., 2007. Accuracy evaluation of weather data generation and disaggregation methods at finer timescales. Advances in Water Resources 30 (5), 1286–1300.

Dessai, S., Hulme, M., Lempert, R., Pielke Jr., R., 2009. Do We Need Better Predictions to Adapt to a Changing Climate? Eos, Transactions American Geophysical Union 90 (13), 111–112.
URL https://agupubs.onlinelibrary.wiley.com/doi/abs/10.1029/2009EO130003

Dong, W., Li, Y., Xiang, J., 2016. Optimal sizing of a stand-alone hybrid power system based on battery/hydrogen with an improved ant colony optimization. Energies 9 (10).

Douglas, C. H., 2006. Small Island States and Territories: Sustainable Development Issues and Strategies. Challenges for Changing Islands in a Changing World. Sustainable Development 14, 75–80.

Duffie, J. A., Beckman, W. A., 2013. Solar engineering of thermal processes. John Wiley & Sons.

Duić, N., Da Graça Carvalho, M., 2004. Increasing renewable energy sources in island energy supply: Case study Porto Santo. Renewable and Sustainable Energy Reviews 8 (4), 383–399.

Ekren, B. Y., Ekren, O., 2009. Simulation based size optimization of a PV/wind hybrid energy conversion system with battery storage under various load and auxiliary energy conditions. Applied Energy 86 (9), 1387–1394.
URL http://dx.doi.org/10.1016/j.apenergy.2008.12.015

Elbaset, A. A., 2011. Design, modeling and control strategy of PV/FC hybrid power system. Journal of Electrical Systems 7, 270–286.

Erdinc, O., Uzunoglu, M., 2012. Optimum design of hybrid renewable energy systems: Overview of different approaches. Renewable and Sustainable Energy Reviews 16 (3), 1412–1425.

European Commission (EC), 2009. Decision No 406/2009/EC of the European Parliament and of the Council of 23 April 2009 on the Effort ofMember States to Reduce Their Greenhouse Gas Emissions toMeet the Community's Greenhouse Gas Emission Reduction Commitments up to 2020. Tech. rep., European Commission, Brussels.

European Commission (EC), 2011. Communication from the commission to the European Parliament, the Council, the European economic and social committee and the committee of the regions. Energy Roadmap 2050. Tech. rep., European Commission, Brussels.

European Commission (EC), 2016. EU Reference Scenario 2016. Energy, Transport and GHG Emissions. Trends to 2050. Tech. rep.

European Commission (EC), 2017. Political Declaration on Clean Energy for EU Islands.
URL https://ec.europa.eu/energy

Fant, C., Schlosser, C. A., Strzepek, K., 2016. The impact of climate change on wind and solar resources in southern Africa. Applied Energy 161, 556–564.
URL http://www.sciencedirect.com/science/article/pii/S0306261915003268

French, S., 1986. Decision Theory: An Introduction to the Mathematics of Rationality. Halsted Press, New York.

Ghalavand, Y., Hatamipour, M. S., Rahimi, A., 2015. A review on energy consumption of desalination processes. Desalination and Water Treatment 54 (6), 1526–1541.
URL https://doi.org/10.1080/19443994.2014.892837

Ghile, Y. B., Taner, M. Ü., Brown, C., Grijsen, J. G., Talbi, A., jan 2014. Bottom-up climate risk assessment of infrastructure investment in the Niger River Basin. Climatic Change 122 (1), 97–110.
URL https://doi.org/10.1007/s10584-013-1008-9

Giudici, F., Castelletti, A., Garofalo, E., Giuliani, M., Maier, H. R., 2019a. Dynamic, multi-objective optimal design and operation of water-energy systems for small, off-grid islands. Applied Energy 250, 605–616.

Giudici, F., Castelletti, A., Garofalo, E., Maier, H. R., 2019b. Exploring the effects of climate change and technological innovation on the robust design of off-grid hybrid energy systems. Nature Energy (in preparation).

Giudici, F., Castelletti, A., Giuliani, M., Maier, H. R., 2019c. An active learning approach for identifying the smallest subset of informative scenarios for robust planning under deep uncertainty. Environmental Modelling & Software (Under Review).

Giuliani, M., Castelletti, A., apr 2016. Is robustness really robust? How different definitions of robustness impact decision-making under climate change. Climatic Change 135 (3), 409–424.
URL https://doi.org/10.1007/s10584-015-1586-9

Giuliani, M., Castelletti, A., Pianosi, F., Mason, E., Reed, P. M., 2016. Curses, Tradeoffs, and Scalable Management: Advancing Evolutionary Multiobjective Direct Policy Search to Improve Water Reservoir Operations. Journal of Water Resources Planning and Management 142 (2), 04015050.
URL http://ascelibrary.org/doi/10.1061/(ASCE)WR.1943-5452.0000570

Haasnoot, M., Kwakkel, J. H., Walker, W. E., ter Maat, J., 2013. Dynamic adaptive policy pathways: A method for crafting robust decisions for a deeply uncertain world. Global Environmental Change 23 (2), 485–498.
URL http://www.sciencedirect.com/science/article/pii/S095937801200146X

Hadka, D., Reed, P., 2013. Borg: An auto-adaptive many-objective evolutionary computing framework. Evolutionary Computation 21 (2), 231–259.

Hakimi, S., Tafreshi, S., Kashefi, A., 2007. Unit Sizing of a Stand-alone Hybrid Power System Using Particle Swarm Optimization (PSO). 2007 IEEE International Conference on Automation and Logistics, 3107–3112.

Hall, J. W., Lempert, R. J., Keller, K., Hackbarth, A., Mijere, C., McInerney, D. J., 2012. Robust Climate Policies Under Uncertainty: A Comparison of Robust Decision Making and Info-Gap Methods. Risk Analysis 32 (10), 1657–1672.
URL https://onlinelibrary.wiley.com/doi/abs/10.1111/j.1539-6924.2012.01802.x

Hamarat, C., Kwakkel, J. H., Pruyt, E., Loonen, E. T., 2014. An exploratory approach for adaptive policymaking by using multi-objective robust optimization. Simulation Modelling Practice and Theory 46, 25–39.
URL http://www.sciencedirect.com/science/article/pii/S1569190X14000380

Hamiche, A. M., Stambouli, A. B., Flazi, S., 2016. A review of the water-energy nexus. Renewable and Sustainable Energy Reviews 65, 319–331.
URL http://dx.doi.org/10.1016/j.rser.2016.07.020

Harrison, P. A., Dunford, R., Savin, C., Rounsevell, M. D. A., Holman, I. P., Kebede, A. S., Stuch, B., feb 2015. Cross-sectoral impacts of climate change and socio-economic change for multiple, European land- and water-based sectors. Climatic Change 128 (3), 279–292.
URL https://doi.org/10.1007/s10584-014-1239-4

Hashimoto, T., Stedinger, J. R., Loucks, D. P., 1982. Reliability, resiliency, and vulnerability criteria for water resource system performance evaluation. Water Resources Research 18 (1), 14–20.

Herman, J. D., Giuliani, M., 2018. Policy tree optimization for threshold-based water resources management over multiple timescales. Environmental Modelling & Software 99, 39–51.
URL http://www.sciencedirect.com/science/article/pii/S1364815217306540

Herman, J. D., Reed, P. M., Zeff, H. B., Characklis, G. W., 2015. How Should Robustness Be Defined for Water Systems Planning under Change? Journal of Water Resources Planning and Management 141 (10).

Herman, J. D., Zeff, H. B., Reed, P. M., Characklis, G. W., 2014. Beyond optimality: Multistakeholder robustness tradeoffs for regional water portfolio planning under deep uncertainty. Water Resources Research 50 (10), 7692–7713.
URL https://agupubs.onlinelibrary.wiley.com/doi/abs/10.1002/2014WR015338

Hijioka, Y., Matsuoka, Y., Nishimoto, H., Masui, T., Kainuma, M., 2008. Global GHG emission scenarios under GHG concentration stabilization targets. Journal of Global Environment Engineering 13, 97–108.

Hurwicz, L., 1953. Optimality criterion for decision making under ignorance.

Ibrahim, H., Younès, R., Ilinca, A., Dimitrova, M., Perron, J., 2010. Study and design of a hybrid wind-diesel-compressed air energy storage system for remote areas. Applied Energy 87 (5), 1749–1762.
URL http://dx.doi.org/10.1016/j.apenergy.2009.10.017

Ibrahim, H., Younès, R., Ilinca, A., Ramdenee, D., Dimitrova, M., Perron, J., Adegnon, M., Boulay, D., Arbez, C., 2011. Potential of a hybrid wind-diesel-compressed air system for nordic remote canadian areas. Energy Procedia 6, 795–804.

Intergovernmental Panel on Climate Change (IPCC), 2014. Climate Change 2014: Impacts, adaptation and vulnerability. Part a: Global and sectoral aspects. Tech. rep., Intergovernmental Panel on Climate Change.

International Renewable Energy Agency (IRENA), 2013. International off-grid renewable energy conference. Key findings and recommendations. Tech. rep., International Renewable Energy Agency, Abu Dhabi.

International Renewable Energy Agency (IRENA), 2015. Off-grid renewable energy systems: Status and methodological issues. Tech. rep., International Renewable Energy Agency.

Jerez, S., Tobin, I., Vautard, R., Montávez, J. P., López-Romero, J. M., Thais, F., Bartok, B., Christensen, O. B., Colette, A., Déqué, M., Others, 2015. The impact of climate change on photovoltaic power generation in Europe. Nature communications 6, 10014.

Kakazu, H., 1994. Sustainable development of small island economies. Westview Press, Inc., Boulder, Colorado, USA.

Kaldellis, J. K., 2010. Stand-alone and hybrid wind energy systems: technology, energy storage and applications. Elsevier.

Kaldellis, J. K., Gkikaki, A., Kaldelli, E., Kapsali, M., 2012. Investigating the energy autonomy of very small non-interconnected islands. A case study: Agathonisi, Greece. Energy for Sustainable Development 16 (4), 476–485.
URL http://dx.doi.org/10.1016/j.esd.2012.08.002

Kaldellis, J. K., Kavadias, K. A., Kondili, E., 2004. Renewable energy desalination plants for the Greek islands - Technical and economic considerations. Desalination 170 (2), 187–203.

Kaldellis, J. K., Kavadias, K. A., Kondili, E., 2006. Energy and clean water coproduction in remote islands to face the intermittent character of wind energy. International Journal of Global Energy Issues (IJGEI) 25 (3/4).

Kalogirou, S. A., 2005. Seawater desalination using renewable energy sources. Progress in Energy and Combustion Science 31 (3), 242–281.

Karagiannis, I. C., Soldatos, P. G., 2007. Current status of water desalination in the Aegean Islands. Desalination 203 (1-3), 56–61.

Kasprzyk, J. R., Nataraj, S., Reed, P. M., Lempert, R. J., 2013. Many objective robust decision making for complex environmental systems undergoing change. Environmental Modelling & Software 42, 55–71.
URL http://www.sciencedirect.com/science/article/pii/S1364815212003131

Kaygusuz, K., 2011. Energy services and energy poverty for sustainable rural development. Renewable and Sustainable Energy Reviews 15 (2), 936–947.
URL http://dx.doi.org/10.1016/j.rser.2010.11.003

Khatib, T., Elmenreich, W., 2015. A model for hourly solar radiation data generation from daily solar radiation data using a generalized regression artificial neural network. International Journal of Photoenergy 2015.

Koutroulis, E., Kolokotsa, D., Potirakis, A., Kalaitzakis, K., 2006. Methodology for optimal sizing of stand-alone photovoltaic/wind-generator systems using genetic algorithms. Solar Energy 80 (9), 1072–1088.

Koutsoyiannis, D., Makropoulos, C., Langousis, A., Baki, S., Efstratiadis, A., Christofides, A., Karavokiros, G., Mamassis, N., 2009. HESS opinions: "Climate, hydrology, energy, water: Recognizing uncertainty and seeking sustainability". Hydrology and Earth System Sciences 13 (2), 247–257.
URL https://www.hydrol-earth-syst-sci.net/13/247/2009/

Kristoferson, L., O'Keefe, P., Soussan, J., 1985. Energy in Small Island Economies. Ambio 14 (4/5), 242–244.
URL http://www.jstor.org/stable/4313156

Kwakkel, J. H., Eker, S., Pruyt, E., 2016. How Robust is a Robust Policy? Comparing Alternative Robustness Metrics for Robust Decision-Making. Robustness Analysis in Decision Aiding, Optimization, and Analytics, 221–237.
URL https://doi.org/10.1007/978-3-319-33121-8{_}10

Lacavalla, M., Bonanno, R., Sperati, S., 2017. Definizione di un dataset di rianalisi meteorologica per lo studio di eventi meteo rilevanti per il sistema elettrico italiano. Deliverable 11, PAR 2017.

Lall, U., Sharma, A., 1996. A nearest neighbor bootstrap for resampling hydrologic time series. Water Resources Research 32 (3), 679–693.

Laplace, P. S., 1951. A Philosophical Essay on Probabilities, 6th Edition. Dover Publications, New York.

Larsen, G. K., van Foreest, N. D., Scherpen, J. M., 2014. Power supply-demand balance in a Smart Grid: An information sharing model for a market mechanism. Applied Mathematical Modelling 38 (13), 3350–3360.
URL http://dx.doi.org/10.1016/j.apm.2013.11.042

Lechón, Y., De La Rúa, C., Cabal, H., 2018. Impacts of Decarbonisation on the Water-Energy-Land (WEL) Nexus: A Case Study of the Spanish Electricity Sector. Energies 11 (5), 1203.

Lempert, R. J., 2002. A new decision sciences for complex systems. Proceedings of the National Academy of Sciences 99 (suppl 3), 7309–7313.
URL https://www.pnas.org/content/99/suppl{_}3/7309

Lempert, R. J., Collins, M. T., 2007. Managing the Risk of Uncertain Threshold Responses: Comparison of Robust, Optimum, and Precautionary Approaches. Risk Analysis 27 (4), 1009–1026.
URL https://onlinelibrary.wiley.com/doi/abs/10.1111/j.1539-6924.2007.00940.x

Lempert, R. J., Popper, S. W., Bankes, S. C., 2003. Shaping the Next One Hundred Years: New Methods for Quantitative, Long-term Policy Analysis. RAND Corporation, Santa Monica CA.

Lempert, R. J., Schlesinger, M. E., jun 2000. Robust Strategies for Abating Climate Change. Climatic Change 45 (3), 387–401.
URL https://doi.org/10.1023/A:1005698407365

Lubega, W. N., Farid, A. M., 2014. Quantitative engineering systems modeling and analysis of the energy-water nexus. Applied Energy 135, 142–157.
URL http://dx.doi.org/10.1016/j.apenergy.2014.07.101

Luna-Rubio, R., Trejo-Perea, M., Vargas-Vázquez, D., Ríos-Moreno, G. J., 2012. Optimal sizing of renewable hybrids energy systems: A review of methodologies. Solar Energy 86 (4), 1077–1088.

Macknick, J., Sattler, S., Averyt, K., Clemmer, S., Rogers, J., 2012. The water implications of generating electricity: Water use across the United States based on different electricity pathways through 2050. Environmental Research Letters 7 (4).

Magnano, L., Boland, J. W., Hyndman, R. J., 2008. Generation of synthetic sequences of half-hourly temperature. Environmetrics: The official journal of the International Environmetrics Society 19 (8), 818–835.

Mahmoud, M., Liu, Y., Hartmann, H., Stewart, S., Wagener, T., Semmens, D., Stewart, R., Gupta, H., Dominguez, D., Dominguez, F., Hulse, D., Letcher, R., Rashleigh, B., Smith, C., Street, R., Ticehurst, J., Twery, M., van Delden, H., Waldick, R., White, D., Winter, L., 2009. A formal framework for scenario development in support of environmental decision-making. Environmental Modelling & Software 24 (7), 798–808.
URL http://www.sciencedirect.com/science/article/pii/S1364815208002211

Maier, H. R., Guillaume, J. H. A., van Delden, H., Riddell, G. A., Haasnoot, M., Kwakkel, J. H., 2016. An uncertain future, deep uncertainty, scenarios, robustness and adaptation: How do they fit together? Environmental Modelling and Software 81, 154–164.
URL http://dx.doi.org/10.1016/j.envsoft.2016.03.014

Maier, H. R., Razavi, S., Kapelan, Z., Matott, L. S., Kasprzyk, J., Tolson, B. A., 2019. Introductory overview: Optimization using evolutionary algorithms and other metaheuristics. Environmental Modelling & Software 114, 195–213.
URL http://www.sciencedirect.com/science/article/pii/S1364815218305905

Matrosov, E. S., Padula, S., Harou, J. J., mar 2013. Selecting Portfolios of Water Supply and Demand Management Strategies Under Uncertainty - Contrasting Economic Optimisation and 'Robust Decision Making' Approaches. Water Resources Management 27 (4), 1123–1148.
URL https://doi.org/10.1007/s11269-012-0118-x

McPhail, C., Maier, H. R., Kwakkel, J. H., Giuliani, M., Castelletti, A., Westra, S., 2018. Robustness Metrics: How Are They Calculated, When Should They Be Used and Why Do They Give Different Results? Earth's Future 6 (2), 169–191.
URL https://agupubs.onlinelibrary.wiley.com/doi/abs/10.1002/2017EF000649

Mentis, D., Karalis, G., Zervos, A., Howells, M., Taliotis, C., Bazilian, M., Rogner, H., 2016. Desalination using renewable energy sources on the arid islands of South Aegean Sea. Energy 94, 262–272.
URL http://dx.doi.org/10.1016/j.energy.2015.11.003

Merei, G., Berger, C., Sauer, D. U., 2013. Optimization of an off-grid hybrid PV–Wind–Diesel system with different battery technologies using genetic algorithm. Solar Energy 97, 460–473.

Mizani, S., Yazdani, A., 2009. Design and operation of a remote microgrid. IECON Proceedings (Industrial Electronics Conference), 4299–4304.

Mohamed, M., Eltamaly, A., 2018. A PSO-Based Smart Grid Application for Optimum Sizing of Hybrid Renewable Energy Systems. Studies in Systems, Decision and Control, 53–60.

Mohtar, R. H., Lawford, R., 2016. Present and future of the water-energy-food nexus and the role of the community of practice. Journal of Environmental Studies and Sciences 6 (1), 192–199.

Moody, P., Brown, C., 2013. Robustness indicators for evaluation under climate change: Application to the upper Great Lakes. Water Resources Research 49 (6), 3576–3588.
URL https://doi.org/10.1002/wrcr.20228

Moss, R. H., Edmonds, J. A., Hibbard, K. A., Manning, M. R., Rose, S. K., Van Vuuren, D. P., Carter, T. R., Emori, S., Kainuma, M., Kram, T., Others, 2010. The next generation of scenarios for climate change research and assessment. Nature 463 (7282), 747.

Nazemi, A. A., Wheater, H. S., 2014. Assessing the Vulnerability of Water Supply to Changing Streamflow Conditions. Eos, Transactions American Geophysical Union 95 (32), 288.
URL https://agupubs.onlinelibrary.wiley.com/doi/abs/10.1002/2014EO320007

Nolan, P., Lynch, P., McGrath, R., Semmler, T., Wang, S., 2012. Simulating climate change and its effects on the wind energy resource of Ireland. Wind Energy 15 (4), 593–608.

Olsson, G., 2015. Water and energy: threats and opportunities. IWA publishing.

Palone, F., Portoghese, P., Buono, L., Necci, A., Rosati, C., Rosati, D., 2017. Replacing diesel generators with hybrid renewable power plants: Giannutri Smart Island project. In: Conference Proceedings - 2017 17th IEEE International Conference on Environment and Electrical Engineering and 2017 1st IEEE Industrial and Commercial Power Systems Europe, EEEIC / I and CPS Europe 2017.

Papaefthymiou, S. V., Karamanou, E. G., Papathanassiou, S. A., Papadopoulos, M. P., 2010. A Wind Hydro Pumped Storage Station Leading to High RES Penetration in the Autonomous Island System of Ikaria. IEEE TRANSACTIONS ON SUSTAINABLE ENERGY 1 (3).

Pašičko, R., Branković, Č., Šimić, Z., 2012. Assessment of climate change impacts on energy generation from renewable sources in Croatia. Renewable Energy 46, 224–231.

Pate, R., Hightower, M., Cameron, C., Einfeld, W., 2007. Overview of Energy-Water Interdependencies and the emerging energy demands on Water Resources. Tech. rep.

Patlitzianas, K. D., Christos, K., 2012. Effective financing for provision of renewable electricity and water supply on islands. Energy for Sustainable Development 16 (1), 120–124.
URL http://dx.doi.org/10.1016/j.esd.2011.11.003

Patlitzianas, K. D., Ntotas, K., Doukas, H., Psarras, J., 2007. Assessing the renewable energy producers' environment in EU accession member states. Energy Conversion and Management 48 (3), 890–897.

Paton, F. L., Maier, H. R., Dandy, G. C., 2014. Including adaptation and mitigation responses to climate change in a multiobjective evolutionary algorithm framework for urban water supply systems incorporating GHG emissions. Water Resources Research 50 (8), 6285–6304.
URL https://agupubs.onlinelibrary.wiley.com/doi/abs/10.1002/2013WR015195

Poff, N. L., Brown, C. M., Grantham, T. E., Matthews, J. H., Palmer, M. A., Spence, C. M., Wilby, R. L., Haasnoot, M., Mendoza, G. F., Dominique, K. C., Baeza, A., sep 2015. Sustainable water management under future uncertainty with eco-engineering decision scaling. Nature Climate Change 6, 25.

Poggi, P., Notton, G., Muselli, M., Louche, A., 2000. Stochastic study of hourly total solar radiation in Corsica using a Markov model. International journal of climatology 20 (14), 1843–1860.

Pryor, S. C., Barthelmie, R. J., 2010. Climate change impacts on wind energy: A review. Renewable and Sustainable Energy Reviews 14 (1), 430–437.
URL http://www.sciencedirect.com/science/article/pii/S1364032109001713

Quinn, J. D., Reed, P. M., Giuliani, M., Castelletti, A., 2017. Rival framings: A framework for discovering how problem formulation uncertainties shape risk management trade-offs in water resources systems. Water Resources Research 53 (8), 7208–7233.
URL https://agupubs.onlinelibrary.wiley.com/doi/abs/10.1002/2017WR020524

Quinn, J. D., Reed, P. M., Giuliani, M., Castelletti, A., Oyler, J. W., Nicholas, R. E., 2018. Exploring How Changing Monsoonal Dynamics and Human Pressures Challenge Multireservoir Management for Flood Protection, Hydropower Production, and Agricultural Water Supply. Water Resources Research 54 (7), 4638–4662.
URL https://agupubs.onlinelibrary.wiley.com/doi/abs/10.1029/2018WR022743

Ray, P. A., Watkins Jr., D. W., Vogel, R. M., Kirshen, P. H., 2014. Performance-Based Evaluation of an Improved Robust Optimization Formulation. Journal of Water Resources Planning and Management 140 (6).

Rehman, S., El-Amin, I., Ahmad, F., M. Shaahid, S., M. Al-Shehri, A., Bakhashwain, J., Shash, A., 2007. Feasibility study of hybrid retrofits to an isolated off-grid diesel power plant. Renewable and Sustainable Energy Reviews 11, 635–653.

Roach, T., Kapelan, Z., Ledbetter, R., Ledbetter, M., 2016. Comparison of Robust Optimization and Info-Gap Methods for Water Resource Management under Deep Uncertainty. Journal of Water Resources Planning and Management 142 (9).

Salazar, J. Z., Reed, P. M., Quinn, J. D., Giuliani, M., Castelletti, A., 2017. Balancing exploration, uncertainty and computational demands in many objective reservoir optimization. Advances in Water Resources 109, 196–210.
URL http://www.sciencedirect.com/science/article/pii/S0309170817305419

Santhosh, A., Farid, A. M., Youcef-Toumi, K., 2014. Real-time economic dispatch for the supply side of the energy-water nexus. Applied Energy 122, 42–52.
URL http://dx.doi.org/10.1016/j.apenergy.2014.01.062

Sawle, Y., Gupta, S. C., Bohre, A. K., 2018. Review of hybrid renewable energy systems with comparative analysis of off-grid hybrid system. Renewable and Sustainable Energy Reviews 81, 2217–2235.

Schaeffer, R., Szklo, A. S., de Lucena, A. F. P., Borba, B. S. M. C., Nogueira, L. P. P., Fleming, F. P., Troccoli, A., Harrison, M., Boulahya, M. S., 2012. Energy sector vulnerability to climate change: A review. Energy 38 (1), 1–12.
URL http://www.sciencedirect.com/science/article/pii/S0360544211007870

Schneller, G. O., Sphicas, G. P., 1983. Decision making under uncertainty: Starr's domain criterion. Theory and Decision 15 (4), 321–336.

Scott, C. A., Kurian, M., Wescoat, J. L., 2015. The Water-Energy-Food Nexus: Enhancing Adaptive Capacity to Complex Global Challenges. Springer International Publishing, Cham, pp. 15–38.
URL https://doi.org/10.1007/978-3-319-05747-7{_}2

Scott, C. A., Pierce, S. A., Pasqualetti, M. J., Jones, A. L., Montz, B. E., Hoover, J. H., 2011. Policy and institutional dimensions of the water-energy nexus. Energy Policy 39 (10), 6622–6630.
URL http://dx.doi.org/10.1016/j.enpol.2011.08.013

Segurado, R., Madeira, J. F., Costa, M., Duić, N., Carvalho, M. G., 2016. Optimization of a wind powered desalination and pumped hydro storage system. Applied Energy 177, 487–499.

Setiawan, A. A., Zhao, Y., Nayar, C. V., 2009. Design, economic analysis and environmental considerations of mini-grid hybrid power system with reverse osmosis desalination plant for remote areas. Renewable Energy 34 (2), 374–383.
URL http://dx.doi.org/10.1016/j.renene.2008.05.014

Shaahid, S. M., El-Amin, I., 2009. Techno-economic evaluation of off-grid hybrid photovoltaic–diesel–battery power systems for rural electrification in Saudi Arabiaï¿½a way forward for sustainable development. Renewable and Sustainable Energy Reviews 13 (3), 625–633.

Shaahid, S. M., Elhadidy, M. A., 2007. Technical and economic assessment of grid-independent hybrid photovoltaic-diesel-battery power systems for commercial loads in desert environments. Renewable and Sustainable Energy Reviews 11 (8), 1794–1810.

Shamshad, A., Bawadi, M. A., Hussin, W. M. A. W., Majid, T. A., Sanusi, S. A. M., 2005. First and second order Markov chain models for synthetic generation of wind speed time series. Energy 30 (5), 693–708.

Sharif, M., Burn, D. H., Wey, K. M., 2007. Daily and hourly weather data generation using a k-nearest neighbour approach. In: Canadian Hydrotechnical Conference. CHC Winnipeg, pp. 1–10.

Shepherd, T. G., Boyd, E., Calel, R. A., Chapman, S. C., Dessai, S., Dima-West, I. M., Fowler, H. J., James, R., Maraun, D., Martius, O., Senior, C. A., Sobel, A. H., Stainforth, D. A., Tett, S. F. B., Trenberth, K. E., van den Hurk, B. J. J. M., Watkins, N. W., Wilby, R. L., Zenghelis, D. A., dec 2018. Storylines: an alternative approach to representing uncertainty in physical aspects of climate change. Climatic Change 151 (3), 555–571.
URL https://doi.org/10.1007/s10584-018-2317-9

Singal, S. K., Varun, Singh, R. P., 2007. Rural electrification of a remote island by renewable energy sources. Renewable Energy 32 (15), 2491–2501.

Singh, R., Wagener, T., Crane, R., Mann, M. E., Ning, L., 2014. A vulnerability driven approach to identify adverse climate and land use change combinations for critical hydrologic indicator thresholds: Application to a watershed in Pennsylvania, USA. Water Resources Research 50 (4), 3409–3427.
URL https://agupubs.onlinelibrary.wiley.com/doi/abs/10.1002/2013WR014988

Sovacool, B. K., 2012. Deploying off-grid technology to eradicate energy poverty. Science 338 (6103), 47–48.

Spyrou, I. D., Anagnostopoulos, J. S., 2010. Design study of a stand-alone desalination system powered by renewable energy sources and a pumped storage unit. Desalination 257 (1-3), 137–149.

Stanton, M. C. B., Dessai, S., Paavola, J., 2016. A systematic review of the impacts of climate variability and change on electricity systems in Europe. Energy 109, 1148–1159.
URL http://www.sciencedirect.com/science/article/pii/S0360544216305679

Steinbach, J., Staniaszek, D., 2015. Discount rates in energy system analysis. Fraunhofer ISI, Building Performance Institute Europe (BPIE): Karlsruhe, Germany.

Takriti, S., Ahmed, S., jan 2004. On robust optimization of two-stage systems. Mathematical Programming 99 (1), 109–126.
URL https://doi.org/10.1007/s10107-003-0373-y

Ter-Gazarian, A., Kagan, N., 1992. Design model for electrical distribution systems considering renewable, conventional and energy storage units. IEE Proceedings C Generation, Transmission and Distribution 139 (6), 499.
URL http://digital-library.theiet.org/content/journals/10.1049/ip-c.1992.0069

Tingstad, A. H., Groves, D. G., Lempert, R. J., 2014. Paleoclimate Scenarios to Inform Decision Making in Water Resource Management: Example from Southern California’s Inland Empire. Journal of Water Resources Planning and Management 140 (10).

Trindade, B. C., Reed, P. M., Characklis, G. W., 2019. Deeply Uncertain Pathways: Integrated Multi-City Regional Water Supply Infrastructure Investment and Portfolio Management. Advances in Water Resources, 103442.

Trindade, B. C., Reed, P. M., Herman, J. D., Zeff, H. B., Characklis, G. W., 2017. Reducing regional drought vulnerabilities and multi-city robustness conflicts using many-objective optimization under deep uncertainty. Advances in Water Resources 104, 195–209.
URL http://www.sciencedirect.com/science/article/pii/S0309170816307333

United Nations (UN), 2019. Sustainable Development Goals Knowledge Platform.
URL https://sustainabledevelopment.un.org

United States Environmental Protection Agency (EPA), 2017. Inventory of U.S. Greenhouse Gas Emissions and Sinks. Tech. rep.

Uusitalo, L., Lehikoinen, A., Helle, I., Myrberg, K., 2015. An overview of methods to evaluate uncertainty of deterministic models in decision support. Environmental Modelling & Software 63, 24–31.
URL http://www.sciencedirect.com/science/article/pii/S1364815214002813

van Vliet, M. T. H., Yearsley, J. R., Ludwig, F., Vögele, S., Lettenmaier, D. P., Kabat, P., 2012. Vulnerability of US and European electricity supply to climate change. Nature Climate Change 2 (9), 676–681.
URL https://doi.org/10.1038/nclimate1546

Voivontas, D., Arampatzis, G., Manoli, E., Karavitis, C., Assimacopoulos, D., 2003. Water supply modeling towards sustainable environmental management in small islands: The case of Paros, Greece. Desalination 156 (1-3), 127–135.

Wald, A., 1950. Statistical Decision Functions. Wiley, New York.

Watson, A. A., Kasprzyk, J. R., 2017. Incorporating deeply uncertain factors into the many objective search process. Environmental Modelling & Software 89, 159–171.
URL http://www.sciencedirect.com/science/article/pii/S1364815216310593

Weisser, D., 2004. On the economics of electricity consumption in small island developing states: A role for renewable energy technologies? Energy Policy 32 (1), 127–140.

World Resources Institute (WRI), 2017. CAIT Climate Data Explorer.
URL http://cait.wri.org

Yan, S., Minsker, B., 2011. Applying Dynamic Surrogate Models in Noisy Genetic Algorithms to Optimize Groundwater Remediation Designs. Journal of Water Resources Planning and Management 137 (3), 284–292.

Yang, H., Wei, Z., Chengzhi, L., 2009. Optimal design and techno-economic analysis of a hybrid solar-wind power generation system. Applied Energy 86 (2), 163–169.

Zeff, H. B., Herman, J. D., Reed, P. M., Characklis, G. W., 2016. Cooperative drought adaptation: Integrating infrastructure development, conservation, and water transfers into adaptive policy pathways. Water Resources Research 52 (9), 7327–7346.
URL https://agupubs.onlinelibrary.wiley.com/doi/abs/10.1002/2016WR018771